OPEN ACCESS

University of BRISTOL

Spicer, R. A., Farnsworth, A., & Su, T. (2020). Cenozoic Topography, Monsoons and Biodiversity Conservation within the Tibetan Region: An Evolving Story. *Plant diversity*, *42*(4), 229-254. https://doi.org/10.1016/j.pld.2020.06.011

Publisher's PDF, also known as Version of record

License (if available):
CC BY-NC-ND

Link to published version (if available):
10.1016/j.pld.2020.06.011

Link to publication record in Explore Bristol Research
PDF-document

This is the final published version of the article (version of record). It first appeared online via Elsevier at https://doi.org/10.1016/j.pld.2020.06.011 . Please refer to any applicable terms of use of the publisher.

University of Bristol - Explore Bristol Research
General rights

This document is made available in accordance with publisher policies. Please cite only the published version using the reference above. Full terms of use are available:
http://www.bristol.ac.uk/red/research-policy/pure/user-guides/ebr-terms/

Plant Diversity 42 (2020) 229–254

Contents lists available at ScienceDirect

Plant Diversity

journal homepage: http://www.keaipublishing.com/en/journals/plant-diversity/
http://journal.kib.ac.cn

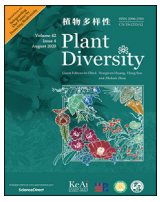

Research paper

Cenozoic topography, monsoons and biodiversity conservation within the Tibetan Region: An evolving story

Robert A. Spicer [a, b, *], Alexander Farnsworth [c], Tao Su [a]

[a] CAS Key Laboratory of Tropical Forest Ecology, Xishuangbanna Tropical Botanical Garden, Chinese Academy of Sciences, Xishuangbanna 666303, China
[b] School of Environmental, Earth and Ecosystem Sciences, The Open University, Walton Hall, Milton Keynes, MK7 6AA, UK
[c] School of Geographical Sciences, University of Bristol, Bristol, BS8 1SS, UK

ARTICLE INFO

Article history:
Received 18 April 2020
Received in revised form
11 June 2020
Accepted 11 June 2020
Available online 17 July 2020

Keywords:
Tibet
Himalaya
Hengduan Mountains
Landscape
Fossils
Conservation

ABSTRACT

The biodiversity of the Himalaya, Hengduan Mountains and Tibet, here collectively termed the Tibetan Region, is exceptional in a global context. To contextualize and understand the origins of this biotic richness, and its conservation value, we examine recent fossil finds and review progress in understanding the orogeny of the Tibetan Region. We examine the deep-time origins of monsoons affecting Asia, climate variation over different timescales, and the establishment of environmental niche heterogeneity linked to topographic development. The origins of the modern biodiversity were established in the Eocene, concurrent with the formation of pronounced topographic relief across the Tibetan Region. High (>4 km) mountains to the north and south of what is now the Tibetan Plateau bounded a Paleogene central lowland (<2.5 km) hosting moist subtropical vegetation influenced by an intensifying monsoon. In mid Miocene times, before the Himalaya reached their current elevation, sediment infilling and compressional tectonics raised the floor of the central valley to above 3000 m, but central Tibet was still moist enough, and low enough, to host a warm temperate angiosperm-dominated woodland. After 15 Ma, global cooling, the further rise of central Tibet, and the rain shadow cast by the growing Himalaya, progressively led to more open, herb-rich vegetation as the modern high plateau formed with its cool, dry climate. In the moist monsoonal Hengduan Mountains, high and spatially extensive since the Eocene but subsequently deeply dissected by river incision, Neogene cooling depressed the tree line, compressed altitudinal zonation, and created strong environmental heterogeneity. This served as a cradle for the then newly-evolving alpine biota and favoured diversity within more thermophilic vegetation at lower elevations. This diversity has survived through a combination of minimal Quaternary glaciation, and complex relief-related environmental niche heterogeneity. The great antiquity and diversity of the Tibetan Region biota argues for its conservation, and the importance of that biota is demonstrated through our insights into its long temporal gestation provided by fossil archives and information written in surviving genomes. These data sources are worthy of conservation in their own right, but for the living biotic inventory we need to ask what it is we want to conserve. Is it 1) individual taxa for their intrinsic properties, 2) their services in functioning ecosystems, or 3) their capacity to generate future new biodiversity? If 2 or 3 are our goal then landscape conservation at scale is required, and not just seed banks or botanical/zoological gardens.

Copyright © 2020 Kunming Institute of Botany, Chinese Academy of Sciences. Publishing services by Elsevier B.V. on behalf of KeAi Communications Co., Ltd. This is an open access article under the CC BY-NC-ND license (http://creativecommons.org/licenses/by-nc-nd/4.0/).

1. Introduction

Mountain regions are recognized widely for their role in nurturing biodiversity (Antonelli, 2015; Spicer, 2017; Hoorn et al., 2018; Rahbeck et al., 2019a, b) and this is particularly true for the Himalaya, the Hengduan Mountains, and what is today the Tibetan Plateau. Our understanding of the history of life across this region is undergoing a fundamental revision brought about by advances in

* Corresponding author. CAS Key Laboratory of Tropical Forest Ecology, Xishuangbanna Tropical Botanical Garden, Chinese Academy of Sciences, Xishuangbanna 666303, China.
E-mail address: r.a.spicer@open.ac.uk (R.A. Spicer).
Peer review under responsibility of Editorial Office of Plant Diversity.

https://doi.org/10.1016/j.pld.2020.06.011
2468-2659/Copyright © 2020 Kunming Institute of Botany, Chinese Academy of Sciences. Publishing services by Elsevier B.V. on behalf of KeAi Communications Co., Ltd. This is an open access article under the CC BY-NC-ND license (http://creativecommons.org/licenses/by-nc-nd/4.0/).

how we measure ancient topography quantitatively, our understanding of how landscapes interact with climate, extraordinary fossil finds, and new insights into patterns of diversification provided by molecular phylogeny. The Tibetan Region, which in the context of this paper we regard as spanning the area today collectively occupied by the Tibetan Plateau, the Hengduan Mountains and the Himalaya, is the world's greatest natural laboratory for geologists interested in collisional tectonics and paleoaltimetry and, as infrastructure has improved, so has access to remote sites within the region to the extent that it can legitimately now also be regarded as a 'natural laboratory for studying organic evolution and environmental change' (Zhou and Deng, 2020). New fossil discoveries and age revisions, not only across Tibet but within adjacent areas such as Yunnan, have all revealed that the region's biodiversity arose in a more complex topographic environment than that envisaged just a few years ago, and that the modernization of the biota took place much earlier than previously thought. The Tibetan region has served as a generator of novel taxa and a locus of intercontinental taxon interchange (Deng et al., 2020). These new insights impact upon the ways we might conserve and manage the exceptional biodiversity that characterizes this part of the world.

In this overview we summarize current knowledge of the topographic development of the Tibetan Region (sections 1.1 and 2), climate (including monsoon) variability (section 1.2) and what is known about the conserved fossil archives of the region. Although we focus on plants (section 3), we do not completely ignore faunal data. We then consider the complementary insights provided by molecular phylogenetics (section 4), and discuss how all this information might influence attitudes and approaches to conservation (section 5). Not all the recent advances can be reviewed here. We knowingly sacrifice some detail in favour of breadth, because bringing together diverse lines of evidence from different disciplines facilitates a more holistic synthesis.

Terrestrial biodiversity tends to be concentrated in mountain systems (Rahbeck et al., 2019a, b) and the Tibetan Region today hosts several of Earth's great biodiversity 'hotspots' (Myers et al., 2000) which, because of human aspirations, are under threat of destruction (Chakraborty, 2020). Seed plant diversity is today greatest in the Hengduan Mountains, which in a recent census hosts 8439 species of trees, shrubs and herbs, while the Himalaya are home to 5468 species (Yu et al., 2020). In comparison, the modern Tibetan Plateau is species-poor (3908 species), but comparatively rich in herbs which make up 81.5% of plateau seed plants (Yu et al., 2020). Knowledge of how such exceptional diversity came about provides an important perspective on how special the biota of the Tibetan Region is, and how imperative it is that the context in which it arose it is not destroyed as climate and landscapes undergo inevitable future changes. Fossil archives show that Tibetan Region biodiversity took on its modern aspect at least 30 million years ago and arose in the context of unique geological events. Once destroyed, we will never get that biodiversity back and we will also loose the potential for future ecosystem resilience.

The two key conditions for generating high biodiversity are complex topographic relief and a dynamic climate (Spicer, 2017, and references therein; Rahbeck et al., 2019a), both of which are found across the Tibetan Region. Recent work has shown that the Asian monsoon, regardless of topography, is a consistent feature arising from the regional land-sea temperature gradient (Acosta and Huber, 2020). Like the biodiversity, the monsoon has a long history, which has shaped both the biota and the landscape. While regional topographic controls on climate are complex (Acosta and Huber, 2020; Boos and Kuang, 2010; Molnar et al., 2010), it is not just the topography of the Tibetan Region but paleogeographical constraints further afield that influence monsoon dynamics (Farnsworth et al., 2019). We also now know that models of Tibetan orogeny favoured a few years ago, the most recent of which envisaged the plateau expanding outward from a high Paleogene "Proto Plateau" (Dai et al., 2012; Wang et al., 2014), require substantial revision in the light of new fossil discoveries, and that those discoveries are changing radically our knowledge of how Asian biodiversity was generated (Spicer et al., 2020).

1.1. Building topography

As we will show, geologically speaking the Tibetan Plateau is a very recent construct and its modern high (>4.5 km), relatively flat (low topographic relief) surface only came into being after ~15 Ma. Because the plateau is such a recently formed feature we cannot refer to a plateau when we are talking about Tibet in the past, so we will use the term 'Tibet', without any administrative implications, to refer to the region presently occupied by the plateau irrespective of its topography.

How such a large elevated expanse of low-relief landscape came into being has been a matter of considerable debate amongst geologists and, inevitably, ideas have changed over time. One early concept in which Tibet rose recently (within the last 10 million years) as an already flat landscape (e.g. England and Houseman, 1988) has dominated thinking for the last three decades, but we now know that idea is too simplistic and that Tibet has a longer and more complex history (see references in Spicer et al., 2020). That history has profoundly impacted the linked evolution of climate and biodiversity across Asia, and understanding that context is crucial for conservation efforts. For example, only with such a background can rare species in decline be distinguished from those that are rare because they are newly evolved.

The simplistic view of a monolithic Tibetan Plateau uplift has influenced disciplines as diverse as molecular phylogenetics (Renner, 2016, and references therein) and climate modelling (e.g. Botsyun et al., 2019). However, the pre-existing geology must have influenced any rise, and instead of acting as a monolithic block Tibetan topography formed by the complex accretion of pieces of Gondwana that collided with Asia at various times during the Mesozoic. After assembly, this complex geological structure responded idiosyncratically under compression from the accretion of India (Kelly et al., 2019). It has long been known that even before the onset of the India-Eurasia collision Tibetan topography encompassed substantial relief produced by earlier tectonic block (terrane) accretions (Allègre et al., 1984; Dewey et al., 1988; Şengör, 1984; Yin and Harrison, 2000). This piecemeal building of Tibet (Guillot et al., 2019; Kapp and DeCelles, 2019; Liu et al., 2016), and what it means for orographic evolution, is now becoming more appreciated and is explored more fully in Section 2.

1.2. A dynamic climate

1.2.1. Monsoon dynamics

In addition to revising our concepts of plateau formation, recent research has brought about a transformation in our understanding of Asia's dynamic climate, and in particular how Asian monsoon systems have evolved. Monsoons do not just affect Asia, but occur at low latitudes worldwide (Zhang and Wang, 2008). They are an inevitable consequence of seasonal migrations of the Inter-tropical Convergence Zone (ITCZ) brought about by Earth's axial tilt (Ramage, 1971; Webster and Fasullo, 2003), and so must have existed throughout most of Earth's history (Spicer et al., 2017). These ITCZ monsoons can, however, be variously modified and amplified by changes in astronomical drivers (Earth's axial tilt, orbital shape etc.) and the configuration of the continents and

topography, but are minimally affected by atmospheric CO_2 concentrations (Farnsworth et al., 2019).

For a long time, the presence of a high and spatially extensive Tibetan Plateau has been invoked as the primary driver for intensifying the Asian monsoon system, serving as a kind of 'hotplate in the sky' (Yanai and Wu, 2006) whereby sensible summer heating of mountain slopes and the plateau leads to convective instability. This in turn triggers air parcel ascent and the resulting surface low pressure draws in Southerly warm moist air from over the Indian Ocean towards the low pressure centre. This process is termed 'thermal forcing'.

Topography can also act to direct airflow either vertically or around such features such as mountains and plateaus (mechanical forcing). The mechanical forcing effect in the Tibetan Region can be twofold, i) the inhibition of dry airflow from central Asia into the Asian monsoon region, which disrupts more tropical airflow from the south and ii) direct forcing of airflow vertically, so initiating convective processes and an inflowing pressure gradient (Boos and Kuang, 2010; Molnar et al., 2010). While both thermal and mechanical forcing impact the monsoon, Wu et al. (2012) showed thermal forcing to be the main driver (ignoring the insulating effect the Iranian, Tibetan/Himalayan topography to dry northerly flow) because the impinging mechanical flow from the south towards the Tibetan Plateau is weak. This complex interplay between both thermal and mechanical forcing has undoubtedly changed through time as the topography evolved, and was integral to the formation and intensity of the Asian summer monoon throughout the Cenozoic (Molnar et al., 1993).

Asian monsoons are broadly divisible into a South Asia Monsoon (SAM) that today affects India, southern Tibet, Myanmar and Thailand, and an East Asia Monsoon (EAM) that predominantly affects most of China and Japan (Molnar et al., 2010; Wang and Ho, 2002; Zhang and Wang, 2008). Each have different characteristics (Molnar et al., 2010; Wang and Ho, 2002), but often the distinctions are not easy to detect in the geological record and have likely changed through time (Spicer et al., 2017). Moreover, the two systems interact in a so-called Transition Area over Yunnan and adjacent provinces (Wang and Ho, 2002). This makes tracking monsoon evolution solely using proxies a challenging exercise, especially when considering spatio-temporal biases (Spicer et al., 2016). Previously, monsoon origins have been linked to a rapid Neogene uplift of a coherent Tibetan Plateau (e.g. An et al., 2001), but it is becoming clear that such a recent rise of Tibet in its entirety never occurred, and that to a greater or lesser extent Asia has been exposed to monsoon climates for hundreds of millions of years.

During the late Paleozoic and early Mesozoic a giant "C" shaped supercontinent, Pangea, straddled the equator in a more or less symmetrical fashion (Fig. 1a), and this symmetry modified the ITCZ migration (Armstrong et al., 2016). In the boreal summer the part of Pangea that was in the Northern Hemisphere, including the region that would become Asia, heated up strongly so developing a pronounced summer low-pressure system, while in the winter (southern) hemisphere the Southern Hemisphere portion of Pangea developed a cold high-pressure centre, with the result that seasonally alternating thermal forcing amplified the ITCZ migration and cross-equatorial wind reversals. These seasonal wind reversals are fundamental to monsoon climate systems (Ramage, 1971; Webster and Fasullo, 2003) and it used to be thought that a global "megamonsoon" system might have dominated Earth's climate throughout the time that Pangea existed (Dubiel et al., 1991; Parrish, 1993), only weakening later in the Mesozoic as Pangea separated into Gondwana (South America, Antarctica, India, Africa, Madagascar, Australia, New Zealand) and Laurasia (North America, Greenland Europe and Asia north of what would become the Himalaya). Further fragmented towards the end of the Mesozoic (Fig. 1b) produced continental configurations approaching those of today (Fig. 1c). More recent modelling shows such megamonsoons are unlikely to have existed, but nevertheless well-developed monsoons were present in the Pangean world. Their main characteristic is that they formed strong near-equatorial belts similar to that which would occur in a 'water world' planet without continents, but these belts were strongly modified near land by thermal forcing arising from land - sea contrasts (Fig. 1a). Clearly continental configuration, topography and global climate conditions constrain monsoon characteristics and all change with time.

Proxy data and modelling show that, although still present in the early Cretaceous, a monsoon climate all but disappeared over southern China during the late Cretaceous and early Paleocene (see Farnsworth et al., 2019, and references therein) (Fig. 1b). In part, this was due to a globally warm climate that generated only a weak Siberian winter low pressure system, and we know the late Cretaceous continental interior of Siberia had a much-reduced mean annual range of temperature compared to that of colder times, such as the present (Spicer et al., 2008). As global climate cooled in the later Cenozoic, a strong winter Siberian High re-established and the EAM strengthened to a zenith in the 'supermonsoon' and peak rainfall of the late Miocene and Pliocene (Farnsworth et al., 2019).

Today's SAM, while in part influenced by the climate of the Siberian Interior, is strongly modified by the complex orography of the Tibetan Region (Boos and Kuang, 2010; Molnar et al., 2010), and today's distinctive attributes of the SAM system must have evolved as the topography of the Tibetan Region developed. Moreover, SAM influences on the Indian subcontinent have changed both as a function of topographic development in Asia and India's latitudinal position. As the Indian plate tracked northward different parts of the sub-continent passed through the ITCZ monsoon belt at different times, beginning at ~150 Ma (Fig. 1) and, subsequently, the SAM likely intensified and changed its characteristics as the Himalaya rose as a consequence of the India-Eurasia collision. This would have meant that monsoon influences on the evolution of Indian biodiversity must have been quite different from those affecting the rest of southern Asia.

1.2.2. Orbital cycles

Global and regional climate is always in a state of flux over millennial timescales, irrespective of monsoon dynamics, purely because the amount and distribution of solar energy received by Earth's surface varies due to what are known as Milankovitch–Croll cycles. These astronomical cycles are driven by the interplay of changes in precession (19 and 23 kyr cycles caused by rotational wander in the direction that Earth's spin axis points), obliquity (41 kyr and 1.2 Myr - changes in the angle of Earth's spin axis relative to the orbital plane) and eccentricity (100 kyr, 405 kyr and 2.4 myr cycles caused by changes in the shape of Earth's orbit around the Sun) (Berger and Loutre, 1994; Berger et al., 2006; Hays et al., 1976; Leuschner and Sirocko, 2003), and such 'orbital forcing' has a direct impact on monsoon (Leuschner and Sirocko, 2003) and vegetation dynamics (Claussen et al., 2006; Tuenter et al., 2006). Orbital forcing famously acted as a 'pacemaker' for the waxing and waning of Quaternary ice sheets (Hays et al., 1976), and there is evidence of its impact on the Tibetan environment over the past 1.74 million years (Zhao et al., 2020).

Orbital forcing has operated throughout Earth's history, and is widely exploited in cyclostratigraphy (Weedon, 2005; Weedon et al., 2004), so it will have impacted the distribution of temperature and precipitation, and thus vegetation, across the Tibetan Region throughout the Cenozoic, and not just in the Quaternary. Usually climate change is thought of in terms of changes in the thermal regime and orbital forcing will have driven plant and animal altitudinal migrations over timescales long enough to have

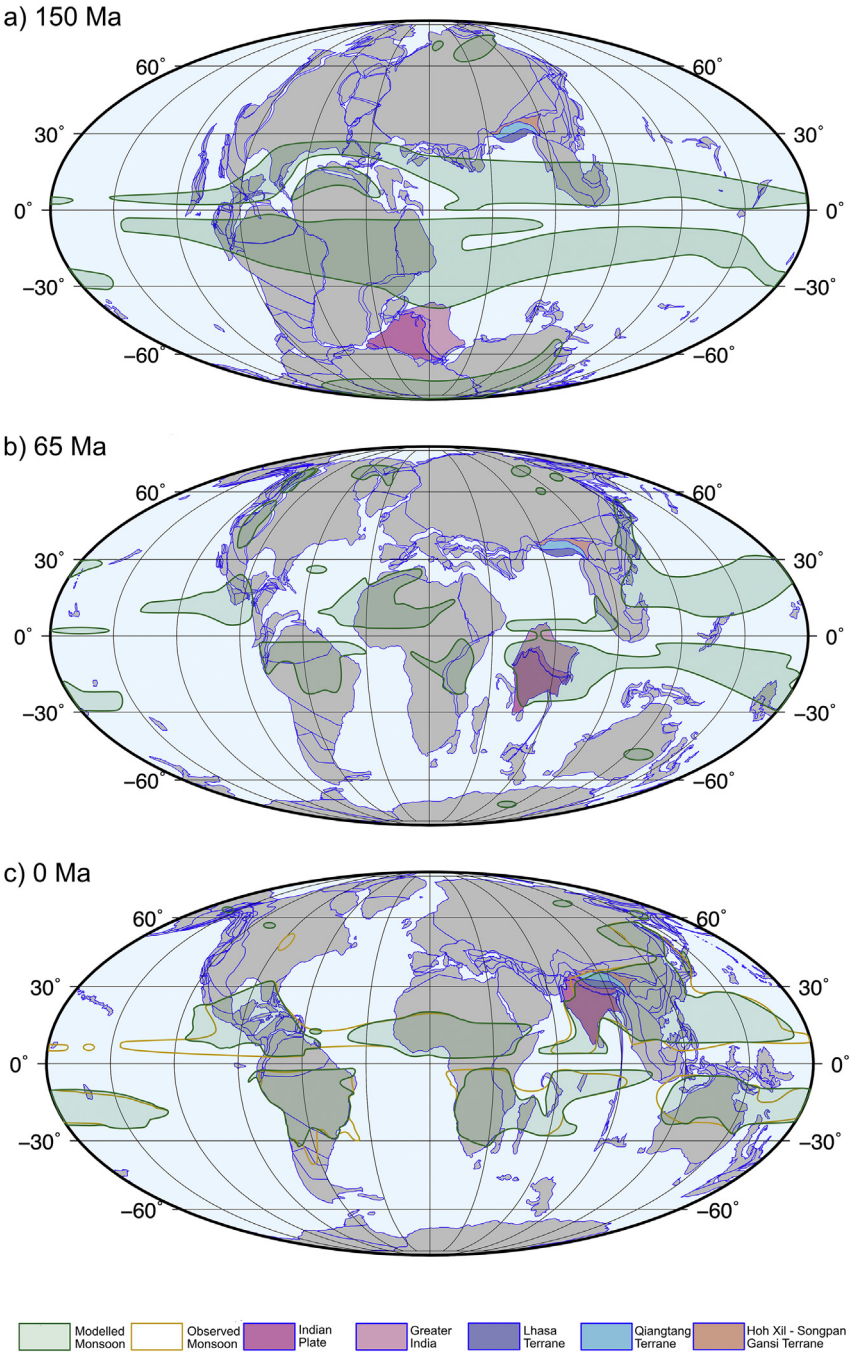

Fig. 1. Paleogeographic reconstructions and monsoon distributions as indicated by computer modelling (green shaded areas) using the HADCM3L General Circulation Model (Valdes et al., 2017). Monsoon definitions follow those of Wang et al. (2011). a) Plate reconstruction for 150 Ma showing the Supercontinent Pangea just beginning to break up into Gondwana in the southern hemisphere and Laurasia in the north. The India plate (dark pink), and greater India (light pink) are in high southern latitudes. Greater India is now subducted beneath Asia and its extent before collision is poorly known. The Lhasa (lilac), Qiangtang (light blue) and Hoh Xil-Songpan Gansi (orange) terranes are already accreted to Asia. Over the ocean two broad monsoon belts lie either side of the equator within the latitudinal migration of the ITCZ, but these belts become wider and fragmented near and over land. b) at the end of the Cretaceous (65 Ma) the monsoon belts have broken up as the continents disperse, but India and Greater India are dominated by the southern hemisphere ITCZ monsoon that extends into the western Pacific. South China and the Tibetan Region are non-monsoonal. c) In the present day (pre-Industrial model boundary conditions) monsoons affect India (SAM) and extend across China, and southern Asia (EAM). Modern observed monsoon limits are shown by a yellow line, indicating that the modelling shows skill at reproducing monsoon distribution. Sources: (Armstrong et al., 2016; ODSN).

resulted in significant shifts in gene pools, but temperature variations will also have impacted the hydrological regime, including monsoon dynamics (Leuschner and Sirocko, 2003). Because of its pace and repetitive nature orbital cycle-driven climate change is likely a key component of the biodiversity 'pump' (Fig. 2) (*sensu* Spicer, 2017).

2. The topographic evolution of the Tibetan Region

2.1. The assembly of Tibet

In the Paleozoic, several microcontinents began separating from Gondwana to travel northwards, a path that the Indian plate would

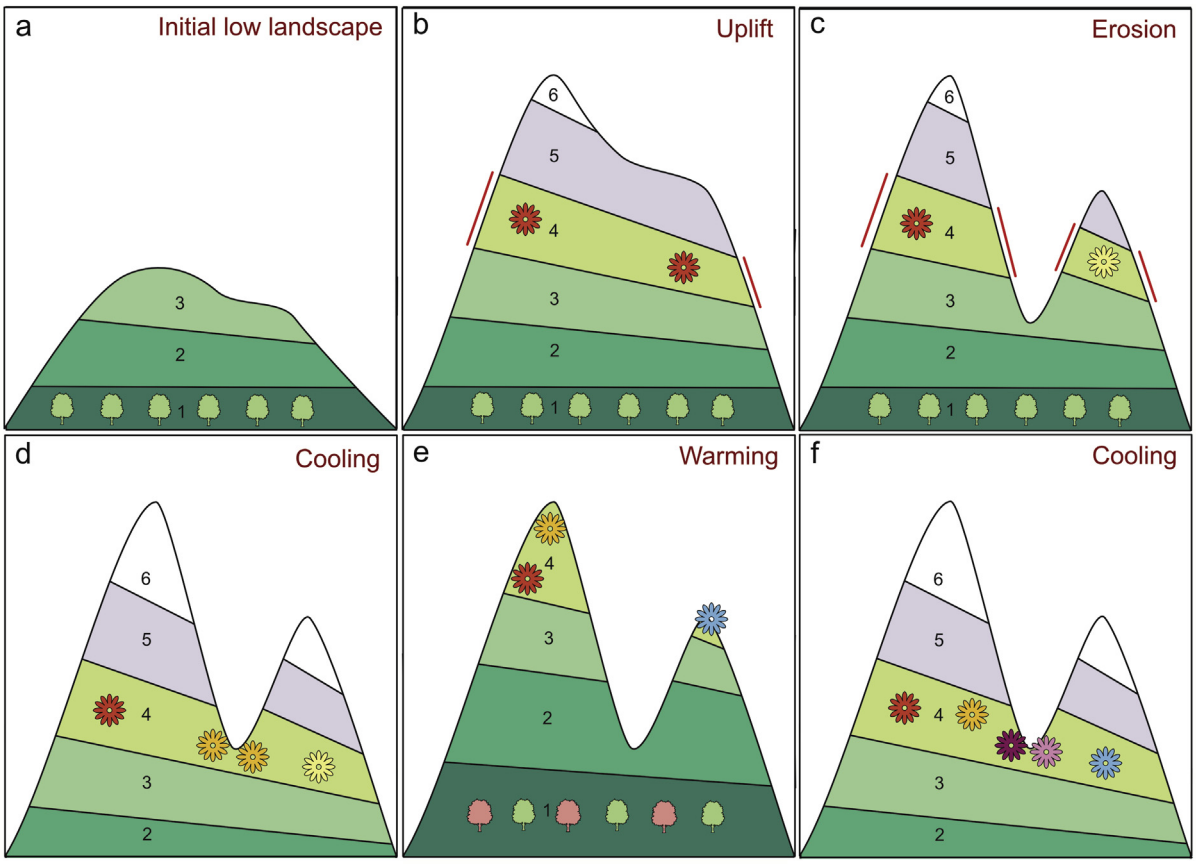

Fig. 2. Cartoons showing the biodiversity pump relationship between topography and climate. a) initially a low elevation landscape can accommodate only a few altitude-related climate and vegetation zones 1–3. Zone 1 composition is indicated by green tree icons. b) uplift creates more altitudinal range and thus more vegetation zones or biome assemblages (1–6) develop through immigration. Here Zone 4 hosts a plant taxon indicated by the red flower symbol. c) Erosion dissects the landscape exposing more land area (indicated by red lines) for occupation, creating more complex niche space and isolating populations that over time, due to such processes as genetic drift, become new species, as indicated by the yellow flower symbol. d) climate cooling due to changes in orbital configuration drive Zone 4 plants to lower elevations and the red and yellow populations hybridize to form a new species indicated by the orange flower. Zone 1 plants (green trees) are eliminated from the area. e) climate warming, again due to a change in orbital configuration, drives Zone 4 plants upslope where isolation produces another genetic variant (blue flower). Zone 1 is re-established, but this time with new immigrants (pink trees). f) cooling again offers another opportunity for hybridization producing pink and purple flowers. Repeated altitudinal migration driven by cyclical climate fluctuations produce more and more species. In reality some taxa will go extinct during this process, but the net result should be an increase in biodiversity.

later also follow, to eventually collide with Asia. These micro-continental collisions took place throughout the Mesozoic (Guillot et al., 2019; Lai et al., 2019; Li et al., 2019; Li et al., 2019; Kapp and DeCelles, 2019, and references therein), so what we now know as the Tibetan Plateau was formed piece by piece (Fig. 3) with each collision marked by deep-rooted suture zones and pronounced relief.

The best documented ancient Tibetan mountain range is that which forms the southern border of the Lhasa Terrane: the Andean-type Gangdese Arc uplands. The Gangdese Mountains formed a high southern flank to Tibet before the growth of the Himalaya, and in places had reached an altitude of at least ~4.5 km in the Eocene (~56 Ma) (Ding et al., 2014). To the north, the uplands of the Qiangtang Terrane, today referred to as the Tanggula Mountains, began to rise from sea level at ~125 Ma after the last marine units were deposited (Li and Batten, 2004). By the Eocene, parts of the Qiangtang uplands had reached, and possibly exceeded, the elevation of the Gangdese Mountains (Xu et al., 2013) and the Tanggula appear to have been a significant topographic high since ~70 Ma, shedding sediment north into the Hoh Xil basin and south into the Bangong-Nujiang Suture Zone (Dai et al., 2012; DeCelles et al., 2007a; Staisch et al., 2014).

The Bangong-Nujiang Suture Zone (BNSZ) is the approximately E–W aligned junction between the Lhasa and Qiangtang terranes. The suture zone, an area we will refer to here as 'central Tibet', was occupied initially by the remnants of the Meso-Tethys Ocean until ~96 Ma (Kapp and DeCelles, 2019), and thereafter the lowlands along the BNSZ suffered significant N–S narrowing throughout the late Cretaceous under compression from the approaching India. Despite this compression the northern part of the Lhasa terrane was maintained at an elevation no higher than 1 km until ~55 Ma by peneplanation, that is to say rivers laterally migrating, eroding and flushing out sediment in an overall arid landscape (Hetzel et al., 2011; Strobl et al., 2012; Xu et al., 2015). One such river, the ancient Lhasa River, appears to have cut through the Gangdese highland (Laskowski et al., 2019) until the rising Himalaya blocked it, most likely sometime in the late Eocene. This is marked by sedimentation in central Tibet switching from being fluvially-dominated to lacustrine, as evidenced by the contrasting dominant sedimentary facies of the Paleocene-Eocene Niubao Formation and Oligocene-Pliocene Dingqing Formation. Continued N–S deformation, coupled with some sediment accumulation, raised the valley floor (probably by no more than 1.5 km) during the Eocene, and by the Oligocene the valley had become more enclosed and host to large lakes surrounded by diverse sub-tropical vegetation in a humid climate (Su et al., 2019; Wu et al., 2017) (Section 3).

Today the junction between the Indian plate and Eurasia is marked by the Yarlung-Tsangpo suture zone (YTSZ) (Fig. 3), but

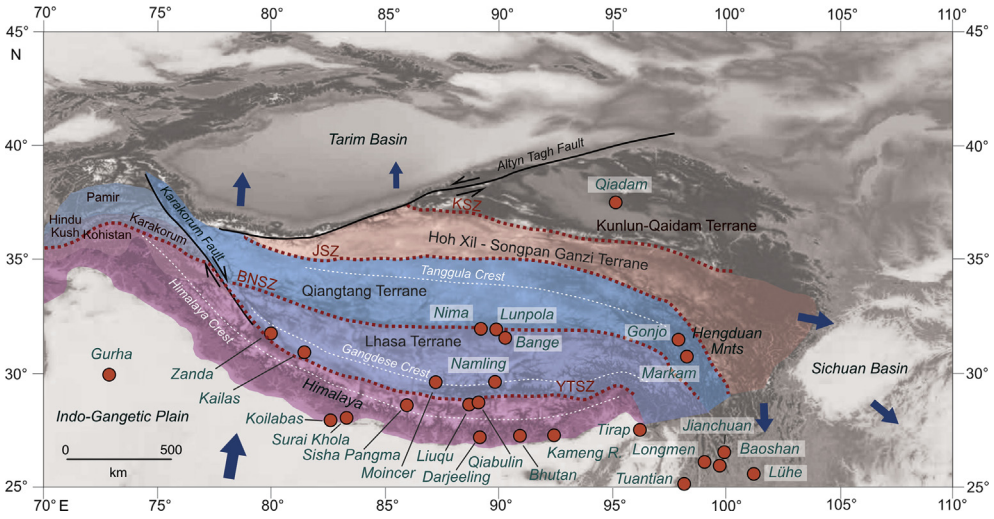

Fig. 3. Map of the Tibetan Region showing major tectonic features, component tectonic terranes and fossil localities (red filled circles) mentioned in the text. Colour coding is as in Fig. 1. Blue arrows indicate ongoing relative tectonic motion based on Wang et al. (2014).

exactly when the onset of continental collision began is still a matter of considerable debate, with estimates ranging between 65 Ma (Ding et al., 2005, 2017a; Yin and Harrison, 2000) and 20 Ma (van Hinsbergen et al., 2012), while recent evidence from mammal exchange points to a land bridge becoming established (as distinct from subduction of oceanic plate) early in the Paleogene, or even the latest Cretaceous (Ni et al., 2020). Contact did not take place simultaneously along the entire length of the YTSZ, and in the west the collision even incorporated a volcanic island system known as the Kohistan Arc (Khan et al., 1997, 2009; Treloar et al., 1996) that may have acted as a 'stepping stone' for biotic exchange as India approached (Kapur et al., 2017; Smith et al., 2016). Locally marine sediments were still being deposited south of the Gangdese Arc as late as 50–55 Ma (Ding et al., 2005).

Once continent–continent contact was made India's northward passage began to slow against increasing resistance (Molnar and Stock, 2009; Meng et al., 2017). A particularly significant slowdown occurred at ~52 Ma (Li et al., 2020c) coinciding with substantial deformation across Tibet at that time (Clark et al., 2010; Jin et al., 2018; Kapp et al., 2007; Li et al., 2015b; Spurlin et al., 2005). Several events in succession followed the collision. The first was the modification of the Tibetan landscape inherited from the earlier terrane collisions, another was the uplift of eastern Tibet and the Hengduan Mountains (section 2.2), and a third was start of the uplift of the Himalaya (Section 2.3). These events are summarized in Fig. 4 and will now be explored further.

2.1.1. The Paleogene lowlands of central Tibet

The evidence for lowlands in Tibet throughout the Paleogene, comes largely from recent fossil finds, and what they suggest is in stark contrast to the high elevations (≥4.5 km) and a proto-plateau suggested by stable isotope paleoaltimetry (DeCelles et al., 2007b; Mulch and Chamberlain, 2006; Rowley and Currie, 2006). The discovery of fossils of the air-breathing climbing perch, *Eoanabas thibetana* Wu, Miao, Chang et al. (Anabantidae) in the lacustrine lower Dingqing Formation of the Lunpola Basin (Fig. 3) (Wu et al., 2017) meant that the area had to have been warm and free of seasonal ice formation on the paleolake surface. Initial estimates constrained the lake surface elevation to have been ~1 km at ~25 Ma (Wu et al., 2017), but this implicitly assumed a modern thermal lapse rate, which is inappropriate for paleoaltimetry (Meyer, 2007; Spicer, 2018), and the age is only loosely constrained but likely to be at least late Oligocene if not a little older. Even assuming a late Oligocene age for *Eoanabas,* this discovery pushed back the origin of the anabantids by at least 20 million years (Wu et al., 2017) and suggests an early Eocene Southeast Asian origin of the group (Wu et al., 2018).

Along with fish, the section also yielded insects, including the water strider *Aquarius lunpolaensis*, again indicative of a low paleoelevation, and a diversity of plant fossils with a sub-tropical affinity (Wu et al., 2017). Among these plants were large (~1 m long) palm leaves assigned to *Sabalites tibetensis* T. Su et Z.K. Zhou (Su et al., 2019). This find was significant because all palms are intrinsically cold-sensitive (Reichgelt et al., 2018) due to their internal structure, particularly when seedlings. Using a conservative +5.2 °C cold month mean temperature (CMMT) as the lowest survivable by natural palm populations (Reichgelt et al., 2018), and by using CMMT terrestrial lapse rates derived using climate models constrained by Oligocene (Chattian) boundary conditions with an array of different Tibetan orographies, Su et al. (2019) determined that the Lunpola lake-margin vegetation was growing below an elevation of 2.3 km.

Very recently older plant fossils have been recovered from five distinct horizons in middle Eocene (Lutetian) mudstones within the Niubao Formation, which underlies the Dingqing Formation in the nearby Bange Basin. Also located along the BNSZ, this flora is more diverse than that of the Dingqing Formation and contains several taxa with affinities to Eocene genera found in the western USA (Green River Formation), the UK (London Clay), Germany (Messel) and even Africa (Del Rio et al., 2020; Liu et al., 2019; Tang et al., 2019). In general, Eocene vegetation across the Northern Hemisphere was notably more uniform than today. By contrast only one taxon, *Ailanthus maximus* T. Su et Z.K. Zhou, has been shown, so far, to have links with India (Liu et al., 2019), suggesting a significant barrier to biotic exchange existed between India and the Interior of Tibet in the middle Eocene. This barrier was most likely the Gangdese Mountains given that the ocean 'moat' between India and Eurasia no longer existed. However, the Gangdese barrier cannot have been complete and was likely penetrated by the ancestral Lhasa River (Laskowski et al., 2019) until sometime in the Eocene (Section 2.3). Limited exchange with Indian taxa was possible through the deep connecting gorge, and it may have looked like the Tsangpo River gorge in SE Tibet today. During the early phases of Himalayan growth gorge erosion may have kept

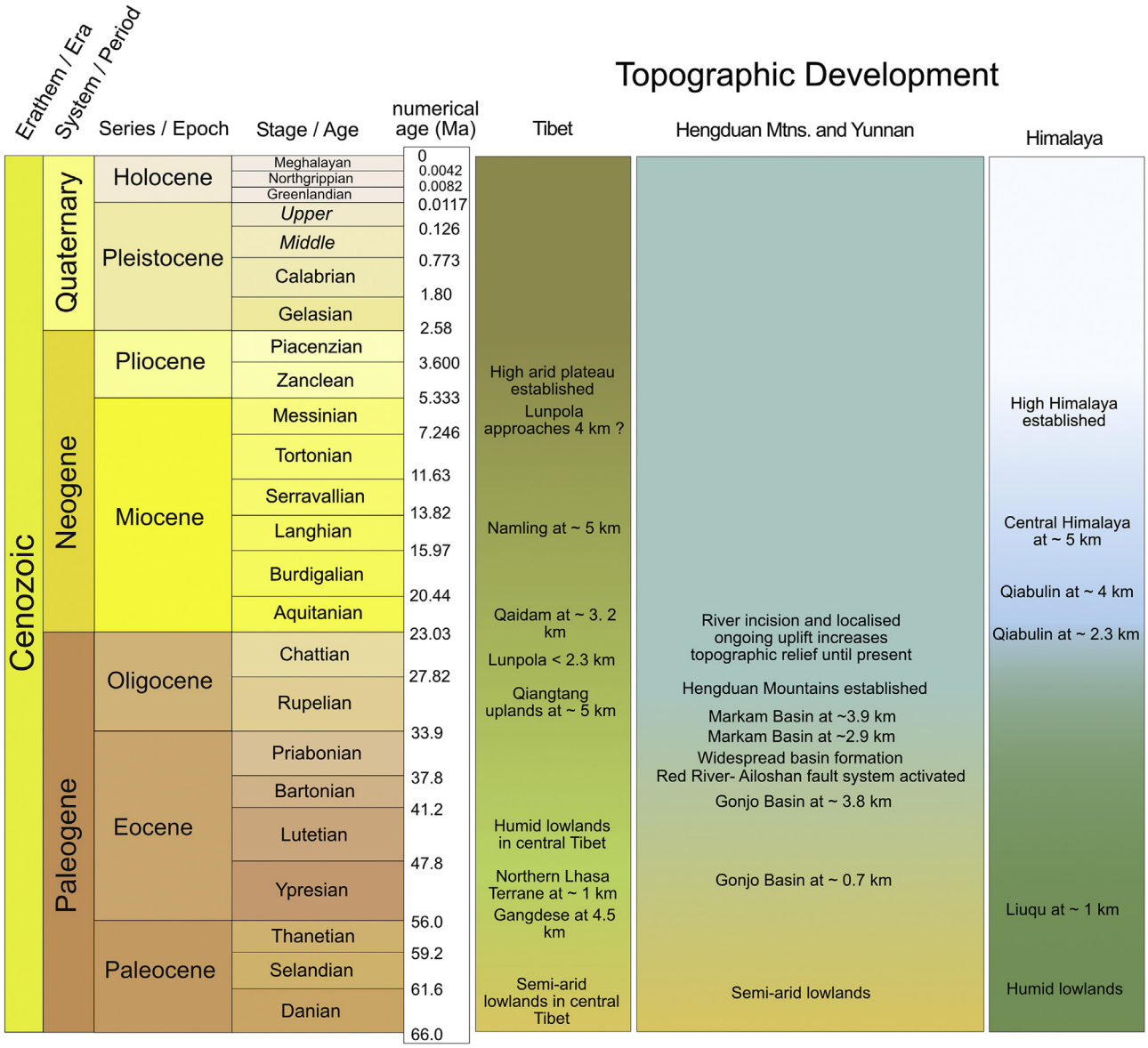

Fig. 4. Summary of the known milestones in the topographic development of the Tibetan region. Timescale from Cohen et al. (2013, updated 2019). Throughout the Paleogene Tibet exists as two major east-west trending mountain ranges with elevations exceeding 4.5 km, bounding a lowland <2.3 km above mean sea level. The modern plateau developed gradually in the Neogene through a combination of ongoing north-south compressions and sediment infilling basins. The Hengduan Mountains achieve near-present elevations by the end of the Paleogene and so before the formation of a high plateau in Tibet and the High Himalaya. The Himalaya is the most recent part of the Tibetan region to be uplifted, only exceeding the height of the old Gangdese highland in the mid Miocene. For vegetation changes see Tables 1–3. Details and references are given in the text.

pace with uplift but eventually, as the pace of uplift accelerated, the connection between Tibet and India was cut and central Tibet became internally drained to host large lake systems.

Like those of the Dingqing flora, the plants within the Niubao Formation are typical of those found growing under a sub-tropical climate and must indicate humid conditions at low elevation. The question then arises as to why there is such a contradiction between the high and dry central Tibet suggested by stable isotopes (e.g. Rowley and Currie, 2006; DeCelles et al., 2007b) and the low, humid environment indicated by the biota reviewed above.

This difference can be reconciled by considering where isotopic fractionation takes place. As a parcel of air approaches a mountain front it is forced upwards and cools, causing entrained moisture to condense and clouds to form. Ultimately moisture in that air parcel rains out, preferentially taking with it the heavy isotopes (^{18}O and Deuterium) from that air parcel (Garzione et al., 2000). This process is known as Rayleigh fractionation (Mulch, 2016; Mulch and Chamberlain, 2018; Rowley et al., 2001) and is most cleanly evidenced where moisture is delivered to the windward side of a single mountain system close to a moisture source (i.e. an ocean).

Such a situation existed in the case of the Gangdese highland, and still persists to a large extent along the southern flank of the Himalaya (Currie et al., 2016; Ding et al., 2014, 2017b). As a consequence, the northward-moving air cresting such mountain tops is depleted in heavy isotopes relative to the isotopic composition of the air parcel when it started its rise, so light isotopes preferentially enter any valley on the leeward side of the mountain range. In the case of the Paleogene central Tibetan lowlands a monsoon climate would have meant that most moisture likely entered from the south in the summer after cresting the Gangdese, while in the winter isotopically lighter and dryer air from the Asian

interior will have had to have passed southwards over the Qiangtang (Tanggula) highlands, again delivering isotopically light moisture to the valley. This resulted in sediments and organic matter that accumulated in the lowland lakes also being isotopically light and so appearing to represent a 'phantom' plateau with a surface height reflecting the elevation of the surrounding mountain crests (Su et al., 2019; Spicer et al., 2020). Both stable isotope paleoaltimetry, which is biased towards reflecting the elevation of highlands, and paleoaltimetry based on paleontology, in which lowland biotas are preferentially preserved in depositional basins, are required to reconstruct the complexity of past landscapes.

The central Tibetan lowland environments did not remain static throughout the Paleogene because they were subject to changes in climate, drainage patterns and tectonics. Continued deformation and sediment infilling raised the elevation of the lowlands such that by the middle Miocene they were approaching their modern elevation (Liu et al., 2016), and thus the modern plateau formed after ~15 Ma, with all that entailed for the on-plateau climate, its biota, and regional monsoon dynamics.

2.2. The building of the Hengduan Mountains

The Hengduan Mountains lie in an area on the south-eastern margin of the modern Tibetan Plateau, accommodating the eastward extrusion of parts of the Qiangtang Terrane and the Indo-China and Chuandian blocks (Li et al., 2020b,c; Searle et al., 2011; Tapponnier et al., 1982, 2001; Tong et al., 2017). This area has experienced strong episodic deformation since the late Cretaceous (Cao et al., 2019; Liu-Zheng et al., 2018; Tian et al., 2014; Wang et al., 2012, 2018), resulting in several major strike-slips fault systems, tightly folded synclines and anticlines (YBGMR, 1990; Burchfiel and Chen, 2012), and a complex of regional high elevation but low-relief relictual landscapes that have become deeply dissected by large rivers draining from the plateau (Clark et al., 2006; Liu-Zheng et al., 2008).

The idea that the rise of eastern Tibet, including the Hengduan Mountains, may have been largely the result of extrusion of part of the Qiangtang Terrane is not new (Searle et al., 2011; Tapponnier et al., 1982, 2001), but at issue until recently had been the timing of uplift tectonics. Many Cenozoic depositional basins across the eastern Tibet and Yunnan had been assigned Miocene ages because they contained modern-looking pollen and plant megafossil assemblages, with the result that paleoaltimetry derived from them (Hoke et al., 2014; Li et al., 2015a) pointed to a Miocene uplift. However, recent radiometric dating of the Jianchuan, Lühe, and Markam basins have shown them all to be late Paleogene and not Neogene (Gourbet et al., 2017; Linnemann et al., 2018; Su et al., 2018), and not only does this make the fossil floras they host older, but also moves the dates of basin formation back to be coincidental with the onset of movement along major fault systems (e.g. the Ailoshan-Red River) near the end of the Eocene (Cao et al., 2011; Leloup et al., 1995; Tapponnier et al., 1990; Li et al., 2020b). The synchronicity of basin formation and initiation of fault movement in the late Eocene/early Oligocene (~35 Ma) points to a common tectonic mechanism, which appears to have involved semi-rigid re-organisation of eastern Tibet, clockwise rotation of the Indo China Block, and inevitably must have involved significant topographic development (Li et al., 2020b, c).

New paleoaltimetric work (Xiong et al., 2020) shows that uplift of what would become the Hengduan Mountains actually predates even those late Eocene/early Oligocene tectonics and that major uplift of the Gonjo Basin, in the eastern Qiangtang Terrane (Fig. 3), took place during the early Eocene, rising from ~700 m at 54–50 Ma to ~3800 m by no later than 40 Ma. The nearby Markam Basin, also part of the Qiangtang Terrane and today part of the Hengduan Mountains, appears to have reached its current elevation by the early Oligocene with active uplift in the late Eocene to earliest Oligocene (Su et al., 2018). Thus, it seems that the building of eastern Tibet, the Hengduan Mountains, and even the topography into central and southern Yunnan, began in the early Eocene with widespread near-modern elevations being achieved within the Paleogene and significant uplift continuing in places into the late Miocene (Li et al., 2020a).

Uplift is not the only process producing pronounced relief because erosion is also important. Subject to the dating being correct, large-scale river incision is thought to have taken place in the Miocene and this phenomenon was used to infer uplift at that time (Clark et al., 2005, 2003, 2004; Royden et al., 1997, 2008). However, erosion can also be accelerated by increases in rainfall, and monsoon intensification in the mid Miocene is also likely to have caused the incision and the creation of pronounced relief across eastern Tibet and the Hengduan Mountains (Nie et al., 2018). These regional river systems appear to long predate the Miocene and recent U–Pb dated detrital zircon analysis points to a major river connection between what is now south-eastern Tibet and the South China Sea in the Eocene, but which underwent major disruption around the Eocene-Oligocene (E-O) transition at ~ 35 Ma (Clift et al., 2020).

Currently available evidence points to a rise of eastern Tibet and the Hengduan mountains beginning in the early Eocene, and uplift progressing south-eastwards through the Eocene such that by the end of the Eocene tectonic restructuring had elevated the landscape across large parts of Yunnan. The initial mechanism for this uplift seems to have been largely extrusion and semi-rigid deformation and rotations of the key tectonic blocks in the region (Li et al., 2017), but then perhaps also including lower crustal flow whereby plastic material was extruded at depth (Royden et al., 1997; Clark and Royden, 2000; Schoenbohm et al., 2006). This process may be ongoing. Recent analysis of seismic data suggests marked anisotropic changes at depth (Han et al., 2020) as would be expected with some form of lower crustal flow. Whatever the dominant uplift mechanisms, which may have changed with time, relief was amplified during and after uplift by river incision creating a mosaic of aspect, elevational differences, microclimates, complex geology and soils that must have increased niche heterogeneity and stimulated increases in biodiversity (Antonelli et al., 2018).

2.3. The building of the Himalaya

The onset of the growth of the Himalaya is evidenced by a rise of the land surface immediately south of the YTSZ and Gangdese uplands, and by ~56 Ma what previously had been deep ocean had reached an elevation~1 km (Ding et al., 2017b). This rise was quantified through CLAMP analysis of leaf form (physiognomy) (http://clamp.ibcas.ac.cn) exhibited by the radiometrically-dated diverse tropical Liuqu Formation flora (Fang et al., 2005). An overlying (23 Ma, Aquitanian) fossil leaf assemblage within the Qiuwu Formation, the temperate Qiabulin flora, yielded a paleoelevation of 2.3 km using the same phytopaleoaltimetric technique, as well as stable isotope paleoaltimetry (Ding et al., 2017b; Xu et al., 2018). Higher in the Qiabulin Formation stable isotope paleoaltimetry indicates an elevation of ~4 km had been achieved by 19 Ma (Burdigalian) (Ding et al., 2017b), and so it appears that the young central Himalaya matched the height of the Gangdese uplands early in the Miocene (Xu et al., 2018). Since then the Himalaya have continued to build to their present mean elevation of ~6 km (Fig. 4).

The uplift of the Himalaya had important consequences for the Neogene climate of southern Asia in that their rise increased mechanical forcing, preventing cool air from the north from ventilating north-western India and Pakistan where the hottest regional summer temperatures are recorded today (Molnar et al., 2010), and intensifying the deflection of wet summer air from the south to produce today's intense rainfall across north-eastern India, Myanmar and northern Thailand (Boos and Kuang, 2010). While deflection produces extremely wet conditions in north-eastern India today, to the north of the Himalaya it resulted in a rain shadow (Ding et al., 2017b), coincidental with plateau formation since the middle Miocene. All these atmospheric phenomena are features of the modern SAM.

While the rain shadow affect is an important one it is not the only reason why a high Tibet is also dry. Climate modelling shows that raising Tibet as a plateau surface will, by itself and without an elevated Himalaya, result in drying as shown both in the Lutetian (Fig. 5) and in the modern (Paeth et al., 2019). The reason for this is complex. Mechanical forcing of a moist airmass rising over a topographical front will cause 'rain out' as that airmass ascends leaving a drier airmass to traverse the plateau. Theoretically a higher plateau should preferentially deplete entrained moisture more than a lower one as a result of adiabatic cooling. This phenomenon is seen on both the southern and northern flanks of the plateau in Fig. 5. However, a higher plateau will increase the flux of moisture towards it due to greater thermal forcing as a deeper low-pressure system develops. Also, Farnsworth et al. (2019) showed that a plateau of half the height of today's Tibetan Plateau can limit convective processes, capping them in the lower troposphere and so inhibiting precipitation as seen today on the Iranian Plateau.

There is also the impact of large-scale circulation and the location of the Hadley Cell, in particular where air descends and a high-pressure belt develops (typically at around 30° latitude and thus across the Tibetan Region). Again, this inhibits convective processes and precipitation, producing a dry environment. What is clear from Fig. 5 is that a 'plateau' in the Tibetan Region, at any of the theorised heights, will be dry and so not able to sustain the type of vegetation that is evidenced by the new fossil finds. This supports the existence of a more complex topography for Tibet, such as suggested by Su et al. (2019), but strong thermal and mechanical forcing would still be important in determining the regional climate. Moreover, a central deep valley system between the Gangdese and Qiangtang uplands hosting large lakes fed by mountain streams would have generated strong within-valley water cycling and provided a more habitable region in terms of the temperature and precipitation regime within it. Further work is required to better understand this, but it is clear that past biotas 'conserved' in natural geological archives are essential to inform our knowledge of past landscapes.

3. An overview of the Cenozoic biota of the Tibetan Region

To understand the evolutionary history of the Cenozoic biota of Tibet, the Himalaya and the Hengduan Mountains it is useful to begin at the end of the Cretaceous because at the start of the Cenozoic the Maastrichtian biota was inevitably inherited, despite events at the K/Pg boundary, which seem to have had little effect on plant diversity outside of the Americas (Spicer and Collinson, 2014). At this time the Gangdese mountains were rising and separated from the Qiangtang uplands by a wide low and arid valley (Kapp and DeCelles, 2019), while eastern Tibet, and Yunnan, were generally at low elevations and India was separated from Eurasia by an oceanic moat. The width of the moat remains poorly constrained.

3.1. India pre-collision

The extent to which India was biotically isolated during its passage northwards and across the Equator is a matter of considerable contention (e.g. Briggs, 2003; Chatterjee and Scotese, 1999; Chatterjee et al., 2013), but it is clear that some taxonomic interchange was possible during the late Cretaceous because Laurasian taxa were already in India (Jaeger et al., 1989; Prasad and Sahni, 1999; Sahni and Bajpai, 1991; Samant et al., 2013) admixed with those of a typical Gondwanan origin (Krause et al., 1997; Prasad and Sahni, 1999, 2009; Sahni and Prasad, 2008) and those that were exclusively Indian (Whatley and Bajpai, 2006). Biotic connection could only have increased as India drew closer to Eurasia and wind and ocean currents driven by monsoon circulation allowed increasing numbers of taxa to cross diminishing ocean barriers (Spicer et al., 2017).

Rapid movement across several climate zones would have imposed unique selection pressures on the Indian 'raft' biota leading to some extinctions, but also favouring novel adaptations to tolerate a wide range of fluctuating climates. Immediately prior to docking India already supported a number of taxa with affinities to Africa and Eurasia (Briggs, 2003; Chatterjee and Scotese, 1999, 2010; Chatterjee et al., 2013) tolerant of a range of climate stresses.

In the late Maastrichtian what is central India today was a lowland coastal zone with abundant mangrove palms (*Nipa*) represented by the pollen *Spinizonocolpites*, other mangrove taxa (e.g. *Sonneratia*) and the mangrove fern *Acrostichum intertrappeum* (Bande and Prakash, 1984; Chitaley, 1960; Chitaley and Nambudiri, 1995; Kathal et al., 2017; Prakash et al., 1990; Prasad et al., 2018; Shete and Kulkarni, 1982).

Away from the coast infratrappean sediments, deposited prior to the onset of Deccan volcanic activity, contain pollen indicating an association of gymnosperms (e.g *Araucariacites*,

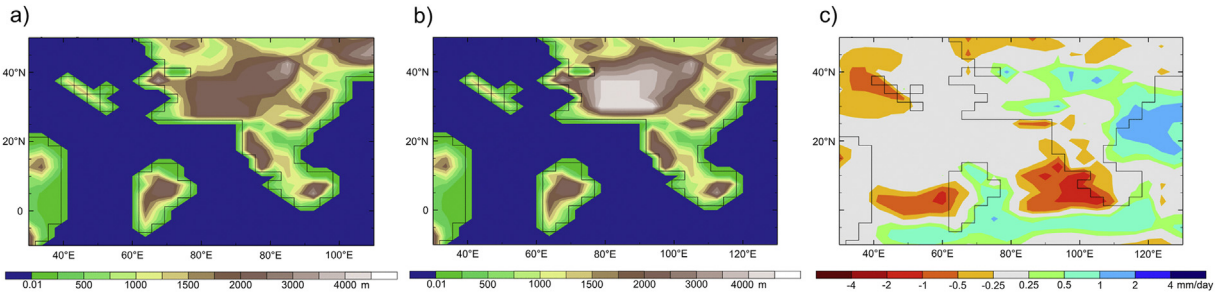

Fig. 5. Climate model experiment showing the difference in middle Eocene (Lutetian) precipitation between Tibet set as a plateau at 2500 m and when raised to 5000 m. a) plateau set at 2500 m, b) paleotopography with a plateau set at 5000 m, c) difference map showing excess moisture when the precipitation for plateau condition b is subtracted from condition a. The higher plateau (b) leads to more intense rainfall on the southern and northern flanks, but across the central part of both low (a) and high (b) plateaus there is no difference in rainfall showing the low plateau is just as dry as the high one.

Classopollis) and angiosperms (e.g. *Cretacaeiporites*, *Compositoipollenites*, *Palmaepollenites*), but in response to the onset of volcanic activity and more disturbed landscapes favouring opportunistic 'weed' taxa, floral turnover resulted in angiosperm-pteridophyte-dominated palynoassemblages in the intertrappeans, (Samant and Mohabey, 2014). Angiosperms seem to dominate (55%) over ferns and fern allies (~13%) (Prasad et al., 2018).

The presence of dipterocarp pollen (*Dipterocarpuspollenites cretacea*) in latest Cretaceous sediments points to a possible Gondwanan origin for this important group of trees that characterize humid tropical forests in southern Asia today (Prasad et al., 2018). The presence of humid tropical forests, presumably away from the most disturbed habitats, is also indicated by the presence of *Retiacolpites pigafettaensis*. This pollen grain can be present in large numbers and shows morphological similarity with that of the extant Arecaceous palm genus *Pigafetta*, which, like dipterocarps, is found in modern SE Asian rain forests.

Fossil woods and other megafossils in non-marine intertrappean beds provide a more site-specific record of vegetation in India than palynomorphs, which can be transported long distances from their parent plants (Rousseau et al., 2004, 2006, 2008). In a recent review Wheeler et al. (2017) noted the woods from Late Cretaceous-Paleocene non-marine Deccan beds were 'surprisingly modern' with a good representation of Malpighiales, Malvales and Sapindales, and provide the earliest fossil records for the families Anacardiaceae, Lamiaceae, Lecythidaceae, Malvaceae, Moraceae, Myrtaceae, Salicaceae, Simaroubaceae and Vitaceae.

3.2. Central Tibet

Because year-round rainfall was low across southern Eurasia, and particularly southern China, northern Thailand and Vietnam, the late Cretaceous arid climate there could not be described as being monsoonal despite its low latitude (Farnsworth et al., 2019; Hasegawa et al., 2012), although later in the Paleocene sedimentary and geochemical data suggests an intermittent transition to a wetter regime in some places (Yan et al., 2007).

3.2.1. Paleocene and Eocene

In the Paleocene the centre of the region currently forming the Tibetan Plateau was at a low (<1 km) elevation until ~55 Ma (Hetzel et al., 2011; Strobl et al., 2012), and somewhat further south (~25°N, Fig. 9 of Li et al., 2020c) of its current position. After the transition from marine to non-marine sedimentation, the late Cretaceous through to early Paleogene environment along the BNSZ was arid, hosting dune fields but with flashy discharge rivers draining from the rising Gangdese and Qiangtang uplands (Hetzel et al., 2011; Kapp and DeCelles, 2019; Laskowski et al., 2019; Strobl et al., 2012; Xu et al., 2015). The preservation potential for plant megafossils, especially leaves, in such dry and predominantly erosional conditions is very low, so we have to rely on surviving pollen and spore assemblages. Despite the aridity it is likely the margins of lowland rivers draining from the surrounding mountains were vegetated, much as are the rivers draining from today's Atlas Mountains (Morocco) into the western Sahara (Fig. 6). Upland regions, if they were high enough, would have supported a more diverse woody angiosperm flora admixed with conifers, the exact mix depending on elevation.

Numerous palynological studies were conducted before absolute age constraints became available, so the ages and attributions to formations given in the older literature have to be regarded with some caution. With that in mind, what appears to be an early Eocene assemblage in the Lunpola Basin (32.033°N, 89.767°E, 4655 m a.m.s.l.) yields an assemblage containing mostly angiosperm pollen representing wind pollinated seasonally deciduous temperate broadleaved taxa (Table 1, panel 1) and subordinate subtropical evergreen plants. The conifers are represented by easily wind-blown pollen such as that of *Pinus* and *Picea*, while other gymnosperms and ferns are rare (Table 1, panel 1) (Wang et al., 1975). This unlikely co-existence of temperate and sub-tropical taxa probably represents two distinct vegetation types living at different elevations on the nearby mountain slopes rather than a community in the valley bottom, which was likely to have been arid to semi-arid based on the surviving lithology.

In the lower part of the Niubao Formation (most likely early Eocene) the palynoassemblage is reportedly dominated by coniferous elements such as of *Taxodium* (which may indicate swampy conditions), together with other conifers (Table 1, panel 2). *Ginkgo* pollen is also moderately abundant. Comprising just over a third of the total pollen diversity are grains representing both temperate angiosperms and some subtropical forms (Table 1, panel 2). Pteridophytes are very rare (Wang et al., 1975). Further up section, but still supposedly within the Niubao Formation and perhaps representing the middle Eocene, the abundance of subtropical taxa, including palms, increases (Table 1, panel 3) (Wang et al., 1975). This increase in thermophilic taxa may represent evidence of warming, but given that from 50 Ma onwards the Eocene is characterized by a general global cooling trend (Zachos et al., 2001) it is more likely to reflect an increase in humidity that allowed areas in the valley lowlands to transition from an arid, sparsely vegetated, landscape to one supporting more extensive forests surrounding the depositional sites.

The problem with palynological assemblages is that pollen and spores can be transported and reworked leading to a degradation in spatial and temporal precision when trying to reconstruct past

Fig. 6. Modern scene in the western margin of the Sahara Desert, Morocco, looking west towards the Atlas Mountains. Similar xerophytic 'ribbon vegetation' along river courses is likely to have existed in the arid Paleocene BNSZ lowlands of Tibet.

Table 1
Pollen record from Central Tibet (Lunpola Basin) as reported by Wang et al. (1975). Panels 1–6 summarize key identified taxa at different points in time with the numerically most abundant palynomorphs shown in bold. In the Eocene pollen records there is a notable mix of cool temperate and warm temperate taxa, representing vegetation at different elevations. The presence of thermophilic taxa such as cycads, palms and subtropical evergreen taxa support the concept of warm lowland vegetation. These taxa disappear at the end of the Eocene to be replaced by temperate taxa such as *Quercus* and a rise in herbs as the climate cools and dries as a high plateau forms.

Age	Pollen Composition
1) ? Early Eocene	***Ulmus, Zelkova, Celtis, Trema, Quercus, Salix, Betula*** (deciduous temperate broadleaved) *Myrica*, *Engelhardia*, *Magnolia*, *Liquidambar*, *Anacardium*, *Platanus*, *Ilex*, *Liriodendron*, *Camellia*, *Araliaceae*, *Nymphaceae*, *Rutaceae*, *Myrtaceae*, *Euphorbiaceae* (subtropical evergreen, broadleaved angiosperms). *Pinus*, *Picea*, *Cedrus*, *Dacrydium, Podocarpus*, and *Taxodium* (conifers) *Cycas, Ginkgo* (gymnosperms). Pteridophyte spores (mostly Polypodiaceae, Cyatheaceae, Osmundaceae, Lycopodiaceae, and *Selaginella*).
2) Early Eocene (Lower Niubao Fm.	***Taxodium*, Taxodiaceae** (now included in the Cupressaceae)**, Taxaceae,** Cupressaceae, *Pinus*, and *Podocarpus* (conifers). *Ulmus, Quercus, Pterocarya, Juglans, Ilex* (temperate broadleaved angiosperms). Proteaceae, Lauraceae, Myrtaceae (subtropical evergreen broadleaved angiosperms). Rare Pteridophytes including *Onychium, Pteridium, Salvinia.*
3) ? Middle Eocene, Niubao Fm.	***Rhus, Nyssa, Magnolia, Salix, Corylus, Carya,*** *Liquidambar, and Myrica* (subtropical broadleaved angiosperms). Palmae (palms, monocots.
4) Late Oligocene, lower Dingqing Fm.	**Quercus**, *Rhus*, *Alnus*, *Betula*, *Ulmus*, *Castanea* and *Celtis* (mostly deciduous broadleaved angiosperms). ***Pinus***, *Picea*, *Abies*, *Cedrus*, *Tsuga*, and Taxodiaceae (conifers). Chenopodiaceae, Compositae, Plantaginaceae, Liliaceae and Graminae (herbaceous).
5) Early Miocene, Dingqing Fm.	***Quercus,*** *Salix*, *Juglans*, *Fagus*, *Alnus*, *Corylus*, *Betula*, *Celtis*, *Castanea*, and *Carpinus* (mostly deciduous broadleaved angiosperms). *Pinus*, *Picea*, *Abies*, and representatives of the Taxodiaceae (conifers). Chenopodiaceae, Compositae, Leguminosae, Cruciferae, Sparganiaceae, Potamogetonaceae, and Gramineae (herbaceous).
6) Middle Miocene Dingqing Fm.	***Quercus, Salix,*** *Rhus*, *Juglans*, *Betula*, *Celtis*, *Magnolia*, *Acer*, *Corylus*, *Carya* and *Liquidambar* (mixed broadleaved evergreen and deciduous angiosperms). *Pinus* (conifer). Chenopodiaceae, Plantaginaceae, Liliaceae, Gramineae and Compositae (herbaceous).

vegetation. This explains the ecologically unlikely juxtaposition of cool temperate, warm temperate and subtropical taxa seen in these assemblages. Without detailed depositional facies context it is difficult to interpret such assemblages in terms of vegetational communities and altitudinal zonation, but because the Niubao Formation reflects mostly sediments deposited by rivers draining from the nearby mountains we can assume a mix of high and low elevation palynomorphs are present in the assemblages. The same phenomenon will arise by wind transport. Now that it is clear that Tibet was not a plateau in the Paleogene, but exhibited considerable topographic relief, it becomes easier to understand these strange taxon combinations.

Other than palynological assemblages, paleontological evidence for Paleocene and early Eocene biodiversity in central Tibet is lacking, but based on recent megafossil discoveries from the Lunpola, Nima, and Bange basins (Fig. 3) by the middle Eocene the region hosted low elevation sub-tropical humid vegetation (Del Rio et al., 2020; Liu et al., 2019; Tang et al., 2019). Late in the Paleocene fluvial influences in the valley waned and by the Oligocene extensive and persistent lakes formed, some of which were saline and others freshwater (Ma et al., 2017). At around 47 Ma the BNSZ lowland supported a diverse flora and to date 69 fossil morphotypes of different kinds have been found in the middle Niubao Formation consisting of leaves (41 morphotypes), fruits, seeds (34 morphotypes), flowers, branches and tubers (Del Rio et al., 2020; Jia et al., 2019; Liu et al., 2019). Systematic analysis is ongoing, but many of the remains represent taxa that no longer exist in Tibet.

3.2.2. Oligocene

The flora near the base of the Dingqing Formation (Wu et al., 2017) was preserved in deep water sedimentary facies some distance from the shoreline. It is likely, therefore, to offer only a biased sample of the source vegetation (Spicer, 1981, 1991), and thus is unsuitable for a reliable CLAMP analysis. Nevertheless, the assemblage contains the palm *S. tibetensis* (Su et al., 2019), *Cedrelospermum tibeticum* (Jia et al., 2019), leaves of the 'golden rain tree' *Koelreuteria lunpolaensis* and *K. miointegrifolia* (Jiang et al., 2019), a *Pistacia* leaflet, a leaf of Araliaceae, a palmately compound leaf of *Handeliodendron* sp., with six leaflets, leaves of the water plant *Limnobiophyllum pedunculatum* (Low et al., 2019), leaves of *Exbucklandia* sp., Magnoliales, *Salix* sp., several unidentified toothed and untoothed woody dicot leaves, and the lake margin monocot *Typha* (Wu et al., 2017). Examples of the material are shown in Fig. 7.

These megafossils are accompanied by conifer pollen, with *Pinus* being the most abundant. Angiosperm pollen is dominated by *Quercus*, which is similar to *Pinus* in abundance, together with other warm temperate taxa (Table 1, panel 4) (Wang et al., 1975). It is at this point in time that herbs start to increase in abundance in central Tibet as represented by Chenopodiaceae, Compositae, Plantaginaceae, and Liliaceae (Wang et al., 1975). Of particular significance is the rise of Gramineae (grasses) which, alongside the herbs and the presence of saline lakes (Ma et al., 2017), suggests a more arid and open landscape than earlier in the Eocene. Ferns are few and overall the palynological assemblage is similar to those of the Hongxiakou and Youshashan Formations in the Qaidam Basin.

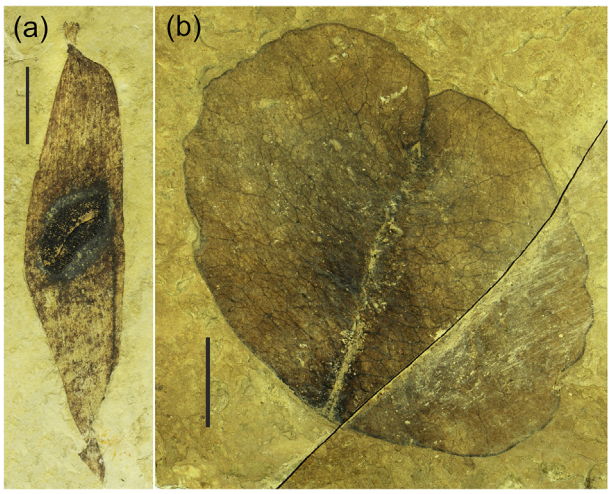

Fig. 7. Specimens from the Dingqing Formation, Lunpola Basin. a) *Ailanthus maximus*, b) *Koelreuteria lunpolensis*. Scale bars = 1 cm.

The mixed coniferous and deciduous broad-leaved composition dominated by pines and oaks was originally thought to reflect a warm temperate moist climate (Wang et al., 1975), but again it likely represents a mix of taxa from different elevations dominated by wind pollinated taxa from cooler upland sites. This lower Dingqing flora, in respect of both the palynological and megafossil records, appears adapted to a slightly drier and possibly a cooler climate than in the middle Eocene, likely reflecting the global cooling trend and a slightly higher elevation, but one that was still low compared to today (Su et al., 2019). Located at the base of the Dingqing Formation the flora must be older than 23.6 Ma derived from U–Pb ages of zircons in a tephra (He et al., 2012; Mao et al., 2019) ~100 m stratigraphically above it. At present it is assumed to be ~25 Ma, but more precise dating is required.

3.2.3. Miocene

The Miocene palynoflora of the Dingqing Formation is dominated by angiosperm pollen with numerous temperate tree genera being represented and *Quercus* reaching almost a third of the total count in some samples, but also a wide range of herbaceous taxa (Table 1, panel 5) (Wang et al., 1975). Gymnosperm pollen makes up 34–48% of the total. With a further small component of ferns, if taken as a whole this assemblage represents a mixed deciduous warm moist temperate broad-leaved and coniferous forest (Wang et al., 1975), but again there is likely to be some mixing of taxa from different elevations.

Higher in the Dingqing Formation angiosperm pollen becomes even more dominant, reaching 88–91% of the total diversity. *Quercus* pollen, along with that of *Salix* predominate, while *Pinus* is less abundant than before and herbs now make up around a third of all angiosperm pollen (Table 1, panel 6). Wang et al. (1975) interpreted this to reflect a warm temperate moist deciduous broad-leaved forest.

Regrettably, when these comprehensive palynological investigation were undertaken, absolute (radiometric) dating was not available. Subsequent work in the Dingqing Formation has provided some better age control (He et al., 2012; Mao et al., 2019), but more work needs to be done to construct a detailed time-line for vegetation and topographic evolution as central Tibet transitioned into a plateau. If the base of the Dingqing Formation dates from ~25 Ma then the floor of the central Tibetan valley was no higher than 2.3 km at that time and experienced a sub-humid sub-tropical to warm temperate climate (Su et al., 2019). As the Miocene began, moderate compression-driven uplift and sediment infill would have raised the valley floor and, coupled with some northward movement to approach the present latitude of ~29°N, the climate seems to have cooled to become warm temperate, but maintained enough moisture to support an angiosperm-dominated woodland landscape. In the upper part of the Dingqing Formation (~15 Ma and younger), the palynoloflora suggests a reduction of conifer pollen input (Table 1, panel 6). This may in part be due to the MMCO warming, but equally it could reflect drying because the input of herb pollen increases, perhaps indicating a more open landscape. Note, however, that although the plateau was beginning to form and the Himalaya were starting to exceed the height of the Gangdese, both phenomena that would induce drying, the monsoon was also intensifying at this point. This would have increased moisture supply to the incipient plateau and partly offset the elevation-related drying. The continued rise of Himalaya above 5 km could also have progressively partially blocked wind-blown pollen, including that of conifers, from the windward slopes of the Himalaya.

3.3. The Hengduan Mountains - an engine of biodiversity

Today the Hengduan Mountains host an exceptionally diverse flora with over 3030 species of alpine seed plants alone (Li et al., 2014) and overall hosts more taxa that either the Himalaya or the Tibetan Plateau (Yu et al., 2020), so for conservation purposes it is important to understand the environmental evolution of the area. Parts of Eastern Tibet and the Hengduan Mountains, north and central Yunnan, rose to near their present elevations throughout the Eocene and early Oligocene (see section 2.2) and thus, together with the Gangdese and Qiangtang uplands, formed the first expansive region of elevated land surface in the Cenozoic history of the Tibetan Region. Extending north to southern Qinghai this elevated landscape also encompassed a wider band of latitudes and a greater climatic range than the E–W trending Gangdese uplands and Himalaya, and as the EAM and SAM systems developed the Hengduan Mountains and Yunnan is where they interacted and where they still form a so-called 'Transitional Area' today (Wang and Ho, 2002). The essentially Eocene-Oligocene rise of much of eastern Tibet also sealed off what had been lowland central Tibet earlier in the Paleogene from contemporary biotas across southern China. Even today the so called 'Tanaka Line', roughly aligned with the Red River - Ailao Shan fault system, separates the floras of the Tibetan Region to the west from that of the Sino-Japanese flora to the east (Tanaka, 1954; Wu et al., 2006).

Apart from forming a significant orographic barrier, the rise also created an altitude- and aspect-related landscape heterogeneity that greatly enhanced environmental niche diversity. Subsequent dissection by erosion, as drainages of the Salween, Mekong (Lancang), Yangtze and Red rivers incised into the elevated landscape (Clark et al., 2004; Nie et al., 2018), further granulated the environmental mosaic and enhanced close-proximity niche complexity.

Relief-related niche heterogeneity is crucial for creating biodiversity (Spicer, 2017) (Fig. 2) because over millennial timescales quasi-cyclical orbital forcing both separates and brings into juxtaposition different gene pools (Spicer, 2017; Rahbeck et al., 2019a). Reproductive isolation allows populations to develop genetic divergence through mutation and genetic drift, while population juxtaposition allows for novel genomes to arise through hybridization. Separation mostly occurs as populations move upslope in times of warming into 'sky islands', while cooling drives populations downslope again to mingle in the lowlands. So, if this model of a biodiversity 'pump' (Spicer, 2017) is correct we should see rapid increases in diversity occurring due to hybridization during cool climate phases, while more gradual genetic shifts take place during the isolation phases in times of warmth.

For the Tibetan Region climate varies seasonally as well as over longer timescales (Section 1.2). During all of the Cenozoic the region was subject to strong seasonal climate variation as a function of monsoon circulation, but monsoon characteristics changed as topography evolved and secular climate fluctuated. While this seasonal variation in climate does not drive genetic modifications in the same way as longer-term climate change, it does select for characters that allow the organism (particularly plants) to tolerate a range of climate-induced stresses (e.g. drought tolerance in the dry season and water saturation in the wet season), and that pre-adapts them to tolerate different environmental constraints that may arise over millennial timescales. At present, proxy evidence is too sparse for detailed monsoon characterisation at temporal and spatial fine-scale resolution, but what there is supports patterns derived from paleoclimate modelling (Farnsworth et al., 2019), through which some detail can be inferred.

Modelling indicates that Cenozoic EAM intensity was weak in the Paleogene, but rose throughout the Eocene to Miocene peaking in a 'supermonsoon' in the Zanclean (early Pliocene, Fig. 4) before weakening slightly to the present (Farnsworth et al., 2019). There was, of course considerable spatial heterogeneity in the pattern and, for example, the Pliocene leaf physiognomy in north-eastern India suggests even the dry season there was wet, so reducing seasonal variation in rainfall and the monsoon index in this region (Hazra et al., 2020), while after the middle Miocene drier winters led to the extirpation of *Metasequoia* from Yunnan (Wang et al., 2019). This kind of work needs to be replicated across the monsoon-impact regions and compared with climate modelling to fully understand spatial and temporal variability in monsoon dynamics.

3.3.1. *The evolution of the Hengduan Mountains and its exceptional biodiversity*

In the Paleocene and Eocene global climate was characterized by a series hyperthermal events superimposed upon an already exceptionally warm climate, which wrought changes to the hydrological system and atmospheric composition (Anagnostou et al., 2016; Carmichael et al., 2017; Foster et al., 2018; Inglis et al., 2019; Zachos et al., 2010). The impact of such extremes early in the Paleogene in the central Tibetan lowland and across to Yunnan is difficult to determine because of a dearth of fossil evidence, but widely distributed 'red bed' sediments suggest an extremely arid climate in which only specialist xeromorphic plants and palms would have survived, and then most likely only near river courses (e.g. Fig. 6). A small window into these conditions is offered by *Sabalites* palm remains discovered in the Gonjo Basin (30.833°N, 96.416°E, 3686 m a.m.s.l.) (BGMRX, 1993), as well as the pollen flora. The Paleocene/earliest Eocene Gonjo Formation palynological assemblage is dominated by representatives of woody taxa, which comprise 75–85% of total pollen diversity (Table 2, panel 1). They include a range of both porate and colpate angiosperm pollen while gymnosperm pollen are represented mostly by *Ephedripites* (considered to represent a drought-adapted plant similar to *Ephedra*), with the notable absence of Pinaceae and Podocarpaceae. The ferns comprise just 5–10% of the total. As with all pollen floras this assemblage is derived from plants growing at different distances and elevations from the depositional site, but it clearly includes a significant proportion of plants growing in a low elevation subtropical semi-arid climate (Song and Li, 1982).

There is convincing evidence that the Gonjo Basin underwent a rapid increase in elevation from ~700 m a.m.s.l. at ~54–50 Ma to 3800 m by ~44–40 Ma (Xiong et al., 2020). This rise of more than 3 km in ~10 million years was determined using radiometrically-dated clumped isotope data validated using isotope-enabled climate modelling. As local uplift took place surface conditions would have cooled and become more humid, so favouring more diverse vegetation. At ~3000 m, at the end of the Eocene, the vegetation in the Markam Basin (~100 km to the southeast of the Gonjo Formation) (Fig. 3) as represented by 36 woody dicot megafossil taxa, consisted of abundant evergreen round cupule oaks (*Quercus* subg. *Cyclobalanopsis*) with members of the Betulaceae (*Alnus* and *Betula*) (Table 2 panel 2) (Xu et al., 2016). Conifers are represented by *Pinus*, *Chamaecyparis*, *Tsuga* and *Abies* (Su et al., 2018). It is likely that such vegetation existed at many similar elevations throughout the Hengduan Mountains at that time and suggests that forests extended to the highest elevations for which we have direct evidence.

3.3.2. *Oligocene*

A major cooling event across the E–O transition is recorded in deep sea sediments (Zachos et al., 2001), but this drop in temperature was not experienced uniformly across continental latitudes and altitudes (Pound and Salzmann, 2017). The effect at low

Table 2
Examples of megafloral and microfloral fossil records for the Hengduan Mountains and parts of Yunnan. Each panel summarizes identified taxa from different depositional basins, with those in bold being the numerically most abundant specimens.

Age and References	Composition
1) Early Eocene, Gonjo Basin (Song and Li, 1982)	Microflora: porate *Triporopollenites*, *Subtriporopollenites*, *Caryaopollenites*, *Plicapollis*, *Ulmipollenites*, *Oculopollis* and *Tetrapollis*, while colpate forms are *Euphorbiacites*, *Tricolpopollenites*, *Retitricolpites*, *Quercoidites*, *Cupuliferoipollenites*, *Cyrillaceaepollenites*, *Rutaceoipollis*, *Meliaceoidites*, *Fraxinoipollenites*, *Nyssapollenites*, *Talisiipites*, *Faguspollenites*, *Tricolpites* (broadleaved angiosperms). *Ephedripites*, *Taxodiaceaepollenites*, and *Inaperturopollenites* (Gymnosperms). Megaflora: *Sabalites* (palm).
2) Latest Eocene (35–34 Ma), Markam Basin (Su et al., 2018; Zhou et al., 2020). Assemblage MK3	Megaflora: ***Quercus* subg. *Cyclobalanopsis***, *Alnus, Berhamniphyllum* and *Betula* (evergreen and deciduous broadleaved angiosperms). *Pinus, Chamaecyparis, Tsuga* and *Abies* (conifers).
3) Earliest Oligocene (33 Ma), Markam Basin (Su et al., 2018). Assemblage MK1	Megaflora: ***?Salix,*** *Rosa,* deciduous oaks and *Alnus* (deciduous broadleaved angiosperms). *Picea* (conifer).
4) Early Oligocene (33 Ma), Markam Basin (Su et al., 2018). Assemblage MK2	Megaflora: *Alnus*, *Betula*, alpine oak (*Quercus* section *Heterobalanus*) and *Rhododendron* (sclerophyllous deciduous and evergreen broadleaved angiosperms).
5) Early Oligocene (32 Ma) Lühe Basin, Yunnan, (Yi et al., 2003; Linnemann et al., 2018).	Megaflora: *Ailanthus, Dipteronia, Acer, Populus, Fraxinus, Machilus, Palaeocarya, Quercus, Cyclobalanopsis, Castanopsis, Ostrya, Alnus, Carpinus, Betula, Mahonia,* and *Ilex,* (mixed evergreen and deciduous broadleaved angiosperms). *Equisetum* (sphenophyte). *Sequoia, Metasequoia, Cryptomeria*, cf. *Cunninghamia, Calocedrus, Picea, Tsuga* and *Pinus* (conifers).
6) Late Miocene (10–12.7 Ma) Xioalongtan Flora, Yunnan (Tao, 2000; Huang et al., 2016)	Megaflora: *Sophora, Albizzia, Cassia, Dalbergia, Dodonaea, Ficus, Indigofera, Jasminum, Passiflora, Smilax, Cinnamomum, Litsea, Ormosia, Pithecellobium, Alangium, Erythrophleum, Desmos, Rhamnella,* ***Cyclobalanopsis****, Distylium, Exbucklandia, Machilus, Nothaphoebe, Phoebe, Acer, Castanea, Juglans, Myrica,* ***Quercus****, Salix, Berchemia, Castanopsis, Desmodium, Gleditsia, Lespedeza, Magnolia,* ***Lithocarpus****, Robinia, Pterocarya, and Laurus* (mostly evergreen broadleaved angiosperms). *Typha* (monocot)
7) Late Pliocene (3.6–2.6 Ma) Longmen Flora (Huang et al., 2016; Su et al., 2013; Tao, 1988)	Megaflora: ***Quercus*** sect. ***Heterobalanus,*** *Acer*, *Cupressus*, *Pinus*, *Populus*, *Rhododendron*, *Salix, and Lithocarpus* (sclerophyllous woodlands, mixed deciduous and evergreen broadleaved angiosperms). *Trapa*
8) Late Pliocene (3.6–2.6 Ma) Tuantian Flora (Huang et al., 2016)	Megaflora: *Dioscorea*, *Ilex, Cinnamomum*, *Ormosia Mallotus*, *Syzygium, Evodia, Garcinia, Cyclea*, *Cyclobalanopsis*, *Exbucklandia*, *Heterosmilax*, *Machilus*, *Rhodoleia, Betula*, *Carpinus*, *Castanea*, *Cornus*, *Fraxinus*, *Juglans*, *Myrica*, *Ulmus, Berchemia*, *Castanopsis*, *Lindera*, *Mahonia*, and *Robinia* (mostly evergreen broadleaved angiosperms).

latitudes in the Tibetan Region seems to have been muted even at high elevations. In the Markam Basin (paleolatitude ~29°N at 34 Ma) (Fig. 3), which preserves this transition, the mean annual temperature reduction at ~3000 m was only ~1.5 °C as revealed by leaf physiognomy (Su et al., 2018). Coupled with changes in the moisture regime, this small cooling did, however, mark a transition from warm temperate evergreen vegetation to one that was less taxonomically diverse, more deciduous, and best characterized as cool temperate deciduous (Su et al., 2018). In total it consists of 24 woody dicot species, with conifers only represented by *Picea* (Table 2, panel 3). Examples of such specimens are shown in Fig. 8. Slightly higher in the section another small flora (MK2) records a return of some evergreen taxa (Table 2, panel 4) consistent with some warming later within the Oligocene.

Unlike the precipitous other edges of the Tibetan Plateau eastern Tibet, including the modern Hengduan Mountains, ramps down gradually into central and southern Yunnan (Fig. 3). This otherwise low relief surface is deeply dissected by numerous rivers that after leaving the plateau turn more or less southwards, resulting in generally N–S oriented mountain ridges and valleys. In the late Paleogene and early Miocene, before extensive river incision, this ramp may have provided an extended altitudinal and latitudinal migration route in times of changing regional temperatures, so it is worthwhile considering, briefly, some of the Yunnan paleofloras.

3.3.3. *Yunnan at lower elevations*

Yunnan today is well known for being biotically highly diverse (e.g. Wu, 1988; López-Pujol et al., 2011) and hosts approximately 244 families of higher plants within which there are 2300 genera with 16,000 species, nearly half of which are endemic to the province (Huang et al., 2016; Wu, 1979; Wu and Zhu, 1987). Only a tiny fraction of plants alive at any one time end up being preserved in the fossil record, but within Yunnan there are some exceptionally diverse fossil floras (Huang et al., 2016), especially those in lower elevation basins. One such flora is from the radiometrically dated ~32 Ma Lühe Basin (25.141627°N, 101.373840°E, 1890 m a.m.s.l.) (Linnemann et al., 2018), (Fig. 3). Reliable quantitative phytopaleoaltimetry is not yet available due to the lack of a suitable contemporaneous sea level flora, but it is likely to have been close to its present elevation by the time the flora was deposited (Hoke, 2018). The assemblage is remarkably modern in aspect consisting of rhizomes, leaves, fruits and seeds representing taxa (Table 2, panel 5) that today are typically found in temperate, humid climates (Linnemann et al., 2018). Examples are shown in Fig. 9. This cool temperate flora grew around a complex of lakes, marshes and rivers, with some preserved river channels being extremely large (Wissink et al., 2016) and containing numerous accumulations of large logs variously oriented and in contact (Fig. 10a). Many such logs are permineralized by carbonates and display well developed tree rings (Fig. 10b) indicative of a strongly seasonal climate. The rings are uniform in thickness but quite narrow (~1 mm) suggesting growth conditions were in some way restricted by cool temperatures or seasonal water supply. Two wood taxa have been reported, and they show strong similarities to modern *Cryptomeria* and *Cunninghamia* (Yi et al., 2003). *In situ* tree stumps occur in several coals exposed in the Lühe mine.

Although several key floras in Yunnan have been re-dated from Miocene to early Oligocene and so are around 20 million years older than previously thought, some depositional basins do seem to contain Miocene and younger fossil floras. The late Miocene hominid-bearing Baoshan Basin (Fig. 3) yields woods of *Quercoxylon* sp., and *Pterocarya* sp. interpreted to represent a sub-tropical evergreen broadleaved forest (Cheng et al., 2014). Late Pliocene sediments in the basin have yielded leaves of *Quercus yangyiensis* (He et al., 2014), which has some architectural similarities to *Quercus*. sect *Heterobalanus* and has a similar thick coriaceous cuticle that allows it to inhabit high seasonally desiccating environments. More paleoaltimetry work needs to be done in the area.

The late Miocene Xiaolongtan paleoflora (Tao, 2000) is dated as 12.7–10 Ma, Serravallian-Tortonian (Li et al., 2015c; Zhang et al., 2019), and occurs in the Xiaolongtan coalmine (23.5°N, 103.2°E, 1030–1111 m a.m.s.l.), Kaiyuan County, Yunnan Province, southwest China. While the Xiaolongtan Basin is outside the Hengduan Mountains the fossil record it contains it is useful to compare with those that were at a higher elevation. The flora comprises 55 species belonging to 45 genera and 21 families. The late Miocene Xiaolongtan paleoflora (Table 2, panel 6) represents a subtropical broad-leaved evergreen and deciduous forest estimated, using the CLAMP proxy, to have grown at a paleoelevation of 530 ± 900 m (Jacques et al., 2014). Recent dating of early hominid-bearing sediments using paleomagnetostratigraphy shows parts of the Xiaolongtan Basin filled between ~8 and ~3 Ma (Li et al., 2020a).

The late Miocene to the late Pliocene saw distinct changes in the floristic composition of Yunnan (Huang et al., 2016). This was particularly marked at higher elevations and previously mountain building was in part invoked to explain this change (Huang et al., 2016). However, as we have seen much of the regional relief was already established in the late Paleogene and it now seems that progressive global cooling after the mid Miocene is likely to have been primary driver. This cooling, although not expressed as strongly as at higher latitudes, would have lowered the tree line, opened up opportunities for the alpine biome to develop, and compressed altitude-related vegetation zones. This in turn would have increased diversity.

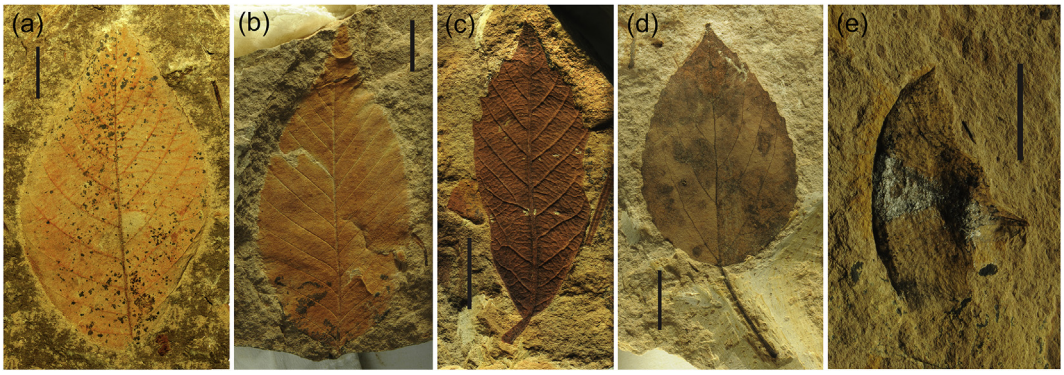

Fig. 8. Representative plant fossil specimens from the latest Eocene of Markam Basin. a) leaf of *Alnus* sp., b) leaf of Betulaceaea, c) leaf of *Cyclobalanopsis tibetensis*, d) leaf of *Populus* sp., e) *Abies* cone scale. Scale bars = 1 cm.

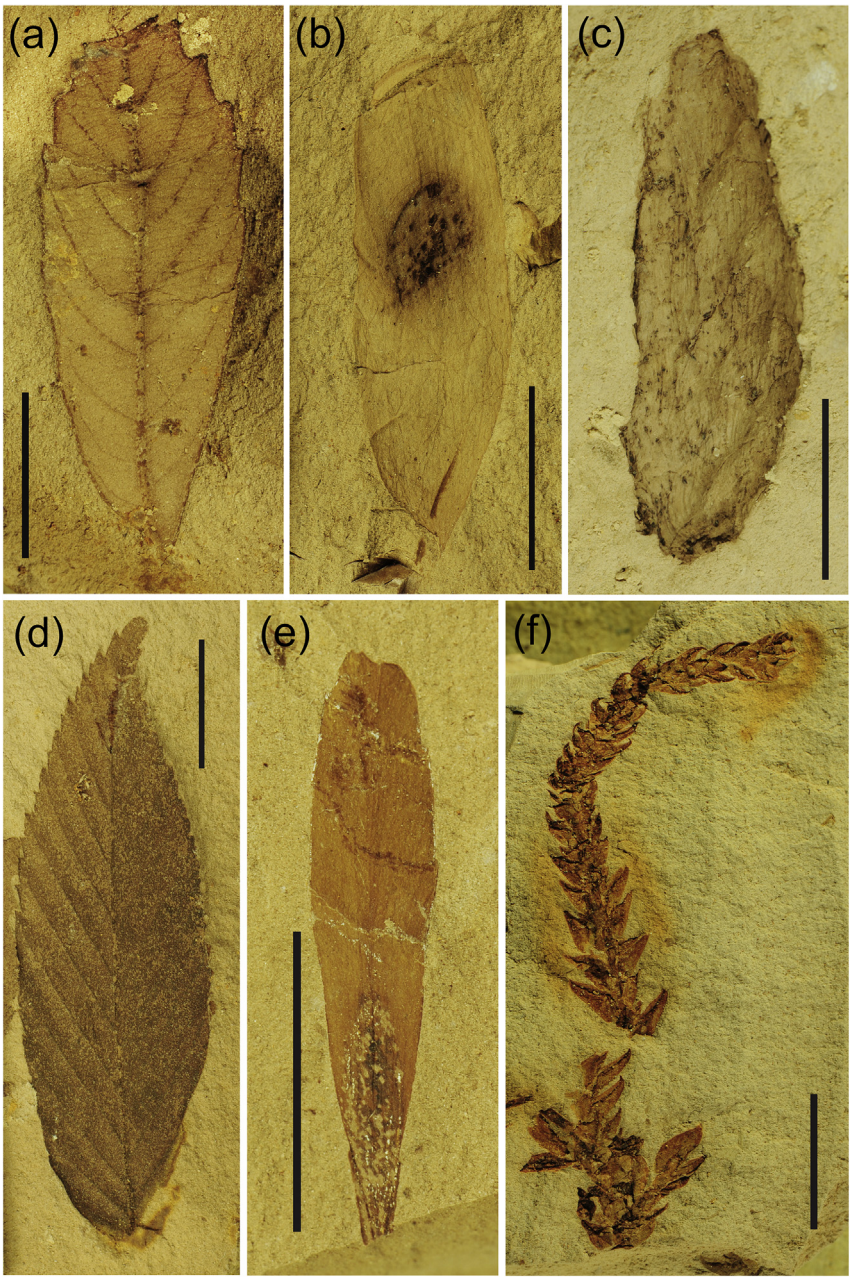

Fig. 9. Examples of plant fossils from the 32 Ma Lühe Basin, Yunnan. a) leaf of *Cyclobalanopsis* sp., b) *Ailanthus* sp. seed, c) *Tsuga asiatica* female cone, d) *Carpinus* sp. leaf, e) fruit of Fraxinus sp., f) *Cryptomeria yunnanensis* leafy shoot. Scale bars = 1 cm.

Based on current dating there are several late Pliocene floras known from Yunnan. Among these the Longmen Flora (Fig. 3) (Table 2, panel 7) represents vegetation in the southern Hengduan Mountains, and is characterized by the dominance of mountain oaks (*Quercus*, sect. *Heterobalanus*) indicative of the kind of sclerophyllous evergreen broad-leaved woodlands that are found throughout north-western Yunnan today (Writing Group of Yunnan Vegetation, 1987). Note, however, that such forests seem to have been established in the Hengduan Mountains as long ago as the Oligocene as evidence by the MK2 assemblage of the Markam Basin (Su et al., 2018) (Table 2, panel 4).

By contrast the lower elevation Tuantian flora (Fig. 3) (Table 2, panel 8) represents a subtropical evergreen broad-leaved forest. In general, there has been a southward and downslope migration of thermophilic forests in Yunnan since the late Miocene (Jacques et al., 2014), largely as a result of climate cooling rather than regional uplift.

3.4. Biodiversity in the Himalaya and Gangdese uplands

In section 3.1 we considered the late Cretaceous - early Paleocene floras on the Indian plate and we assume that at that time similar vegetation would have also occupied the region that today hosts the Himalaya. The earliest known well-dated assemblages representing the early growth of the Himalaya are early Eocene.

3.4.1. Eocene

Despite recent uplift, the Himalaya today host exceptional biodiversity, displaying a rich mosaic of altitudinal zones, aspect and underlying geology. Although the Middle Miocene Climatic

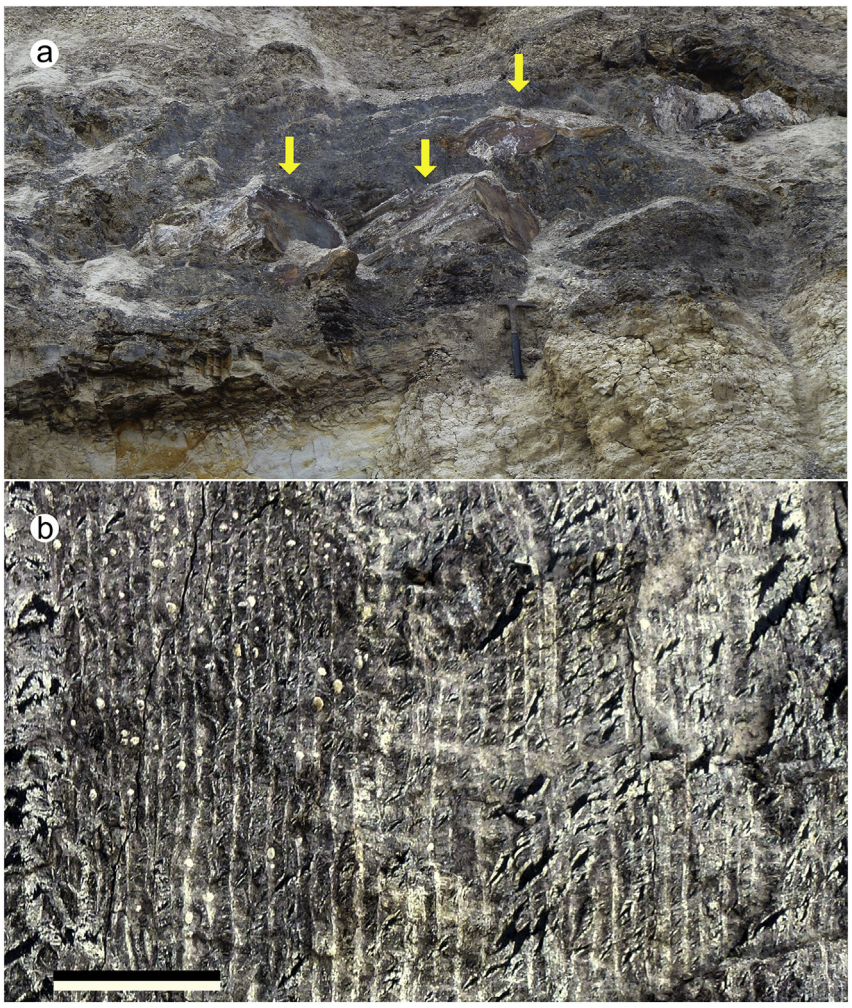

Fig. 10. Woods fossils from the Lühe Basin, Yunnan. a) a log 'jam' in a mudstone lens within a fluvial sandstone in the Lühe mine section. Individual trunks are preserved variously orientated and often in contact with each other. b) rings seen in a carbonate permineralized tree trunk, approximately 0.5 m in diameter, broken transversely. Ring width are uniformly ~1 mm wide suggesting a stable but seasonal climate with moderately restricted growing conditions. Scale bar represents 1 cm.

Optimum (MMCO) saw an influx of taxa from SE Asia to India (Klaus et al., 2016), possibly along a northern expanded megathermal forest belt in the Himalayan foothills (Jacques et al., 2015; Morley, 2000, 2018), the origins of this richness at low elevations clearly can be traced back to early in the uplift process as exemplified by the (~56 Ma, Ypresian) Liuqu flora (Fang et al., 2005) (Fig. 2), and those on India before collision and shortly thereafter (Section 3.1). The youngest age of the Liuqu flora is constrained by U–Pb dating of an overlying tuffite to be ~56 Ma (basal Eocene) (Ding et al., 2017b). In places the Liuqu Fm. is cut through by Miocene dykes, so making unlikely a Miocene age for the Liuqu as is sometimes accepted (e.g. Leary et al., 2016, 2017; Quade et al., 2020).

The Liuqu Formation flora, located today at 29.1° N, 87.65° E; altitude 3986 m, preserves the fern taxon *Cyclosorus*, the gymnosperm *Ginkgoites*, and a wide variety of predominantly evergreen tropical angiosperms (Table 3, panel 1) (Fang et al., 2005; Tao, 1988). A notable feature of this flora is the abundance of palm remains and it represents a humid (mean annual precipitation >2 m) tropical monsoonal forest at a paleoelevation of ~1 km (Ding et al., 2017b; Spicer et al., 2017).

Other supposedly Eocene assemblages come from the Xigatse District Prefecture, Tibet, (29.4° N, 88° E; 3192 m a.m.s.l.). The Donggar village flora (29.3 °N, 89.05 °E, 3836 m a.m.s.l.) and the Gyisong village flora in Ngamring (29.3° N, 89.3° E; altitude 4747 m) have yielded a less diverse woody dicot flora consisting of mixed evergreen and deciduous thermophilic taxa and emergent aquatic monocots (Table 3, panel 2) (Geng and Tao, 1982b) from the lower part of the Qiuwu Formation. A middle Eocene is assigned based on regional stratigraphy and the flora (Guo, 1981), but the ages of these assemblages need to be better constrained, and it may be that they should not be aggregated.

3.4.2. Oligocene

Further west the U–Pb and magnetostratigraphically dated 23.3 Ma late Oligocene flora from the Kailas Basin (31.174° N, 81.313° E, 5300 m a.m.s.l.) (Fig. 3) represents low diversity cool temperate humid vegetation (Table 3 panel 3) (Ai et al., 2019). Compositionally this seems to suggest a moderately high paleoelevation, but the flora is not diverse enough to conduct a CLAMP analysis, and the estimate provided by Ai et al. (2019) of 1500–2900 m may be too low because elevation was inferred from modern altitudinal zonation and no correction was made for secular climate change (the modern day is cooler than the late Oligocene).

Table 3
Megafloras and microfloras from the Gangdese highlands and the Himalaya. From a geological perspective the Gangdese and Himalaya are separate entities, but both formed highlands along the southern margin of Tibet and the Gangdese vegetation likely seeded that of the Himalaya as it rose to match the Gangdese in elevation in the Miocene. For that reason, they are treated together in this table. Panels 1–11 focus on selected paleofloras that chart the vegetation of the Gangdese highland and the high Himalaya, while panels 12–18 illustrate the composition of paleofloras in the more recently uplifted Siwalik succession along the southern flank of the Himalaya. At the time of deposition these Siwalik floras were at sea level but now are found at elevations up to 500 m a.m.s.l..

Age and Reference	Composition
1) earliest Eocene (~56 Ma), Liuqu Formation (Fang et al., 2005; Tao, 1988)	Megaflora: *Annona presanguinea, Caesalpinites* sp., *Cissites* sp., *Cornophyllum* cf. *swidiformis, Corylites megaphylla, Daphnogene polymorpha, Eucalyptophyllum obolongifolia, E. geinitzii, E.* sp.A, *E.* sp. B, *Evodia* sp., *Ficus protobenjamina, Ficus* sp., *Grewia* sp, *Grewiopsis* sp., *Juglans sinustus, Lithocarpus angustus, Litseaphylum presanguinea, Laurophyllum* sp., *Magnolia inglefieldii, Magnolia* sp. (2 species), *Mallotus* sp., *Melanorrhorea alaska, Milletia* sp., *Meliosma* sp., *Myrica* sp., *Nephelium* sp., *Platanus* cf. *comstoki, Platanus* sp., *Populus gigantophylla, Plafkeria rentonensis, Rhamnus preleptophylla, R. marginatus, Sapindus* sp., *Viburnum speciosum.* (mostly evergreen broadleaved angiosperms). *Sabalites* sp., *Livistona tibetica* (palms - monocot). *Typha* sp. (monocot). *Ginkgoites* (ginkgophyte). *Cyclosaurus* (fern).
2) ? Eocene, lower Qiuwu Fm. (Geng and Tao, 1982b) (aggregated Donggar and Gyisong villages assemblages)	Megaflora: *Juglandites sinuatus*, *Quercus orbicularis*, *Ficus daphnogenoides*, *F. stephensoni*, *Cassia fayettensis*, *Celastrus minor*, *Myrtiphyllum (Eucalyptus) angusta*, *M. (Eucalyptus) geinitsi*, *Phrynium tibeticum*, *Dianella longifolia* (mixed evergreen and deciduous broadleaved angiosperms) *Cyperacites heydenii* and *Typha* sp. (monocots)
3) Oligocene (23.3 Ma) Kailas Basin (Ai et al., 2019)	Megaflora: *Quercus* section *Heterobalanus* sp., *Alnus*, *Populus* cf. *glandulifera* Heer., *P.*cf. *balsamoides* Göppert sensu lato, Pinaceae needle, *Betula* and *Carpinus*, together with leaves of several unidentified broadleaved dicots (mixed evergreen and deciduous broadleaved angiosperms)
4) earliest Miocene (~23 Ma) Qiabulin Flora (Geng and Tao, 1982b; Ding et al., 2017b)	Megaflora: *Populus latior*, *P.* sp., *Cercidiphyllum ellipticum*, *Eucalyptus* sp., *Viburnum asperum* and a number of unidentified broadleaved angiosperms (mixed evergreen and deciduous broadleaved angiosperms).
5) mid Miocene (15 Ma) Namling Flora, lower horizon. (Li and Guo, 1976; Guo et al., 2019)	Megaflora: *Populus*, *Salix*, *Betula*, *Alnus*, *Corylus*, *Carpinus*, *Quercus*, *Acer*, *Ribes* and *Rhododendron* (predominantly deciduous broadleaved angiosperms) *Sabina, Cedrus* and *Thuja* (conifers, rare). Microflora: *Pinus*, and *Cedrus* dominate the pollen spectrum.
6) mid Miocene (15 Ma) Namling Flora, upper horizon (Geng and Tao, 1982b; Li and Guo, 1976)	Megaflora: ***Quercus semicarpifolia, Q. senscens*, and *Q. pannosa*** (broadleaved angiosperms *Phragmites* and *Cyperacites* (monocots) *Sabina, Cedrus* and *Thuja* (conifers) Microflora: *Pinus*, *Cedrus, Abies* appear in the pollen spectrum (conifers).
7) ? mid Miocene Moincer Flora (Geng and Tao, 1982b)	Megaflora: *Populus balsamoides*, *P. glandulifera*, *P. latior*, *Populus* sp., *Salix* sp., *Albizia* sp. and *Sophora* sp. (broadleaved angiosperms).
8) ? mid Miocene Moincer Flora (Geng and Tao, 1982b)	Megaflora: *Ficus myrtifolia*, *Myrica* sp., *Cassia marshalensis*, *Rhamnus manchigensis*, *Myrtophyllum (Eucalyptus) geinitzii*, *M. (Eucalyptus)* oblongifolia, *Phrynium tibeticum* and *Cyperacites haydenii)* (Monocots).
9) Pliocene Zanda Basin (Huang et al., 2020; Li and Zhou, 2001; Wu et al., 2014)	Megaflora: *Berberis* sp., *Caragana* sp., *C.* cf. *gerardiana*, *C.* cf. *versicolor*, *Cotoneaster* sp. 1, *Cotoneaster* sp.2, *Spiraea* sp. 1, *Spiraea* sp. 2, *S.* cf. *myrtilloides*, *Hippophae* sp., *Salix*, sp.1, *Salix.* sp. 2, *Salix*.sp. 3, *Polygonum* sp., *Ceratostigma* sp., *Rhododendron*, sp. 1, *Rhododendron* sp. 2, *Lonicera* sp., *L.* cf. *spinosa*, and two unassigned dicot leaf forms (small woody broadleaved angiosperms). *Potentilla fruticosa* (herbaceous dicot) *Kobresia* sp. (herbaceous monocot). Microflora: ***Picea***, ***Abies,*** *Pinus, Podocarpus, Tsuga, Cedrus* (conifers). *Betula*, *Quercus*, *Juglans*, Chenopodiaceae, Compositae (angiosperms). Fern spores.
10) ? Pliocene (but could be as old as Eocene) Yabokang Jialha Flora (Shisha Pangma) (Hsu et al., 1973; Li, 1998)	Megaflora: *Quercus semecarpifolia* (*Quercus* sect. *Heterobalanus*), *and Cypericites* sp.
11) Pliocene (2.48 Ma), Gyabulha Basin Flora, Cho Oyu, Tingri County, Tibet (Shi et al., 1998)	Megaflora: *Populus* sp. and *Lespedeza* sp. (dicot angiosperms) *Sabina recurva* and *Picea spinulosa* (conifers).
12) Mid to late Miocene (15–10 Ma) Kameng River Flora, eastern Siwaliks, N. India (Khan et al., 2014a; Srivastava et al., 2018a)	Megaflora: *Aglaia*, *Sapium*, *Actinodaphne*, cf. *Dipterocarpus*, cf. *Polyalthia*, *Cinnamomum*, *Millettia*, cf. *Millettia* (2 species), *Dysoxylum*, cf. *Cratoxylum*, *Terminalia*, *Antidesma*, *Lannea*, *Albizia*, *Eugenia*, *Anogeissus*, *Cassia*, *Anthocephalus*, *Mesua*, *Callicarpa*, *Combretum*, *Pterocarpus*, *Oxyceros*, *Kayea*, and *Woodfordia* (mostly evergreen tropical broadleaved angiosperms)
13) Mid to late Miocene (15–10 Ma) Darjeeling Flora, eastern Siwaliks, N. India (Antal and Awasthi, 1993; Antal and Prasad, 1996a, b, 1997, 1998; Awasthi, 1992; Khan et al., 2014a)	Megaflora: *Phoebe*, *Garcinia*, *Combretum*, cf. *Cratoxylum*, *Glochidion*, *Lagerstroemia*, *Callicarpa*, cf. *Bridelia*, *Dipterocarpus*, *Persea*, *Medinilla*, *Mesua*, cf. *Woodfordia*, *Hopea*, *Nephelium*, *Uvaria*, cf. *Atalantia*, cf. *Derris* and *Albizia* (mostly evergreen tropical broadleaved angiosperms)
14) Mid to late Miocene (15–10 Ma) Koilabas Flora, Siwaliks, western Nepal (Prasad et al., 1999)	Megaflora: *Miliusa siwalica, Anona koilabasensis, Dillenia palaeoindica, Securidaca miocenica, Ryparosa prekunstelri, Gynocardia miodorata, Mesua tertiara, Kayea kalagarhensis, Isoptera siwalica, Dipterocarpus siwalicus, D. koilabasensis, Hopea mioglabra, Shorea eutapizifolia, Eovodia koilabasensis, Murraya khariense, Atlantia miocenica, Brucea darwajensis, Chloroxylon palaeoswietenia, Aglaia nepalensis, Zizyphus miocenica, Filicium koilabasensis, Euphorea nepalsensis, Otophora miocenica, Nephelium palaeoglabrum, Sabia eopaniculata, Swintonia palaeoschwenckii, Bouea koilabasensis, Tapiria chorkholiensis, Mangifera someshwarica, Albizia siwalica, Pongamia kathgodamensis, Cassia nepalensis, C. miosiamea, C. neosophora, Dalbergia eocultrata, D. miosericea, D. siwalika, D. miovolubilis, Milletia, siwalica, M. koilabasensis, M. imblibasensis, M. miobrandisiana, Ormosia robustoides, Cynometra palaeoiripia, Samanea siwalica, Entada palaeoscandens, Anogeissus eosericea, Clycopteris floribundoides, Terminalia koilabasensis, T. siwalica, T. panandhroensis, Combretum salmii, Lagerstroemia siwalika, Woodfordia

(*continued on next page*)

Table 3 (*continued*)

Age and Reference	Composition
	neofruticosa, Anisphyllea siwalica, Sysygium mioceniccum, S. miooccidentalis, Lonicera mioquinquelocularis, Randia miowallichii, Morinda siwalika, Diospyros koilabasensis, D. pretoposia, D. darwajensis, Tabernaemontana precoronaria, Carissa koilabasensis, Gaertneria siwalica, Datura miocenica, Anacolosa mioluzoniensis, Vitex prenegundo, V. siwalica, Cinnamomum moinuctatum, Ficus precunia, F. retusoides, F. nepalensis, Helicia eorretica, Phyllanthus koilabasensis, P. mioreticulatus, and Antedesma siwalica (mostly moist evergreen broadleaved angiosperms).
15) Mid Miocene (13–11 Ma) Surai Khola (Bankas Formation) Flora, Siwaliks, western Nepal (Srivastava et al., 2018c)	Megaflora: *Albizia microfolia, Cinnamomum nepalensis, Cocculus miotrilobus, Cynometra palaeoiripa, Cleistanthus suraikholaensis, Millettia churiensis, Ficus raptiensis, Koompassia suraikholaensis, Machilus miocenica, Mallotus venkatachalai, Chisocheton suraikholaensis, Mesua tertiara, Mucuna miogigantea, Olax bankasii, Phyllanthus palaeoreticulatus, Polyalthia palaeosimiarum, Xerospermum mioglabratum, and Sterculia mioensifolia* (mostly moist evergreen broadleaved angiosperms).
16) Late Miocene (9.5–6.8 Ma) Surai Khola (Chor Khola Formation) Flora, Siwaliks, western Nepal (Srivastava et al., 2018c)	Megaflora: *Actinodaphne palaeoangustifolia, Albizia siwalika, Goniothalamus chorkholaensis, Chonemorpha miocenica, Bridelia mioretusa, Calophyllum suraikholaensis, Chukrasia miocenica, Ctenolophon chorkholaensis, Diospyros miocenicus, Dipterocarpus siwalicus, Dipterocarpus suraikholaensis, Excoecaria palaeocrenulata, Millettia koilabasensis, Garcinia corvinusiana, Duabanga siwalika, Mallotus kalimpongensis, Stigmaphyllon chorkholaensis, Mangifera suraikholaensis, Dysoxylum raptiensis, Artocarpus nepalensis, Murraya khariensis, Myrsine precapitellata, Ochna siwalika, Harpullia siwalica, Shorea palaeostellata, Sterculia premontana, Syzygium palaeocumini,* and *Zanthoxylum siwalicum* (moist evergreen and deciduous broadleaved angiosperms).
17) Pliocene (5.3–3 Ma) Kameng River, middle Siwaliks, eastern Himalaya (Khan et al., 2014a)	Megaflora: *Annona* cf. *squamosa*, *Persea* cf. *parviflora*, cf. *Lindera*, cf. *Millettia*, *Pimenta* cf. *officinalis*, cf. *Ficus, Shorea siwalika, Calophyllum suraikholaensis, Glochidion* cf. *gamblei*, *Millettia* cf. *cinerea*, *Mallotus* cf. *philippensis*, *Pongamia siwalika*, *Bridelia siwalika*, *Mitragyna tertiara*, *Unona* cf. *discolor*, *Quercus semecarpifolia*, cf. *Calophyllum*, *Terminalia panandhroensis*, cf. *Mitragyna*, *Albizia siwalica*, and *Gynocardia mioodorata* (mostly evergreen tropical broadleaved angiosperms)
18) Late Pliocene to Pleistocene (3 Ma –0.01 Ma) Kameng River, upper Siwaliks, eastern Himalaya (Khan et al., 2014a)	Megaflora: *Actinodaphne palaeoangustifolia*, cf. *Fabaceae*, *Litsea* cf. *salicifolia*, *Quercus* cf. *lamellosa*, *Millettia palaeopachycarpa, Dipterocarpus siwalicus*, *Atalantia palaeomonophylla*, *Chonemorpha miocenica*, *Berchemia siwalica*, *Dysoxylum raptiensis*, *Canarium* cf. *bengalense*, *Dalbergia* cf. *rimosa*, cf. *Shorea*, *Mangifera someshwarica*, *Pongamia siwalika*, *Combretum sahnii*, *Calophyllum suraikholaensis*, *Callicarpa siwalika*, *Millettia* cf. *extensa*, *Lindera* cf. *pulcherrima*, cf. *Albizia*, *Knema* cf. *glaucescens*, *Quercus semicarpifolia*, and *Actinodaphne* cf. *obovata* (mostly evergreen tropical broadleaved angiosperms)

3.4.3. Miocene and Pliocene

The earliest Miocene Qiabulin flora from the Xigatse Prefecture (Fig. 2) is U–Pb dated as ~23 Ma (Aquitanian) (Ding et al., 2017b) and, although it is not well studied, the physiognomy of the dicot leaf forms indicates the assemblage represents a warm temperate evergreen broadleaved forest lacking palms (Geng and Tao, 1982b) (Table 3, panel 4), but growing under a mean annual temperature of ~19 °C, a warm month mean temperature of ~28 °C and a cold month mean temperature of ~9 °C. The growing season was 10–11 months during which time that area received ~1.9 m of rainfall with a wet season almost five times wetter than the dry season and thus borderline monsoonal (Spicer et al., 2017). The paleoelevation based on a CLAMP analysis was ~2.3 km (Ding et al., 2017b).

Other paleofloras from the Xigatse District, so far not well dated but supposedly Miocene, include those from near Zhaxilin Village that has yielded *Salix* cf. *meeki*, *Juglandites sinuatus*, *Ficus daphnogenoides*, *Laurophyllum* sp., *Leguminosites* sp. and *Rhamnites eminens*, another from near Gyalhagong-badong Village in Ngamring County (29.3°N, 89.3°E, 4200–4600 m a.m.s.l.) with just one reported species, *Aralia firma*, and from near Gharlong Village in Sagya County (29.41°N, 85.35°E, 4600 m a.m.s.l.) where *Equisetites* sp., *Leguminosites* sp., *Dictylophyllum* sp., and *Cyperacites* sp. have been recovered (Guo, 1975).

The early Miocene rapid rise of the Himalaya (Ding et al., 2017b) created more niche space at high, and thus cooler, elevations and by the MMCO the Namling-Oiyug Basin (29.7° N, 89.583°E; 4600 m a.m.s.l.) (Fig. 3), just north of the YTSZ on the Gangdese Arc, and so not part of the Himalaya from a geological perspective, hosted an angiosperm-dominated boreal temperate broad-leaved deciduous woodland (Table 3, panel 5) at a paleoelevation of ~5 km (Currie et al., 2016; Khan et al., 2014a; Polissar et al., 2009; Spicer et al., 2003). While inevitably not as rich (25 species in 13 genera and 9 families) as lower elevation and more thermophilic vegetation, the Namling Basin lake sediments contain many genera found today mostly at elevations of 3000 to 4500 m in the Tibetan Region, as well as in northern China (Guo et al., 2019; Li and Guo, 1976). The most diverse leaf-bearing horizon at Namling ($^{40}Ar/^{39}Ar$, dated as 15 Ma) (Spicer et al., 2003) is dominated by woody dicot angiosperms (Table 3, panel 5). Conifers are only represented by rare Juniper-like *Sabina, Cedrus* and *Thuja* in a horizon slightly higher in the section (but still 15 Ma) that is dominated by *Quercus semicarpifolia*, *Q. senscens*, and *Q. pannosa* (Geng and Tao, 1982b). *Phragmites* and *Cyperacites* give an insight into lake margin emergents (Table 3, panel 6) (Geng and Tao, 1982b; Li and Guo, 1976). The pollen record shows the regional presence of conifers (*Pinus*, and *Cedrus*) predominate in the main plant bed and are joined by *Abies* upsection (Song and Liu, 1982), most likely inhabiting the higher elevation slopes on the mountains surrounding the Namling paleolake.

The foliar physiognomic spectrum of this cool temperate Namling flora examined using CLAMP indicates a mean annual temperature of ~8 °C, a warm month mean temperature of ~24 °C and a cold month mean temperature of ~−6 °C (Khan et al., 2014a) falling into climate 'B' in Köppen's global climate classification (Peel et al., 2007). With cool temperatures and high rainfall (1300 mm) during the 6-month growing season, the region was humid and the wet season rainfall, likely coinciding with the growing season, was only three times that of the dry season (Khan et al., 2014a). This high rainfall was due to the close proximity of the Namling Basin to the then southern margin of the Tibetan Region, at a time when the Himalaya had not yet exceeded 5 km.

The Namling flora represents the highest elevation Miocene vegetation so far documented and it is both temporally and altitudinally well constrained. It is compositionally distinct from other contemporaneous regional floras, but most similar to the late Miocene (so far lacking absolute dating but considered to be 11–7 Ma, Tortonian, based on regional stratigraphy) Yemagou Formation Flora exposed in the Moincer Coal Mine, Gar County (29.287°N, 87.223°E, 5105 m a.m.s.l.), Tibet (Fig. 3) . The Moincer plant remains are preserved in clays, sands and silts that are associated with the coals, and the fine-grained sands often display ripple cross-bedding, worm tracks and plant debris indicative of shallow lake or fluvial margin deposits. The coarser sands host internal casts of freshwater bivalves and few whole leaves, while the finer lake sediments are often finely laminated, but lack any obvious biota. The Moincer flora (Table 3, panel 7) (Geng and Tao, 1982b) is indicative of cool temperate deciduous broad-leaved vegetation that probably grew at a similar elevation to that in the

Namling Basin. However, other leaf fossils from the Moincer mine area appear to represent more thermophilic taxa (Table 3, panel 8) (Geng and Tao, 1982a) and display a similarity with those from the lower Qiuwu Formation at Gyisong Town in Ngamring County and at Donggar Town in Xigaze. These seem to represent a mixed evergreen and deciduous forest inhabiting a warm and humid climate. This flora would benefit from more detailed study and a better constrained dating framework, notably because the two quite distinct floral compositions may be indicative of rapid uplift as seen in the Markam Basin. Like that of Namling, the Yemagou Flora is located on the Gangdese highland, but no quantitative paleoaltimetry has been conducted.

Towards the western end of the Gangdese highland the Pliocene flora of the extensional Zanda Basin (31.73°N, 79.56°E, 3990 m a.m.s.l.) (Fig. 3) preserves a megaflora marking the transition from the broadleaved woodlands of the late Miocene to the arid semi-desert conditions of today. The flora consists of leaves representing lake margin vegetation consisting of woody members of the Berberidaceae, Fabaceae, Rosaceae, Eleagnaceae, Salicaceae, Ericacea and Caprifoliaceae with herbaceous taxa such as *Polygonum* and *Kobresia* (Huang et al., 2020) (Table 3, panel 9). Today *Kobresia* forms extensive 'grasslands' across large parts of Tibet. Along with the megaflora, the palynological record attests to a completely different kind of vegetation, one dominated by conifers and ferns. Angiosperm pollen forms only a small part of the overall palynological record. The dominant pollen and spore types are those that are produced in vast quantities by their parent plants and where wind is the dispersal vector, so the lack conifer and fern megafossils points to the palynological record, as elsewhere in Tibet, representing vegetation remote from the depositional site and spanning different elevations. Not only does the palynological record provide an inflated view of local plant diversity it also, as previously discussed, yields highly unreliable estimates of past surface elevation. In respect of the Zanda Basin its location close to the Himalayan front means that isotopic paleoaltimetry is likely to be more liable and this points to the area being at least as high as today at ~9 Ma, and possibly up to 1.5 km higher than today (Saylor et al., 2009). Although likely biased towards the height of the surrounding peaks, this possible fall in surface height is consistent with the extensional setting and is similar to a ~1 km reduction in height since the Miocene seen in the Namling-Oiyug Basin (Khan et al., 2014a). The drop would also account for an increase in local aridity because it would amplify the rain shadow effect from the Himalaya even if they remained static. Although in the Pliocene the Zanda Basin supported a lake system, the vegetation surrounding that lake was still characterized by small leaves and while some of this may have been a taphonomic artefact (Spicer, 1991, p.75), the composition of the Zanda flora (small leaved drought-tolerant shrubs) still suggests a cooler and drier climate (Huang et al., 2020) than prevailed in the Gangdese highlands during the Miocene.

Supposed Pliocene floras in the Himalaya have poorly-constrained ages but contributed greatly to previous ideas concerning the topographic development of the Tibetan Region. An important find was that from the Yabokang Jialha Group at an altitude of 5700–5900m a.m.s.l. on the northern slopes of Shisha Pangma (Gosainthan). This poorly located small flora consists of alpine oaks (Table 3, panel 10) and is reminiscent of the upper flora found at Namling. At first, the Shisha Pangma flora was believed to be Pliocene in age (3.6 Ma) (Hsu et al., 1973; Li, 1998), but it has subsequently been reported that the Yabokang Jialha Group encompasses the late Eocene through to the middle Miocene (38–11 Ma) based on K–Ar dating of granite intrusions in its lower part (Li, 1998). Coupled with the fact that this flora was found as loose blocks and not *in situ*, the age of the flora must remain in question. Nevertheless, it was one of the first Himalayan fossil floras to be used to argue for a recent uplift of Tibet (Shi et al., 1998), erroneously implying that the rise of the Himalaya and Tibet were one and the same thing.

A number of megafossil remains of the cupressaceous *Sabina recurva*, *Picea*, and the deciduous *Populus* sp. and the bush or vine *Lespedeza* sp., have been found from the lacustrine sediments of the Gyabulha Basin (28.78 °N, 87.18 °E; 4865–5100 m a.m.s.l.) (Table 3, panel 11) on the northeastern slope of the Cho Oyu Peak region in Tingryi County, southern Tibet. This is reportedly late Pliocene in age (2.48 Ma) (Shi et al., 1998).

3.4.4. Siwalik floras

Despite concerns regarding dating it is clear that several late Neogene floras in the Himalaya represent cool 'boreal' vegetation typical of that found at high-elevations in the Tibetan Region today. This is perhaps best illustrated by the Namling flora (Guo et al., 2019). Even without quantitative paleoaltimetry it is obvious that floras such as that found at Namling are distinctly different from contemporaneous floras from the Siwaliks that exhibit much greater diversity and contain numerous taxa typical of tropical vegetation (Srivastava et al., 2017, 2018a-c) as well as remains of thermophilic animals (Gilbert et al., 2017; Kundal et al., 2017; Sankhyan and Èeròanský, 2016; Sankhyan et al., 2017; Sankhyan and Chavasseau, 2018).

The Siwalik successions extend along the southern margin of the Himalaya and it has been known for a long time that they contain abundant Miocene plant assemblages (Cautley, 1835), some of which have been well studied in recent years (Table 3, panels 12–18). The assemblages represent Neogene near sea level forest ecosystems and dating is usually based on magnetostratigraphy. In the eastern Siwaliks (Kameng River, 27.04°N, 92.61°E; 250 m a.m.s.l.) (Fig. 3) a mid to late Miocene flora yields a diverse leaf assemblage (72 taxa recognized to date) typical of tropical humid forests (Table 3, panel 12) (Khan et al., 2014a; Srivastava et al., 2018a). Further west near Darjeeling (26.88°N, longitude 88.47°E 194–250 m a.m.s.l.) (Fig. 3) another, smaller, mid to late Miocene flora displays a similar composition also typical of humid tropical to subtropical vegetation (Table 3, panel 13) (Antal and Awasthi, 1993; Antal and Prasad, 1996a, b, 1997, 1998; Awasthi, 1992; Khan et al., 2014a). Further west still, the Koilabas Flora of western Nepal (27.712°N, 82.529°E, ~250 m.a.m.s.l.) (Prasad et al., 1999) (Table 3, panel 14, Fig. 3) contains a diverse leaf assemblage typical of that indicative of tropical evergreen, moist evergreen forest and moist deciduous forests. Eighteen of the taxa today grow in both India and Malaya and most are found in north-eastern and southern India. Table 3, panels 15 and 16 summarize the composition of middle to late Miocene leaf floras from Surai Khola, also in western Nepal (27.8°N, 82.9°E, ~500 m a.m.s.l.) (Srivastava et al., 2018c) (Fig. 3). Here there is an increase in deciduous tropical taxa as the Miocene progresses, accompanied by a perceived small rise in mean and cold month mean temperatures. Using the Co-existence Approach proxy (Mosbrugger and Utescher, 1997; Utescher et al., 2014), Srivastava et al. (2018c) reconstructed a warming trend from the mid to late Miocene with the mid Miocene mean annual temperature (MAT) being 21.1–25.4 °C and 26–27 °C for late Miocene. The cold month mean temperatures (CMMT) also rose from 20.6 to 24.3 °C in the mid Miocene to 24.3–24.7 °C in the late Miocene, accompanied by a mean annual precipitation (MAP) increase from ~2.3 m to 2.9 m and a marked increase in rainfall seasonality from a wet:dry month ratio of ~3.5 in the middle Miocene to ~ 9 in the late Miocene, largely due to marked dry season (winter) drying.

CLAMP analysis of both the Darjeeling and Kameng River regions suggests similar warm wet climates in the middle to late Miocene climate characterized by a MAT of ~25° with a CMMT ~18 °C in Darjeeling and ~21 °C in Kameng River, and markedly seasonal variations in rainfall (i.e. monsoonal) in an otherwise wet regime (the MAP being ~2 m). In Bhutan, a middle to late Miocene leaf flora (26.66–28.417°N, 88.66–92.17°E; ~400 m a.m.s.l.) (Fig. 3) again suggests a very similar monsoonal climate regime (MAT ~24 °C, CMMT ~19 °C, MAP ~1.8 m with seasonal variations similar to those of Kameng River) (Khan et al., 2019).

Pliocene through to Pleistocene eastern Siwalik floras show similar compositions indicative of humid to sub-humid tropical to subtropical vegetation (Table 3, panels 17 and 18) and, depending on age and location, similar compositions to those seen in the region today (Khan and Bera, 2014; Khan et al., 2011, 2014a). The transition to the modern is subtle with small compositional changes over time and, as far as can be determined, the structure of the vegetation was already well established by the mid Miocene. Furthermore, the plant–insect relationships that exist today in the Siwaliks were also already established by that time (Khan et al., 2014b).

The abundance of fossil floras throughout the Siwaliks have yet to be fully investigated and studied form a quantitative paleoclimate perspective, but future studies should illuminate our understanding of how and when the pronounced east to west drying trend seen along the southern margins of the Himalaya today developed. This in turn should help characterize the development of the modern SAM.

4. What explains the apparent Miocene diversification of Asian floras seen in molecular phylogenetics?

Assuming the age constraints are correct, molecular phylogenetics consistently reveals large-scale plant diversification in China taking place in the Miocene (Lu et al., 2018; Renner, 2016). Lu et al. (2018) report that 66% of angiosperm genera in China have evolved since ~23 Ma (early Miocene) and that the flora of eastern China seems to have older divergence times (~25–22 Ma) than that in the west (~19–15 Ma). Significantly, the authors regarded eastern China overall as an evolutionary museum, while they suggest western China (including the Tibetan Region) appears to have served as an evolutionary cradle for herbaceous taxa.

Most of this work has linked the observed diversification to the supposed combined Miocene 'uplift of the Tibetan Plateau' and the development of the Asian monsoon systems (Favre et al., 2015; Lu et al., 2018; Sun and Wang, 2005). However, as we have seen, such an uplift cannot be the explanation because 1) a complex mountainous landscape, with uplands >4 km has existed in the Tibetan Region throughout the Cenozoic, 2) the plateau, although supporting many endemic species, hosts less diversity than nearby areas such as the Hengduan Mountains, the Himalaya and more lowland regions of China (Yu et al., 2020), and 3) the monsoons long pre-date the Miocene and their evolution, although complex, seems to have been gradual. If a post-mid Miocene formation of the Tibetan Plateau had been a key factor in driving greater biodiversity it must have been associated with the development of the kind of cold arid environment we see there today. As noted in Section 2.3 an elevated plateau itself will induce aridity, and dryness will have been intensified by the rise of the Himalaya, so to a large extent monsoon development is irrelevant because monsoon impact on the plateau is minimal compared to that on the southern flank of the Himalaya and across the Hengduan Mountains. Moreover, we know that monsoons affected these areas long before the Miocene. One additional point is that vegetation on the plateau was likely almost extirpated during the Quaternary when cold and aridity generated a hostile growth environment (Kuhle, 1998), whereas the Hengduan Mountains seem to have been minimally glaciated (Shi et al., 2006), and the Hengduan Mountains area with its deep valleys will have provided numerous refugia within the altitudinal and aspect heterogeneity afforded by a spatially extensive, complex and highly dissected landscape.

Plant fossils, both palynomorphs and megafossils (leaves, fruits, seeds woods etc.), provide valuable evidence of the composition and, by inference, structure of past vegetation and, notwithstanding the imperfect nature of the fossil record, normally these remains capture the presence of sufficient taxa to characterize past diversity and community composition. However, this record relies on the accumulation, and survival against erosion, of sediments that entomb and preserve the fossils. This means our paleontological insights into past ecosystems are biased towards archives representing the lower elevations or rarely preserved intermontane basins (e.g. Namling), albeit some insight into upland communities can be gained from the palynological record.

One important and diverse modern biome that is not likely to have been preserved is that which exists above the natural treeline - the Alpine Biome. Alpine plants are typically small, predominantly herbaceous, 'cushion plants' occupying the protected environment between boulders and within a few centimetres of the soil surface. They also tend to be insect pollinated and do not expend large amounts of energy in producing abundant pollen. Their position on high mountain slopes, herbaceous character, small size and low pollen production mean that they have little chance of being represented in the fossil record, and yet today they form a highly diverse group of plants displaying an array of specializations to the harsh environments that they inhabit (e.g. Körner, 2003).

That molecular phylogenetic findings (Lu et al., 2018; and others referenced in Renner, 2016) point to western China being an evolutionary cradle for herbaceous plants may well be due in large part to the emergence of the alpine biome as a significant vegetation type across the already elevated parts of the Tibetan Region (particularly the high and humid Hengduan Mountains) as climate cooled in the late Oligocene and into the Neogene. Cooling would have lowered and compressed altitude-related climate zones, including lowering the tree line, and so making available for the first time significant eco-space for sub-alpine and alpine biomes (e.g. Fig. 2d). This opening up of above-treeline space may have begun in the late Oligocene when the regional climate was sufficiently cool to depress the tree line below ~4.5 km and the humid Hengduan Mountain system had achieved an elevation that exceeded that height over a significant area. Note that for the more southerly-located Gangdese highlands and rising Himalaya, the tree line could have extended to the mountain tops in the Oligocene and the alpine biome may only have become established thereafter in the mid Miocene when the Himalaya were sufficiently high, and global climate sufficiently cool, to lower the tree line below peak height. No doubt the MMCO imposed a bottleneck on this novel biome at ~15 Ma and it is interesting to note that this is around the time when Lu et al. (2018) detect the mean divergence times characteristic of western China. The role that the Tibetan Plateau played in the development of the alpine biome is probably limited because of the aridity that developed in the Neogene through the growth of the Himalaya and plateau formation, which reduced relief-related niche diversity. It is likely that most of the ancient late Oligocene and early Neogene Gangdese alpine biota was extirpated through drying as the Himalaya rose above 5 km, as well as subsequent

glaciations, but some taxa may well survive in the Himalaya today, which makes both the Himalaya and Hengduan mountains key areas for conservation.

5. Questions for conservation

Mountain regions, long protected by their remoteness and difficult access, are now increasingly suffering environmental degradation though deforestation, agriculture, tourism and geological resource extraction (Chakraborty, 2020). The Tibetan Region is no exception, and improved access, while presenting a threat to today's biodiversity, is also revealing the true antiquity and significance of biotic evolution through new fossil discoveries. The fossil assemblages, nature's archives, being newly discovered and securely dated provide unique and invaluable insights into the ancient origins of the Tibetan Region biota, and the circumstances under which it developed before human interference. The fossil record shows that the biota of the Tibetan Region achieved much of its modern aspect (in terms of composition at the generic level and taxon assemblies) in the Eocene, and since then complex tectonics and an everchanging climate have expanded environmental niche space within which the modern biodiversity has arisen. Nevertheless, no matter how much exploration is undertaken and how much discovery is achieved, paleontological archives will always be incomplete, and the gaps in the record are more pronounced at high elevations where erosion dominates over sediment deposition and preservation. Consequently, critical information on the evolution of these floral associations and biomes needs also to be sought elsewhere, for example through molecular phylogenetics.

Our new knowledge of orographic development (Fig. 4), coupled with analysis of modern Chinese plant diversity, shows that the alpine biota is likely the youngest of vegetation types in the Tibetan Region, only becoming established at the end of the Oligocene at the earliest, but undoubtedly then constrained through a MMCO bottleneck at about 15 Ma. Like those provided by the fossil record, the molecular archives conserved in living organisms that are used to reconstruct phylogeny are incomplete and cannot provide insights into extinct lineages or their morphology and interactions with past environments. The image of the past that molecular phylogenetics provides will necessarily be distorted by what has survived until the present, and those lineages lost in ancient diversity bottlenecks cannot be properly represented. However, taken together paleontology and molecular phylogeny do make our window into the past a little clearer than would be the case if we relied only on the distorted view provided by just one of these approaches. In combination paleontology and molecular phylogenetics can help frame conservation strategies.

It is clear that at the heart of generating the globally exceptional diversity that humanity has inherited, and are the custodians of, is not stasis but profound and continuous change in landscape and climate. We cannot control tectonics, but we can manage landscapes and as a species we are, without any forethought or intelligence, changing climate. Within this dynamic context what is it that we are trying to conserve? Is it the library of living taxa as if species were immutable but valuable books, or is it the information (genomes) within them? Why do we want to conserve them? Is it for their intrinsic properties, or their ecosystem services? If the former, gene banks, gardens and zoos are all that are required, but this compromises the capacity of taxa to adapt to changing circumstances and maintain fitness in natural systems. If it is the latter, then conservation in gene banks, garden or zoos is of limited value, because to provide ecosystem services individuals need to function within communities. Botanic gardens and zoos can never provide the complex structure and functional integration that is an intrinsic property of wild ecosystems. Neither can they support the complex web of mutual animal–plant interactions that are critical for healthy ecosystem maintenance. If this complex web is disrupted, for example by the loss of biotic (insect/bird/reptile/mammal) pollen and seed vectors, then plant reproduction is compromised, extinction follows and the ecosystem fails, bringing about further extinctions, the permanent loss of information from the genetic library and a compromised ability to form new species. Ultimately this means a failure of ecosystem services under future changed climates.

The present rate of anthropogenic change is an important component in conservation. Plants can adapt, quite fast geologically speaking, to a changing climate, but the rate of human-induced change we are currently experiencing is well outside any previous natural long-term variability (Neukom et al., 2019) and constraints on the ability of plants to migrate or adapt may lead to extinction level stress on ecosystems, particularly if so-called keystone taxa (Paine, 1969) disappear.

It is clear that treelines are increasing in elevation (Harsch et al., 2009) and the ability to migrate unhindered is especially important given that climate warming is happening far more rapidly than during past extreme thermal events (Foster et al., 2018), and yet migration is currently frustrated by landscape and ecosystem fragmentation (e.g. Tiwari et al., 2019). Furthermore, not all taxa in geologically complex landscapes are able to migrate because they may be uniquely adapted to particular substrates, even though such taxa appear to have already survived extreme Quaternary climate changes (Corlett and Tomlinson, 2019). Here, specialisation may enhance survivorship because potentially competing taxa are excluded by the unusual edaphic conditions, but throughout the Cenozoic survival has been in the context of long-term cooling trends and gradual fluctuations over orbital timescales, not the rapid warming we are experiencing today. Because mountains can be thought of, simplistically, as being conical, in a cooling climate ecosystem space expands for a given taxon as they are driven to lower elevations. However, in a warming scenario that space is diminished as climate tolerance zones rise up mountains until they pass beyond the height of the highest peaks. No matter what the edaphic adaptations sooner or later significant numbers of taxa will run out of habitability space.

Ideally, we should we be trying to conserve the capacity for change and future dynamic diversity and ecosystem resilience (Barnosky et al., 2017). For future ecosystem resilience we need to conserve entire landscapes with niche heterogeneity intact, unfragmented, enabling plants and animal vectors to migrate at will. Only this will conserve the processes of biodiversity dynamics as well as the genetic library and the capacity for future adaptation. For the Tibetan Region this means maintaining migration corridors between protected areas and limiting further fragmentation (Lu et al., 2018). Such corridors need to be of sufficient width and encompass enough niche heterogeneity (edaphic, aspect, microclimate etc.) to support the full spectrum of plant/animal interactions.

Declaration of Competing Interest

The authors declare they have no conflicts of interest.

Acknowledgements

This work was supported by an XTBG International Fellowship for Visiting Scientists to R.A.S., and the NSFC–NERC (Natural Environment Research Council of the United Kingdom) joint research program [nos. 41661134049 and NE/P013805/1]. We thank Teresa Spicer, Gaurav Srivastava and an anonymous reviewer for their comments and suggestions.

References

Acosta, R.P., Huber, M., 2020. Competing topographic mechanisms for the summer indo-asian monsoon. Geophys. Res. Lett. 47 e2019GL085112.

Ai, K., Shi, G., Zhang, K., Ji, J.L., Song, B.W., Shen, T., Guo, S.-X., 2019. The uppermost Oligocene Kailas flora from southern Tibetan Plateau and its implications for the uplift history of the southern Lhasa terrane. Palaeogeography, Palaeoclimatology,. Palaeoecology 515, 142–151.

Allègre, C.J., Courtillot, V., Tapponier, P., Hirn, A., Mattauer, M., Coulon, C., Jaeger, J.J., Achache, J., Schärer, U., Marcoux, J., Burg, J.P., Girardeau, J., Armijo, R., Gariépy, C., Gopel, C., Li, T.D., Xiao, X., Chang, C.F., Li, G.W., Lin, B., Teng, J., Wang, N., Han, T., Wang, X., Den, W., Sheng, H., Cao, Y., Zhou, J., Qiu, H.N., Bao, P., Wang, S., Wang, B., Zhou, Y., Xu, R., 1984. Structure and evolution of the Himalaya-Tibet orogenic belt. Nature 307, 17–22.

An, Z.S., Kutzbach, J.E., Prell, W.L., Porter, S.C., 2001. Evolution of asian monsoons and phased uplift of the himalayan–Tibetan plateau since late Miocene times. Nature 411, 62–66.

Anagnostou, E., Jihn, E.H., Edgar, K.M., Foster, G.L., Ridgwell, A., Inglis, G.N., Pancost, R.D., Lunt, D.J., Pearson, P.N., 2016. Changing atmospheric CO_2 concentration was the primary driver of early Cenozoic climate. Nature 533, 380–384.

Antal, J.S., Awasthi, N., 1993. Fossil flora from the Himalayan foot hills of Darjeeling foot-hills of Darjeeling District,West Bengal and its palaeoecological and phytogeographical significance. Palaeobotanist 42, 14–60.

Antal, J.S., Prasad, M., 1996a. Dipterocarpaceous fossil leaves from grish river section in himalayan foot hills near oodlabari, darjeeling district, West Bengal. Palaeobotanist 43, 73–77.

Antal, J.S., Prasad, M., 1996b. Some more leaf-impressions from the himalayan foothills of darjeeling district, West Bengal, India. Palaeobotanist 43, 1–9.

Antal, J.S., Prasad, M., 1997. Angiospermous fossil leaves from the Siwalik sediments (Middle-Miocene) of darjeeling district, West Bengal. Palaeobotanist 46, 95–104.

Antal, J.S., Prasad, M., 1998. Morphotaxonomic study of some more fossil leaves from the lower Siwalik sediments of West Bengal, India. Palaeobotanist 47, 86–98.

Antonelli, A., 2015. Multiple origins of mountain life. Nature 524, 300–301.

Antonelli, A., Kissling, W.D., Flantua, S.G.A., Bermúdez, M.A., Mulch, A., Muellner-Riehl, A.N., Kreft, H., Linder, P.L., Badgley, C., Fjeldså, J., Fritz, S.A., Rahbeck, C., Herman, F., Hooghiemstra, H., Hoorn, C., 2018. Geological and climatic influences on mountain biodiversity. Nat. Geosci. 11, 718–725.

Armstrong, H.A., Wagner, T., Herroingshaw, L.G., Farnsworth, A.J., Lunt, D.J., Harland, M., Imber, J., Lopston, C., Atar, E.F.L., 2016. Hadley circulation and precipitation changes controlling black shale deposition in the Late Jurassic Boreal Seaway. Paleoceanography 31, 1041–1053.

Awasthi, N., 1992. Changing patterns of vegetation through Siwalik succession. Palaeobotanist 40, 312–327.

Bande, M.B., Prakash, U., 1984. In: Sharma, A.K.e.a. (Ed.), Occurrence of *Evodia, Amoora* and *Sonneratia* from the Plaeogene of India. Symposium of Eovolutionary Botany and Biostratigraphy, Calcutta, pp. 97–114.

Barnosky, A.D., Hadly, E.A., Gonzalez, P., Head, J., Polly, P.D., Lawing, A.M., Eronen, J.T., Ackerly, D.D., Alex, K., Biber, E., Blois, J., Brashares, J., Ceballos, G., Davis, E., Dietl, G.P., Dirzo, R., Doremus, H., Fortelius, M., Greene, H.W., Hellman, J., Hickler, T., Jackson, S.T., Kemp, M., Koch, P.I., Kremen, C., Lindsey, E.L., Looy, C., Marshall, C.R., Mendenhall, C., Mulch, A., Mychajliw, A.M., Nowak, C., Ramakrishnan, U., Schnitzier, J., Shrestha, K.D., Soalari, K., Stegner, L., Stegner, A.A., Stenseth, N.C., Wake, M.H., Zhang, Z., 2017. Merging paleobiology with conservation biology to guide the future of terrestrial ecosystems. Science 355 eaah4787.

Berger, A., Loutre, M.F., 1994. Astronomical forcing through geological time. In: de Boer, P.L., Smith, D.G. (Eds.), International Association of Sedimentologists. Special Publication, pp. 15–24.

Berger, A., Loutre, M.F., Mélice, J.L., 2006. Equatorial insolation: from precession harmonics to eccentricity frequencies. Clim. Past 2, 131–136 hal- 00298053.

BGMRX, 1993. Regional Geology of Xizang (Tibet) Autonomous Region. Geological Publishing House, Beijing.

Boos, W.R., Kuang, Z.-M., 2010. Dominant control of the South Asian monsoon by orographic insulation versus plateau heating. Nature 463, 218–222.

Botsyun, S., Sepulchre, P., Donnadieu, Y., Risi, C., Licht, A., Caves Rugenstein, J.K., 2019. Revised paleoaltimetry data show low Tibetan Plateau elevation during the Eocene. Science 363, eaaq1436.

Briggs, J.C., 2003. The biogeography and tectonic history of India. J. Biogeogr. 30 (381–388), 397–425.

Burchfiel, B.C., Chen, Z., 2012. Tectonics of the southeast Tibetan Plateau and its adjacent foreland. Geol. Soc. Am. Mem. 210, 1–164.

Cao, S.Y., Neubauer, F., Liu, J.l., Censer, J., Leiss, B., 2011. Exhumation of the diancang Shan metamorphic complex along the Ailao Shan-Red river belt, southwestern yunnan, China: evidence from Ar-40/Ar-39 thermochronology. J. Asian Earth Sci. 42, 525–550.

Cao, K., Wang, G.-C., Leloup, P.H., Mahéo, G., Xu, Y., van der Beek, P.A., Replumaz, A., Zhang, K., 2019. Oligocene-Early Miocene topographic relief generation of southeastern Tibet triggered by thrusting. Tectonics 38, 374–391.

Carmichael, J.W., Inglis, G.N., Badger, M.P.S., Naafs, B.D.A., Behrooz, L., Remmelzwaal, S., Monteiro, F.M., Rohrssen, M., Farnsworth, A., Buss, H., Dickson, A.J., Valdes, P.J., Lunt, D.J., Pancost, R.D., 2017. Hydrological and associated biogeochemical consequences of rapid global warming during the Paleocene-Eocene Thermal Maximum. Global Planet. Change 157, 114–138.

Cautley, P.T., 1835. Letter noticing the discovery of further fossils in vast quantity in the Siwalik Range. J. Asia. Soc. Bengal 4, 585–587.

Chakraborty, A., 2020. Mountains as a global heritage: arguments for conserving the natural diversity of mountain regions. Heritage 3, 198–207.

Chatterjee, S., Scotese, C.R., 1999. The breakup of Gondwana-land and the evolution and biogeography of the Indian plate. Proc. Indiana Acad. Sci. 65A, 397–425.

Chatterjee, S., Scotese, C.R., 2010. The wandering Indian plate and its changing biogeography during the Late Cretaceous–Early Tertiary period. In: Bandopadhyay, S. (Ed.), New Aspects of Mesozoic Biogeography. Springer-Verlag, Berlin Heidelberg, Germany, pp. 105–126.

Chatterjee, S., Goswami, A., Scotese, C.R., 2013. The longest voyage: tectonic, magmatic, paleoclimatic evolution of Indian plate during its northward flight from Gondwana to Asia. Gondwana Res. 23, 238–267. https://doi.org/10.1016/j.gr.2012.07.001.

Cheng, Y.-M., Wang, Y.-F., Li, C.S., 2014. Late Miocene wood flora associated with the Yuanmou hominoid fauna from Yunnan, southwestern China and its palaeoenvironmental implication. J. Plaeogeogr. 3, 323–330.

Chitaley, S.D., 1960. A new specimen of *Nipa* fruit from Mohgaonkalan cherts. Nature 186, 495.

Chitaley, S.D., Nambudiri, E.M.V., 1995. Anatomy of *Nypa* fruit reviewed from new specimens from the Deccan Intertrappean flora of India. In: Pant, D.D. (Ed.), Global Environment and Diversification of Plants through Geological Time. South Asian Publishers, Allahabad, pp. 83–94.

Clark, M.K., Royden, L.H., 2000. Topographic ooze: building the eastern margin of Tibet by lower crustal flow. Geology 28, 703–706.

Clark, M.K., Royden, L.H., Whipple, K.X., House, M.A., Zhang, X., Tang, W., Chen, L., 2003. Late Cenozoic uplift of southeastern Tibet: implications for tectonic-climate coupling. "Monsoon Evolution and Tectonics-Climate Linkage in East Asia and its Marginal Seas during the Late Cenozoic". In: Programme with Abstracts Tokyo, pp. 7–8.

Clark, M.K., Schoenbohm, L.M., Royden, L.H., Whipple, K., Burchfiel, B.C., Zhang, B., Tang, W., Wang, E., Chen, L., 2004. Surface uplift, tectonics, and erosion of eastern Tibet from large-scale drainage patterns. Tectonics 23, TC1006.

Clark, M.K., House, M.A., Royden, L.H., Whipple, K.X., Burchfiel, B.C., Zhang, X., Tang, W., 2005. Late cenozoic uplift of southeastern Tibet. Geology 33, 525–528.

Clark, M.K., Royden, L.H., Whipple, K., Burchfiel, B.C., Zhang, X., Tang, W., 2006. Use of a regional, relict landscape to measure vertical deformation of the eastern Tibetan Plateau. J. Geophys. Res. 111, F03002.

Clark, M.K., Farley, K.A., Zheng, D., Wang, Z., Duvall, A.R., 2010. Early Cenozoic faulting of the northern Tibetan Plateau margin from apatite (U–Th)/He ages. Earth Planet Sci. Lett. 296, 78–88.

Claussen, M., Fohlmeister, J., Ganopolsky, A., Brokin, V., 2006. Vegetation dynamics amplifies precessional forcing. Geophys. Res. Lett. 33, L09709.

Clift, P.D., Carter, A., Wysocka, A., Long, H.V., Zheng, H., Neubeck, N., 2020. A late Eocene- Oligocene through-flowing river between the upper Yangtze and south China sea. G-cubed. https://doi.org/10.1029/2020GC009046.

Cohen, K.M., Finney, S.C., Gibbard, P.L., Fan, X.-L., 2013. Updated 2019, the ICS international chronostratigraphic chart. Episodes 36, 199–204.

Corlett, R., Tomlinson, K., 2019. Climate change and edaphic specialists: irresistible force meets immovable object? Trends Ecol. Evol. 35, 367–376.

Currie, B.S., Polissar, P.J., Rowley, D., Ingals, M., Li, S., Olack, G., Freeman, K.H., 2016. Multiproxy palaeoaltimetry of the late oligocene-pliocene Oiyug Basin, southern Tibet. Am. J. Sci. 316, 401–436.

Dai, J., Zhao, X., Wang, C., Zhu, L., Li, Y., Finn, D., 2012. The vast proto-Tibetan plateau: new constraints from Paleogene Hoh Xil basin. Gondwana Res. 22, 434–446.

DeCelles, P.G., Kapp, P., Ding, L., Gehrels, G., 2007a. Late Cretaceous to middle Tertiary basin evolution in the central Tibetan Plateau: changing environments in response to tectonic partitioning, aridification, and regional elevation gain. Geol. Soc. Am. Bull. 119, 654–680.

DeCelles, P.G., Quade, J., Kapp, P., Fan, M., Dettman, D.L., Ding, L., 2007b. High and dry in central Tibet during the late Oligocene. Earth Planet Sci. Lett. 253, 389–401.

Del Rio, C., Wang, T.-X., Liu, J., Liang, S.-L., Spicer, R.A., Wu, F.-X., Zhou, Z.-K., Su, T., 2020. *Asclepiadospermum* gen. nov., the earliest fossil record of Asclepiadoideae (Apocynaceae) from the early Eocene of central Qinghai-Tibetan Plateau, and its biogeographic implications. Am. J. Bot. 107, 1–13.

Deng, T., Wu, F.-X., Zhou, Z.-K., Su, T., 2020. Tibetan Plateau: an evolutionary junction for the history of modern biodiversity. Sci. China Earth Sci. 63, 172–187. https://doi.org/10.1007/s11430-019-9507-5.

Dewey, J.F., Shackleton, R.M., Chang, C.F., Sun, Y., 1988. The tectonic evolution of the Tibetan Plateau. Trans. Royal Soc. London A327, 379–413.
Ding, L., Kapp, P., Wan, X., 2005. Paleocene–Eocene record of ophiolite obduction and initial India–Asia collision, south central Tibet. Tectonics 24, TC3001.
Ding, L., Xu, Q., Yue, Y.H., Wang, H.Q., Cai, F.I., Li, S.Q., 2014. The andean-type gangdese mountains: paleoelevation record from the paleocene–eocene linzhou basin. Earth Planet Sci. Lett. 392, 250–264.
Ding, L., Maksatbeck, S., Cai, F.L., Wang, H.Q., Song, P.P., Ji, W.Q., Xu, Q., Zhang, L.Y., Muhammad, Q., Upendra, B., 2017a. Processes of initial collision and suturing between India and Asia. Sci. China Earth Sci. 60, 635–651.
Ding, L., Spicer, R.A., Yang, J., Xu, Q., Cai, F., Li, S., Lai, Q., Wang, H., Spicer, T.E.V., Yue, Y., Shukla, A., Srivastava, G., Khan, M.A., Bera, S., Mehrotra, R.C., 2017b. Quantifying the rise of the Himalaya orogen and implications for the South Asian monsoon. Geology 45, 215–218.
Dubiel, R.F., Parrish, J.T., Parrish, J.M., Good, S.C., 1991. The pangaean megamonsoon - evidence from the upper triassic chinle formation, Colorado plateau. Palaios 6, 347–370.
England, P.C., Houseman, G.A., 1988. The mechanics of the Tibetan Plateau. Phil. Trans. Roy. Soc. Lond. A326, 301–320.
Fang, A.M., Yan, Z., Liu, X.H., Pan, Y.S., Li, J.L., 2005. The flora of the Liuqu formation in South Tibet and its climate implications. Acta Micropalaeontol. Sin. 44, 435–445.
Farnsworth, A., Lunt, D.J., Robinson, S.A., Valdes, P.J., Roberts, W.H.G., Clift, P.D., Markwick, P.J., S, T., Wrobel, N., Bragg, F., Kelland, S.-J., Pancost, R.D., 2019. Past East Asian monsoon evolution controlled by paleogeography, not CO_2. Sci. Adv. 5, eaax1697.
Favre, A., Packert, M., Pauls, S.U., Jahnig, S.C., Uhl, D., Michalak, I., Muellner-Riehl, A.N., 2015. The role of the uplift of the Qinghai-Tibetan Plateau for the evolution of Tibetan biotas. Biol. Rev. 90, 236–253.
Foster, G.L., Hull, P., Lunt, D.J., Zachos, J.C., 2018. Placing our current 'hyperthermal' in the context of rapid climate change in our geological past. Phil. Trans. Roy. Soc. Lond. 376, 20170086.
Garzione, C.N., David, L.D., D, L., Quade, J., DeCelles, P.G., Butler, R.F., 2000. High times on the Tibetan plateau: palaeoelevation of the thakkhola graben, Nepal. Geology 28, 339–342.
Geng, G.-C., Tao, J.-R., 1982a. Tertiary Plants from Xizang Xizang Palaeontology. Science Press, Beijing, pp. 110–125.
Geng, G.C., Tao, J.R., 1982b. The Tertiary Paleobotany of Tibet. Chinese Academy of Sciences, Beijing.
Gilbert, C.C., Patel, B.A., Singh, N.P., Campisano, C.J., Fleagle, J.G., Rust, K.L., Pugh, K.D., Patnaik, R., 2017. New fossil primates from the lower Siwaliks of India. Am. J. Phys. Anthropol. (Suppl 64).
Gourbet, L., Leloup, P.H., Paquette, J.-L., Sorrel, P., Maheo, G., Wang, G.-C., Xu, Y., Cao, K., Antoine, P.-O., Eymard, I., Liu, W., Lu, H., Replumaz, A., Chevalier, M.-L., Zhang, K., Wu, J., Shen, T., 2017. Reappraisal of the Jianchuan Cenozoic basin stratigraphy and its implications on the SE Tibetan Plateau evolution. Tectonophysics 700–701, 162–179.
Guillot, S., Goussin, F., Airaghi, L., Replumaz, A., deSigoyer, J., Cordier, C., 2019. How and when did the Tibetan plateau grow? Russ. Geol. Geophys. 60, 957–977.
Guo, S.-X., 1975. The Plant Fossils from the Xigaze Group on Mount Jolmo Lungma Feng Region. (A Report of Scientific Expedition on Mount Jolmo Lungma Feng Region) (1965-1968). Science Press, Beijing.
Guo, S.-X., 1981. On the Elevation and Climatic Changes of the Qinghai-Xizang Plateau Based on Fossil Angiosperms, Qinghai-Xizang (Tibet) Plateau. Science Press and Gordon and Breach. Science Publications, Inc, New York, Beijing, pp. 201–206.
Guo, S.-X., Spicer, R.A., Widdowson, M., Herman, A.B., Domogatskaya, K.V., 2019. The composition of the middle Miocene (15 Ma) namling palaeoflora, south central Tibet, in the context of other Tibetan and himalayan floras. Rev. Palaeobot. Palynol. 271, 104088.
Han, C., Xu, M., Huang, Z., Wang, L., Xu, M., Mi, N., Yu, D., Guo, T., Huo, S., Tian, M., Bi, Y., 2020. Layered crustal anisotropy and deformation in the SE Tibetan plateau revealed by Markov-Chain-Monte-Carlo inversion of receiver functions. Phys. Earth Planet. In. https://doi.org/10.1016/j.pepi.2020.106522.
Harsch, M.A., Hulme, P.E., McGlone, M.S., Duncan, R.P., 2009. Are treelines advancing? A global meta-analysis of treeline response to climate warming. Ecol. Lett. 12, 1040–1049.
Hasegawa, H., Tada, R., Jiang, X., Suganuma, Y., Imsamut, S., Charusiri, P., Ichinnorov, N., Khand, Y., 2012. Drastic shrinking of the Hadley circulation during the mid- cretaceous supergreenhouse. Clim. Past 8, 1323–1337.
Hays, J.D., Imbrie, J., N.J., S., 1976. Variations in the Earth's orbit: pacemaker of the ice ages. Science 194, 1121–1132.
Hazra, T., Spicer, R.A., Hazra, M., Mahato, S., Spicer, T.E.V., Bera, S., Valdes, P.J., Farnsworth, A., Hughes, A.C., Yang, J., Khan, A.M., 2020. Latest Neogene monsoon of the Chotanagpur Plateau, eastern India, as revealed by fossil leaf architectural signatures. Palaeogeography, Palaeoclimatology. Palaeoecology 545, 109641.
He, H.-Y., Sun, J., Li, Q., Zhu, R., 2012. New age determination of the Cenozoic Lunpola basin, central Tibet. Geol. Mag. 149, 141–145.
He, Y., Li, N., Wang, Z., Wang, H., yang, G., Xiao, L., Wu, J., Sun, B., 2014. *Quercus yangyiensis* sp. nov. From the late Pliocene of baoshan, yunnan and its paleoclimatic significance. Geologica Sinica 88, 738–747. https://doi.org/10.1111/1755-6724.12234.
Hetzel, R., Dinkl, I., Haider, V., Strobl, M., von Eynatten, H., Ding, L., Frei, D., 2011. Peneplain formation in southern Tibet predates the India-Asia collision and plateau uplift. Geology 39, 983–986.
Hoke, G.D., 2018. Geochronology transforms our view of how Tibet's southeast margin evolved. Geology 46, 95–96.
Hoke, G.D., Liu-Zeng, J., Hren, M.T., Wissink, G.K., Garzione, C.N., 2014. Stable isotopes reveal high southeast Tibetan Plateau margin since the Paleogene. Earth Planet Sci. Lett. 394, 270–278.
Hoorn, C., Perrigo, A., Antonelli, A., 2018. Mountains, climate and biodiversity: an introduction. In: Hoorn, C., Perrigo, A., Antonelli, A. (Eds.), Mountains, Climate and Biodiversity. Wiley-Blackwell, Chichester, UK, pp. 1–13.
Hsu, J., Tao, J.-R., Sun, X.-J., 1973. On the discovery of *Quercus semicarpifolia* bed in Mount Shisha Pangma and its significance in botany and geology. Acta Botan. Sinensis 15, 103–119.
Huang, J., Su, T., Li, S.-F., Wu, F.-X., Deng, T., Zhou, Z., 2020. Pliocene flora and paleoenvironment of Zanda Basin, Tibet, China. Science China. Earth Sci. 63, 212–223. https://doi.org/10.1007/s11430-019-9475-2.
Huang, Y.-J., Jia, L., Wang, Q., Mosbrugger, V., Utescher, T., Su, T., Zhou, Z.-K., 2016. Cenozoic plant diversity of yunnan: a review. Plant Div. 38, 271–282.
Inglis, G.N., Farnsworth, A., Collinson, M.E., Carmichael, M.J., Naafs, B.D.A., Lunt, D.J., Valdes, P.J., Pancost, R.D., 2019. Terrestrial environmental change across the onset of the PETM and the associated impact on biomarker proxies: a cautionary tale. Global Planet. Change 181, 102991.
Jacques, F.M.B., Su, T., Spicer, R.A., Xing, Y.-W., Huang, Y.-J., Zhou, Z.-K., 2014. Late Miocene southwestern Chinese floristic diversity shaped by the southeastern uplift of the Tibetan Plateau. Palaeogeography, Palaeoclimatology. Palaeoecology 411, 208–215.
Jacques, F.M.B., Shi, G., Sua, T., Zhou, Z., 2015. A tropical forest of the middle Miocene of Fujian (SE China) reveals Sino-Indian biogeographic affinities. Rev. Palaeobot. Palynol. 216, 76–91.
Jaeger, J.J., Courtillot, V., Tapponnier, P., 1989. Paleontological view of the ages of the Deccan traps, the Cretaceous/Tertiary boundary, and the India-Asia collision. Geology 17, 316–319.
Jia, L.-B., Su, T., Huang, Y.-J., Wu, F.-X., Deng, T., Zhou, Z.-K., 2019. First fossil record of *Cedrelospermum* (ulmaceae) from the Qinghai–Tibetan plateau: implications for morphological evolution and biogeography. J. Systemat. Evol. 57, 94–104.
Jiang, H., Su, T., Wong, W.-O., Wu, F., Huang, J., Shi, G., 2019. Oligocene *Koelreuteria* (Sapindaceae) from the Lunpola Basin in central Tibet and its implication for early diversification of the genus. J. Asian Earth Sci. 175, 99–108.
Jin, C., Liu, Q., Liang, W., Roberts, A.P., Sun, J., Hu, P., Zhao, X., Su, Y., Jiang, Z., Liu, Z., Duan, Z., Yang, H., Yuan, S., 2018. Magnetostratigraphy of the fenghuoshan group in the Hoh Xil basin and its tectonic implications for India–Eurasia collision and Tibetan plateau deformation. Earth Planet Sci. Lett. 486, 41–53. https://doi.org/10.1016/j.epsl.2018.01.010.
Kapp, P., DeCelles, P.G., 2019. Mesozoic-cenozoic geological evolution of the himalayan-Tibetan orogen and working tectonic hypotheses. Am. J. Sci. 319, 159–254.
Kapp, P., DeCelles, P.G., Leier, A.L., Fabijanic, J.M., He, S., Pullen, A., Gehrels, G.E., Ding, L., 2007. The Gangdese retroarc thrust belt revealed. GSA Today 17, 4–9.
Kapur, V.V., Das, D.B., Bajpai, S., Prasad, G.V.R., 2017. First mammal of Gondwanan lineage in the early Eocene of India. Comptes Rendus Palevol 16, 721–737.
Kathal, P.K., Srivastava, R., Mehrotra, R.C., Alexander, P.O., 2017. *Rhizopalmoxylon nypoides* a new palm root from the Deccan Intertrappean beds of Sagar, Madhya Pradesh, India. J. Earth Syst. Sci. 126, 35.
Kelly, S., Baumont, C., Butler, J.P., 2019. Inherited terrane properties explain enigmatic post-collisional Himalayan-Tibetan evolution. Geology 48, 8–14.
Khan, A.M., Bera, S., 2014. New lauraceous species from the Siwalik forest of Arunachal Pradesh, eastern Himalaya, and their palaeoclimatic and palaeogeographic implications. Turk. J. Bot. 38, 453–464.
Khan, M.A., Stern, R.J., Gribble, R.F., Windley, B.F., 1997. Geochemical and isotopic constraints on subduction polarity, magma sources, and palaeogeography of the Kohistan intra-oceanic arc, northern Pakistan Himalaya. J. Geologi. Soc. london 154, 935–946.
Khan, S.D., Walker, D.J., Hall, S.A., Burke, K.C., Shah, M.T., Sytockli, L., 2009. Did the Kohistan-Ladakh island arc collide first with India? Geol. Soc. Am. Bull. 121, 366–384.
Khan, M.A., Ghosh, R., Bera, S., Spicer, R.A., Spicer, T.E.V., 2011. Floral diversity during plio-pleistocene Siwalik sedimentation (kimin formation) in Arunachal Pradesh, India, and its palaeoclimatic significance. Palaeobiodivers. Palaeoenviron. 91, 237–255.
Khan, M.A., Spicer, R.A., Bera, S., Ghosh, R., Yang, J., Spicer, T.E.V., Guo, S.-X., Su, T., Jacques, F.M.B., Grote, P.J., 2014a. Miocene to Pleistocene floras and climate of the eastern himalayan Siwaliks, and new palaeoelevation estimates for the namling–Oiyug Basin, Tibet. Global Planet. Change 113, 1–10.
Khan, M.A., Spicer, R.A., Spicer, T.E.V., Bera, S., 2014b. Fossil evidence of insect folivory in the eastern Himalayan Neogene Siwalik forests. Palaeogeography, Palaeoclimatology. Palaeoecology 430, 264–277.
Khan, M.A., Bera, M., Spicer, R.A., Spicer, T.E.V., Bera, S., 2019. Palaeoclimatic estimates for a latest miocene-pliocene flora from the Siwalik group of Bhutan: evidence for the development of the south asian monsoon in the eastern Himalaya. Palaeogeography, palaeoclimatology. Palaeoecology 514, 326–335.
Klaus, S., Morley, R.J., Plath, M., Zhang, Y.-P., Li, J.-T., 2016. Biotic interchange between the Indian subcontinent and mainland Asia through time. Nat. Commun. 7, 12132.
Körner, C., 2003. Alpine Plant Life: Functional Plant Ecology of High Mountain Ecosystems. Springer, Berlin Heidelburg.

Krause, D.W., Prasad, G.V.R., Koenigswald, W.V., Sahni, A., Grine, F.E., 1997. Cosmopolitanism among gondwanan late cretaceous mammals. Nature 390, 504–507.
Kuhle, M., 1998. Reconstruction of the 2.4 million km^2 late Pleistocene ice sheet on the Tibetan Plateau and its impact on the global climate. Quat. Int. 45, 71e108.
Kundal, S.N., Bhadur, G., Kumar, S., 2017. *Elephas* cf. *E. planifrons* (elephantidae, mammalia) from upper Siwalik subgroup of samba district, Jammu and Kashmir, India. Vertebr. Palasiat. 55, 59–70.
Lai, W., Hu, X., Garzanti, E., Xu, Y., Ma, A., Li, W., 2019. Early Cretaceous sedimentary evolution of the northern Lhasa terrane and the timing of initial Lhasa-Qiangtang collision. Gondwana Res. 73, 136–152.
Laskowski, A.K., O'rme, D.A., Cai, F., Ding, L., 2019. The ancestral Lhasa River: a late cretaceous trans-arc river that drained the proto–Tibetan plateau. Geology 47, 1029–1033.
Leary, R.J., DeCelles, P.G., Quade, J., Gehrels, G.E., Waanders, G., 2016. The Liuqu Conglomerate, southern Tibet: early Miocene basin development related to deformation within the Greater Counter Thrust system. Lithosphere 8, 427–450.
Leary, R.J., Quade, J., DeCelles, P., 2017. Evidence from paleosols for low to moderate elevation of the India-Asia suture zone during mid-Cenozoic time. Geology 45, 399–402.
Leloup, P.H., Lacassin, R., Tapponier, P., Schärer, U., Zhong, D.-L., Liu, X.-H., Zhang, L.-S., Ji, S.-C., Trong Tring, P., 1995. The Ailao Shan-Red river shear zone (yunnan, China), tertiary transform boundary of indochina. Tectonophysics 251, 3–84.
Leuschner, D.C., Sirocko, F., 2003. Orbital insolation forcing of the Indian Monsoon – a motor for global climate changes? Palaeogeography, Palaeoclimatology. Palaeoecology 197, 83–95.
Li, W.-Y., 1998. Quaternary Vegetation and Environment in China. Science Press, Beijing.
Li, H.-M., Guo, S.-X., 1976. Miocene flora from namling, xizang. Acta Palaeontol. Sin. 15, 7–18.
Li, J.-S., Batten, D.J., 2004. Early cretaceous palynofloras from the Tanggula mountains of the northern qinghai-xizang (Tibet) plateau, China. Cretac. Res. 25, 531–542.
Li, J.G., Zhou, Y., 2001. Pliocene palynoflora from the Zanda Basin west Xizang (Tibet), and the palaeoenvironment (in Chinese). Acta Micropalaeontologica Sinica 18, 89–96.
Li, X.-H., Zhu, X.-X., Niu, Y.-T., Sun, H., 2014. Phylogenetic clustering and overdispersion for alpine plants along elevational gradient in the Hengduan Mountains Region, southwest China. J. Systemat. Evol. 52, 280–288.
Li, S., Currie, B.S., Rowley, D.B., Ingalls, M., 2015a. Cenozoic paleoaltimetry of the SE margin of the Tibetan Plateau: constraints on the tectonic evolution of the region. Earth Planet Sci. Lett. 432, 415–424.
Li, S.-H., Deng, C., Dong, W., Sun, L., Liu, S., Qin, H., Yin, J., Ji, X., Zhu, R., 2015c. Magnetostratigraphy of the Xiaolongtan Formation bearing *Lufengpithecus keiyuanensis* in Yunnan, southwestern China: constraint on the initiation time of the southern segment of the Xianshuihe-Xiaojiang fault. Tectonophysics 655, 213–226.
Li, Y.-L., Wang, C.-S., Dai, J.-G., Xu, G.-Q., Hou, Y.-L., Li, X.-H., 2015b. Propagation of the deformation and growth of the Tibetan-Himalayan orogen: a review. Earth Sci. Rev. 143, 36–61.
Li, S.H., Advokaat, E.L., van Hinsbergen, D.J.J., Koymans, M., Deng, C., Zhu, R., 2017. Paleomagnetic constraints on the Mesozoic-Cenozoic paleolatitudinal and rotational history of Indochina and South China: review and updated kinematic reconstruction. Earth Sci. Rev. 171, 58–77.
Li, L., Garzione, C.N., Fan, M., Li, X.-W., Li, X.-Z., 2019. Jurassic sedimentation in the south-central Qiangtang terrane reveals successive terrane collisions in central Tibet. Geosphere 15. https://doi.org/10.1130/GES01649.1.
Li, S., Yin, C., Guilmette, C., Ding, L., Zhang, J., 2019. Birth and demise of the bangong-nujiang tethyan ocean: a review from the gerze area of central Tibet. Earth-Sci. Rev. 198, 102907. https://doi.org/10.1016/j.earscirev.2019.102907.
Li, S.-H., Ji, X.-P., Harrison, T., Deng, C.-L., Wang, S.-Q., Wang, L., Zhu, R.-X., 2020a. Uplift of the Hengduan Mountains on the southeastern margin of the Tibetan Plateau in the late Miocene and its paleoenvironmental impact on hominoid diversity. Palaeogeography, Palaeoclimatology. Palaeoecology 109794. https://doi.org/10.1016/j.palaeo.2020.109794.
Li, S.-H., Su, T., Spicer, R.A., Xu, C.-L., Sherlock, S., Halton, A., Hoke, G., Tian, Y.-M., Zhou, Z.-K., Deng, C.-L., Zhu, R.-X., 2020b. Oligocene deformation of the Chuandian terrane in the SE margin of the Tibetan Plateau related to the extrusion of Indochina. Tectonics.
Li, S.-H., van Hinsbergen, D.J.J., Najman, Y., Jing, L.-Z., 2020c. Does pulsed Tibetan deformation correlate with Indian plate motion changes? Earth Planet Sci. Lett. 536, 116144.
Linnemann, U., Su, T., Kunzmann, L., Spicer, R.A., Ding, W.-N., Spicer, T.E.V., Zieger, J., Hofmann, M., Moraweck, K., Gärtner, A., Gerdes, A., Marko, L., Zhang, S.-T., Li, S.-F., Tang, H.L., Huang, J., Mulch, A., Mosbrugger, V., Zhou, Z.-K., 2018. New U-Pb dates show a Paleogene origin for the modern Asian biodiversity hot spots. Geology 46, 3–6.
Liu, X.-H., Xu, Q., Ding, L., 2016. Differential surface uplift: Cenozoic palaeoelevation history of the Tibetan Plateau. Sci. China Earth Sci. 59, 2105–2120.
Liu, J., Su, T., Spicer, R.A., Tang, H., Deng, W.-Y.-D., Wu, F.-X., Srivastava, G., Spicer, T.E.V., Van Do, T., Deng, T., Zhou, Z.-K., 2019. Biotic interchange through lowlands of Tibetan plateau suture zones during Paleogene. Palaeogeography, palaeoclimatology. Palaeoecology 524, 33–40.
Liu-Zheng, J., Tapponier, P., Gaudemer, Y., Ding, L., 2008. Quantifying landscape differences across the Tibetan plateau: implications for topographic relief evolution. J. Geophys. Res. 113, F04018.
Liu-Zheng, J., Zhang, J., McPhillips, D., Reiners, P.W., Wang, W., Pik, R., Zeng, L., Hoke, G.D., Xie, K., Xiao, P., Zheng, D., Ge, Y., 2018. Multiple episodes of fast exhumation since Cretaceous in southeast Tibet, revealed by low-temperature thermochronology. Earth Planet Sci. Lett. 490, 62–76.
Low, S.L., Su, T., Spicer, T.E.V., Wu, F.-X., Deng, T., Xing, Y.-W., Zhou, Z.-K., 2019. Oligocene *Limnobiophyllum* (Araceae) from the central Tibetan Plateau and its evolutionary and palaeoenvironmental implications. J. Syst. Palaeontol. 18, 415–431. https://doi.org/10.1080/14772019.2019.1611673.
López-Pujol, J., Zhang, F.-M., Sun, H.-Q., Ying, T.-S., Ge, S., 2011. Centres of plant endemism in China: places for survival or for speciation? J. Biogeogr. 38, 1267–1280.
Lu, L.-M., Mao, L.F., Yang, T.-N., Ye, J.-F., Liu, B., Li, H.-L., Miller, J.T., Mathews, S., Hu, H.-H., Niu, Y.-T., Peng, D.-X., Chen, Y.-H., Smith, S.A., Chen, M., Xiang, K.L., Le, C.-T., Dang, V.C., Lu, A.-M., Soltis, P.S., Soltis, D.E., Li, J.-H., Chen, Z.-D., 2018. Evolutionary history of the angiosperm flora of China. Nature 554, 234–238.
Ma, P., Wang, C., Meng, J., Ma, C., Zhao, X., Li, Y., Wang, M., 2017. Late Oligocene-early Miocene evolution of the Lunpola Basin, central Tibetan Plateau, evidences from successive lacustrine records. Gondwana Res. 48, 224–236.
Mao, Z.-Q., Meng, Q.-Q., Fang, X.-M., Zhang, T., Wu, P., Yang, Y., Zhang, W., Zan, J., Tan, M.-Q., 2019. Recognition of tuffs in the middle-upper Dingqinghu Fm., Lunpola Basin, central Tibetan Plateau: constraints on stratigraphic age and implications for paleoclimate. Palaeogeogr. Palaeoclimatol. Palaeoecol. 525, 44–56.
Meng, J., Coe, R.S., Wang, C.-S., Gilder, S., Zhao, X., Liu, H., Li, Y., Ma, P., Shi, K., Li, S., 2017. Reduced convergence within the Tibetan plateau by 26 Ma? Geophys. Res. Lett. 44 https://doi.org/10.1002/2017GL074219.
Meyer, H.W., 2007. A Review of paleotemperature-lapse rate methods for estimating paleoelevation from fossil floras. Rev. Mineral. Geochem. 66, 155–171.
Molnar, P., Stock, J.M., 2009. Slowing of India's Convergence with Eurasia since 20 Ma and its Implications for Tibetan Mantle Dynamics, Tectonics. American Geophysical Union.
Molnar, P., England, P., Martinod, J., 1993. Mantle dynamics, uplift of the Tibetan Plateau and the Indian monsoon. Rev. Geophys. 31, 357–396.
Molnar, P., Boos, W.R., Battisti, D.S., 2010. Orographic controls on climate and paleoclimate of Asia: thermal and mechanical roles for the Tibetan Plateau. Annu. Rev. Earth Planet Sci. 38, 77–102.
Morley, R.J., 2000. Origin and Evolution of Tropical Rain Forests. John Wiley and Sons, Chichester (UK).
Morley, R.J., 2018. Assembly and division of the South and South-East Asian flora in relation to tectonics and climate change. J. Trop. Ecol. 34, 209–234.
Mosbrugger, V., Utescher, T., 1997. The coexistence approach—a method for quantitative reconstructions of Tertiary terrestrial palaeoclimate data using plant fossils. Palaeogeography, Palaeoclimatology,. Palaeoecology 134, 61–86.
Mulch, A., 2016. Stable isotope paleoaltimetry and the evolution of landscapes and life. Earth Planet Sci. Lett. 433, 180–191.
Mulch, A., Chamberlain, C.P., 2006. Earth science e the rise and growth of Tibet. Mulch, A., Chamberlain, C.P., 2006 Nature 439, 670e671.
Mulch, A., Chamberlain, C.P., 2018. Stable isotope paleoaltimetry: paleotopography as a key element in the evolution of landscapes and life. In: Hoorn, C., Perrigo, A., Antonelli, A. (Eds.), Mountains, Climate and Biodiversity. Wiley Blackwell, pp. 81–93.
Myers, N., Mittermeir, C.G., da Fonseca, G.A.B., Kent, J., 2000. Biodiversity hotspots for conservation priorities. Nature 403, 218–222.
Neukom, R., Steiger, N., Gómez-Navarro, J.J., Wang, J., Werner, J.P., 2019. No evidence for globally coherent warm and cold periods over the preindustrial Common Era. Nature 571, 550–554.
Ni, X.J., Li, Q., Zhang, C., Samiullah, K., Zhang, L., Yang, Y., Cao, W., 2020. Paleogene mammalian fauna exchanges and the paleogeographic pattern in Asia. Sci. China Earth Sci. 63, 202–211.
Nie, J., Ruetenik, G., Gallagher, K., Hoke, G.D., Garzione, C.N., Wang, W., Stockli, D., Hu, X., Wang, Z., Wang, Y., Stevens, T., Danišík, M., Liu, S., 2018. Rapid incision of the Mekong River in the middle Miocene linked to monsoonal precipitation. Nat. Geosci. 11, 944–949.
ODSN (Ocean Drilling Stratigraphic Network) website. http://www.odsn.de/odsn/services/paleomap/paleomap.html. (Accessed 5 March 2020).
Paeth, H., Steger, C., Li, J., Pollinger, F., Mutz, S.G., Ehlers, T.A., 2019. Comparison of climate change from Cenozoic surface uplift and glacial-interglacial episodes in the Himalaya-Tibet region: insights from a regional climate model and proxy data. Global Planet. Change 177, 10–26. https://doi.org/10.1016/j.gloplacha.2019.03.005.
Paine, R.T., 1969. A note on trophic complexity and community stability. Am. Nat. 103, 91–93.
Parrish, J.T., 1993. Climate of the supercontinent pangaea. J. Geol. 101, 215–233.
Peel, M.C., Finlayson, B.L., McMahon, T.A., 2007. Updated world map of the Köppen-Geiger climate classification. Hydrol. Earth Syst. Sci. Discuss. 4, 439–473.
Polissar, P., Freeman, K., Rowley, D., McInerney, F., Currie, B.S., 2009. Paleoaltimetry of the Tibetan Plateau from D/H ratios of lipid biomarkers. Earth Planet Sci. Lett. 287, 64–76.

Pound, M.J., Salzmann, U., 2017. Heterogeneity in global vegetation and terrestrial climate change during the late Eocene to early Oligocene transition. Sci. Rep. 7, 43386. https://doi.org/10.1038/srep43386.
Prakash, T., Singh, R.Y., Sahni, A., 1990. Palynoforal assemblage from the padwar deccan intertrappeans. In: Jabalpur, M.P., Sahni, A., Jolly, A. (Eds.), Proceedings of the International Geological Correlation Programme 216 and 245. Seminar cum Workshop, Chandigarh, pp. 68–89. Sahni, A., Jolly, A. (Eds.), Proceedings of the International Geological Correlation Programme 216 and 245. Seminar cum Workshop, Chandigarh.
Prasad, G.V.R., V, S., Farooqui, A., Murthy, S., Sarate, O.S., Bajpai, S., 2018. Palynological assemblage from the Deccan Volcanic Province, central India: insights into early history of angiosperms and the terminal Cretaceous paleogeography of peninsular India. Cretac. Res. 86, 186–198.
Prasad, G.V.R., Sahni, A., 1999. Were there size constraints on biotic exchanges during the northward drift of the Indian plate? In: Sahni, A., Loyal, R.S. (Eds.), Gondwana Assemblage: New Issues and Perspective. Proceedings of the National Science Academy A, pp. 377–379.
Prasad, G.V.R., Sahni, A., 2009. Late Cretaceous continental vertebrate fossil record from India: palaeobiogeographic insights. Bull. Geologic. Soc. Fr. 180, 369–381.
Prasad, M., Antal, J.S., Tripathi, P.P., Pandey, V.K., 1999. Further contribution to the Siwalik flora from the Koilabas area, western Nepal. Palaeobotanist 48, 49–95.
Quade, J., Leary, R., Dettinger, M.P., Orme, D., Krupa, A., DeCelles, P.G., Kano, A., Kato, H., Waldrip, R., Huang, W., Kapp, P., 2020. Resetting Southern Tibet: The serious challenge of obtaining primary records of paleoaltimetry. Glob. Planet. Change 191, 103194. https://doi.org/10.1016/j.gloplacha.2020.103194.
Rahbeck, C., Borregaard, M.K., Antonelli, A., Colwell, R.K., Holt, B.G., Nogues-Bravo, D., Rasmussen, C.M.Ø., Richardson, K., Rsoing, M.T., Whittaker, R.J., Fjeldså, J., 2019a. Building mountain biodiversity: geological and evolutionary processes. Science 365, 1114–1119.
Rahbeck, C., Borregaard, M.K., Colwell, R.K., Dalsgaard, B., Holt, B.G., Morueta-Holme, N., Nogues-Bravo, D., Whittaker, J.J., GFjeldsa, J., 2019b. Humboldt's enigma: what causes global patterns of mountain biodiversity? Science 365, 1108–1113.
Ramage, C.S., 1971. Monsoon Meteorology. Academic Press, New York.
Reichgelt, T., West, C.K., Greenwood, D.R., 2018. The relation between global palm distribution and climate. Sci. Rep. 8, 4721–4731.
Renner, S.S., 2016. Available data point to a 4-km-high Tibetan Plateau by 40 Ma, but 100 molecular-clock papers have linked supposed recent uplift to young node ages. J. Biogeogr. 43, 1479–1487.
Rousseau, D.-D., Duzer, D., Cambon, G., Jolly, D., Poulsen, U., Ferrier, J., Schevin, P., Gros, R., 2004. Long-distance transport of pollen to Greenland. Geophys. Res. Lett. 30, 1765.
Rousseau, D.-D., Schevin, P., Duzer, D., Cambon, G., Ferrier, J., Jolly, D., Poulsen, U., 2006. New evidence of long distance pollen transport to southern Greenland in Late Spring. Rev. Paleobotany Palynol. 141, 277–286.
Rousseau, D.-D., Schevin, P., Ferrier, J., Jolly, D., Andreasen, T., Ascanius, S.E., Hendriksen, S.-E., Poulsen, U., 2008. Long-distance pollen transport from north America to Greenland in spring. J. Geophys. Res. 113, G02013.
Rowley, D., Currie, B.S., 2006. Palaeo-altimetry of the late Eocene to Miocene Lunpola Basin, central Tibet. Nature 439, 677–681.
Rowley, D., Pierrehumbert, R.T., Currie, B.S., 2001. A new approach to stable isotope-based paleoaltimetry; implications for paleoaltimetry and paleohypsometry of the High Himalaya since the late Miocene. Earth Planet Sci. Lett. 188, 253–268.
Royden, L.H., Burchfiel, B.C., King, R.W., Wang, e., Chen, Z.I., Shen, F., Liu, Y.P., 1997. Surface deformation and lower crustal flow in eastern Tibet. Science 276, 788–790.
Royden, L.H., Burchfiel, B.C., van der Hilst, R.D., 2008. The geological evolution of the Tibetan Plateau. Science 231, 1054–1058.
Sahni, A., Bajpai, S., 1991. Eurasiatic elements in the Upper Cretaceous nonmarine biotas of peninsular India. Cretac. Res. 12, 177–183.
Sahni, A., Prasad, G.V.R., 2008. Geodynamic evolution of the Indian Plate: consequences for dispersal distribution of biota. Gold. Jubilee Memor. Geologi. Soc. India 66, 203–225.
Samant, B., Mohabey, D.M., 2014. Deccan volcanic eruptions and their impact on flora: palynological evidence. Geol. Soc. Am. Spec. Pap. 505, 171e191.
Samant, B., Mohabey, D.M., Paudayal, K.N., 2013. *Aquilapollenites* and other triprojectate pollen from the late cretaceous to early Paleocene deccan intertrappean deposits of India. Palynology 37, 298–315.
Sankhyan, A.R., Chavasseau, O., 2018. New proboscidean fossils from middle Siwaliks of haritalyangar, Himachal Pradesh. India Palaeontologica Electronica. https://doi.org/10.26879/844.
Sankhyan, A.R., Ěeròanský, A., 2016. A first possible chameleon from the Late Miocene of India (the hominoid site of Haritalyangar): a tentative evidence for an Asian dispersal of chameleons. Sci. Nat. 103, 94.
Sankhyan, A.R., Kelley, J., Harrison, T., 2017. A highly derived pliopithecoid from the Late Miocene of Haritalyangar,. India J. Human Evol. 105, 1–12.
Saylor, J.E., Quade, J., Dettman, D.L., DeCelles, P.G., Kapp, P.A., Ding, L., 2009. The late Miocene through present paleoelevation history od southwestern Tibet. Am. J. Sci. 309, 1–42.
Schoenbohm, L.M., Burchfiel, B.C., Liangzhong, C., 2006. Propagation of surface uplift, lower crustal flow, and Cenozoic tectonics of the southeast margin of the Tibetan Plateau. Geology 34, 813–816.
Searle, M.P., Elliott, J.R., Phillips, R.J., Chung, S.-L., 2011. Crustal-lithospheric structure and continental extrusion of Tibet. J. Geol. Soc. (Lond.) 168, 633–672.
Şengör, A.C., 1984. The Cimmeride orogenic system and the tectonics of Eurasia. Spec. Pap. Geol. Soc. Am. 195, 1–74.
Shete, R.H., Kulkarni, A.R., 1982. Contributions to the dicotyledonous woods of the deccan intertrappeans (early tertiary) beds of wardha district Maharashtra, India. Palaeontographica 183, 57–81.
Shi, Y.F., Li, J.J., Li, B.Y., 1998. Uplift and Environmental Changes of Qinghai-Xizang (Tibetan) Plateau in the Late Cenozoic., Uplift and Environmental Changes of Qinghai-Xizang (Tibetan) Plateau in the Late Cenozoic. Guangdong Science and Technology Press, Guangdong, pp. 1–459.
Shi, Y.-F., Cui, Z.-J., Su, Z., 2006. The Quaternary glaciations and environmental variations in China. Shijiazhuang, Heibei Province, China: Heibei Science and Technology Publishing House.
Smith, T., Kumar, K., Rana, R.S., Folie, A., Solé, F., Noiret, C., Steeman, T., Sahni, A., Rose, K.D., 2016. New early Eocene vertebrate assemblage from western India reveals a mixed fauna of European and Gondwana affinities. Geosci. Front. 7, 1–33.
Song, Z.-C., Li, M.Y., 1982. Eocene palynological assemblages from the gongjo formation in qamdün region, xizang (Tibet). People press of Sichuan, Chengdu.
Song, Z.C., Liu, J.L., 1982. The Tertiary Sporo-Pollen Assemblages from Namling of Xizang. Palaeontology of Xizang. Science Press, Beijing, pp. 153–164.
Spicer, R.A., 1981. The sorting and deposition of allochthonous plant material in a modern environment at Silwood Lake, Silwood Park, Berkshire. In: United States Geological Survey Professional Paper, 1143, pp. 1–77.
Spicer, R.A., 1991. Plant taphonomic processes. In: Allison, P.A., Briggs, D.E.G. (Eds.), Taphonomy: Releasing the Data Locked in the Fossil Record. Plenum Press, New York, pp. 71–113. ISBN 0-306-43876-3.
Spicer, R.A., 2017. Tibet, the Himalaya, Asian monsoons and biodiversity - in what ways are they related? Plant Div. 39, 233–244.
Spicer, R.A., 2018. Phytopaleoaltimetry: using plant fossils to measure past land surface elevation. In: Hoorn, C., Perrigo, A., Antonelli, A. (Eds.), Mountains, Climate and Biodiversity. Wiley Blackwell, pp. 95–109.
Spicer, R.A., Collinson, M., 2014. Plants and floral change at the Cretaceous-Paleogene boundary: three decades on. Geol. Soc. Am. Spec. Pap. 505.
Spicer, R.A., Harris, N.B.W., Widdowson, M., Herman, A.B., Guo, S., Valdes, P.J., Wolfe, J.A., Kelley, S.P., 2003. Constant elevation of Southern Tibet over the past 15 million years. Nature 412, 622–624.
Spicer, R.A., Ahlberg, A., Herman, A.B., Hofmann, C.-C., Raikevich, M.I., Valdes, P.J., Markwick, P.J., 2008. The Late Cretaceous continental interior of Siberia: a challenge for climate models. Earth Planet Sci. Lett. 267, 228–235.
Spicer, R.A., Yang, J., Herman, A.B., Kodrul, T., Maslova, N., Spicer, T.E.V., Aleksandrova, G., Jin, J., 2016. Asian Eocene monsoons as revealed by leaf architectural signatures. Earth Planet Sci. Lett. 449, 61–68.
Spicer, R.A., Yang, J., Herman, A.B., Kodrul, T., Aleksandrova, G., Maslova, N., Spicer, T.E.V., Ding, L., Xu, Q., Shukla, A., Srivastava, G., Mehrotra, R.C., Liu, X.-Y., Jin, J., 2017. Paleogene monsoons across India and South China: drivers of biotic change. Gondwana Res. 49, 350–363.
Spicer, R.A., Su, T., Valdes, P.J., Farnsworth, A., Wu, F.-X., Shi, G., Spicer, T.E.V., Zhou, Z.-K., 2020. Why the 'uplift of the Tibetan plateau' is a myth. Natl. Sci. Rev. nwaa091. https://doi.org/10.1093/nsr/nwaa091.
Spurlin, M.S., Yin, A., Horton, B.K., Zhou, J., Wang, J., 2005. Structural evolution of the Yushu-Nangqian region and its relationship to syncollisional igneous activity, east-central Tibet. Geol. Soc. Am. Bull. 117, 1293–1317.
Srivastava, G., Adhikari, P., Mehrotra, R.C., Paudel, L., Uhl, D., Paudayal, K.N., 2017. *Dipterocarpus* Gaertn. (Dipterocarpaceae) leaf from the Middle Siwalik of eastern Nepal and its phytogeographic and climatic significance. J. Nepal Geol. Soc. 53, 39–46.
Srivastava, G., Mehrotra, R.C., Srikarni, C., 2018a. Fossil wood flora from the Siwalik Group of Arunachal Pradesh, India and its climatic and phytogeographic significance. J. Earth Syst. Sci. 127, 2. https://doi.org/10.1007/s12040-017-0903-2.
Srivastava, G., Mehrotra, R.C., Srikarni, C., 2018b. *Lagerstroemia* L. Wood from the Kimin Formation (upper Siwalik) of Arunachal Pradesh and its climatic and phytogeographic significance. J. Geol. Soc. India 91, 695–699.
Srivastava, G., Paudayal, K.N., Utescher, T., Mehrotra, R.C., 2018c. Miocene vegetation shift and climate change: Evidence from the Siwalik of Nepal. Glob. Planet. Change 161, 108–120.
Staisch, L.M., Niemi, N., Hing, C., Clark, M.K., Rowley, D.B., Currie, B.S., 2014. A Cretaceous-Eocene depositional age for the Fenghuoshan Group, Hoh Xil basin: implications for the tectonic evolution of the northern Tibet plateau. Tectonics 33, 281–301.
Strobl, M., Hetzel, R., Niedermann, S., Ding, L., Zhang, L., 2012. Landscape evolution of a bedrock peneplain on the southern Tibetan Plateau revealed by in situ-produced cosmogenic 10Be and 12Ne. Geomorphology 153, 192–204.
Su, T., Jacques, F.M.B., Spicer, R.A., Liu, Y.-S., Huang, Y.-J., Xing, Y.-W., Zhou, Z.-K., 2013. Post-Pliocene establishment of the present monsoonal climate in SW China: evidence from the late Pliocene Longmen megaflora. Clim. Past 9, 1911–1920.
Su, T., Spicer, R.A., Li, S.-H., Xu, H., Huang, J., Sherlock, S., Huang, Y.-J., Li, S.-F., Wang, L., Jia, L.B., Deng, W.-Y.-D., Deng, C.-L., Zhang, S.-T., Valdes, P.J., Zhou, Z.-K., 2018. Climate and biotic changes at the eocene-oligocene transition in south-east Tibet. Natl. Sci. Rev. 6, 495–504.
Su, T., Farnsworth, A., Spicer, R.A., Huang, J., Wu, F.-X., Liu, J., Li, S.-F., Xing, Y.-W., Huang, Y.-J., Deng, W.-Y.-D., Tang, H., Xu, C.-L., Zhao, F., Srivastava, G., Valdes, P.J., Deng, T., Zhou, Z.-K., 2019. No high Tibetan plateau until the Neogene. Sci. Adv. 5, eaav2189.

Sun, X.J., Wang, P., 2005. How old is the Asian monsoon system?——palaeobotanical records from China. Palaeogeography, Palaeoclimatology. Palaeoecology 222, 181–222.
Tanaka, T., 1954. Species Problem in Citrus. Tokyo: Japanese Society for the Promotion of Science. Ueno, Tokyo, pp. 1–15.
Tang, H., Liu, J., Wu, F.-X., Magner, T.E.V., Spicer, R.A., Deng, W.-Y.-D., Xu, C., Zhao, F., Huang, J., Li, S.F., Su, T., Zhou, Z.-K., 2019. An extinct genus *Lagokarpos* reveals a biogeographic connection of the Tibet with other regions in the Northern Hemisphere during the Paleogene. J. Systemat. Evol. 57, 670–677.
Tao, J.-R., 1988. The Fossil Plant Assemblage and its Palaeoclimatical Significance of the Liuqu Formation in Lhaze County, Tibet. Academica Sinica, Beijing.
Tao, J.-R., 2000. The Evolution of the Late Cretaceous —Cenozoic Floras in China. Science Press, Beijing.
Tapponnier, P., Peltzer, G., Le Dain, A.Y., Armijo, R., Cobbold, P.R., 1982. Propagating extrusion tectonics in Asia: new insights from simple experiments with plasticine. Geology 10, 611–616.
Tapponnier, P., Lacassin, R., Leloup, P.H., Scharer, U., Zhong, D.L., Wu, H.W., Liu, X.H., Ji, S.C., Zhang, L.S., Zhong, Y.J., 1990. The Ailao Shan Red river metamorphic belt - tertiary left-lateral shear between indochina and south China. Nature 343, 431–437.
Tapponnier, P., Xu, Z.Q., Roger, F., Meyer, B., Arnaud, N., Wittlinger, G., Yang, J.S., 2001. Oblique stepwise rise and growth of the Tibet Plateau. Science 294, 1671–1677.
Tian, Y.T., Kohn, B.P., Gleadow, A.J.W., Hsu, S.B., 2014. A thermochronological perspective on the morphotectonic evolution of the southeastern Tibetan Plateau. J. Geophys. Res. 119, 676–698.
Tiwari, A., Uprety, Y., Rana, S.K., 2019. Plant endemism in the Nepal Himalayas and phytogeographical implications. Plant Div. 41, 174–182.
Tong, Y., Yang, Z., Mao, C., Pei, J., Pu, Z., Xu, Y., 2017. Paleomagnetism of Eocene redbeds in the eastern part of the Qiangtang Terrane and its implications for uplift and southward crustal extrusion in the southeastern edge of the Tibetan Plateau. Earth Planet Sci. Lett. 475, 1–14.
Treloar, P., Petterson, M.G., Jan, M.Q., Sullivan, M.A., 1996. A re-evaluation of the stratigraphy and evolution of the Kohistan arc sequence, Pakistan Himalaya: implications for magmatic and tectonic arc-building processes. J. Geologi. Soc. london 153, 467–475.
Tuenter, E., Weber, S.L., Hilgen, F.J., Lourens, L.J., 2006. Simulating sub-Milankovitch climate variations associated with vegetation dynamics. Clim. Past 2, 745–769.
Utescher, T., Bruch, A.A., Erdei, B., Francois, L., Ivanov, D., Jacques, F.M.B., Kern, A.K., Liu, Y.-S.C., Mosbrugger, V., Spicer, R.A., 2014. The Coexistence Approach—Theoretical background and practical considerations of using plant fossils for climate quantification. Palaeogeography, Palaeoclimatology,. Palaeoecology 410, 58–73.
Valdes, P.J., Armstrong, E., Badger, M.P.S., Bradshaw, C.D., Bragg, F., Davies-Barnard, T., Day, J.J., Farnsworth, A., Hopcroft, P.O., Kennedy, A.T., Lord, N.S., Lunt, D.J., Marzocchi, A., Parry, L.M., Roberts, W.H.G., Stone, E.J., Tourte, G.J.L., Williams, J.H.T., 2017. The BRIDGE HadCM3 family of climate models: HadCM3@Bristol v1.0. Geosci. Model Develop. 10, 3715–3743.
van Hinsbergen, D.J.J., Lippert, P.C., Dupont-Nivet, G., McQuarrie, N., Doubrovine, P.V., Spakman, W., Torsvik, T.H., 2012. Greater India basin hypothesis and a two-stage cenozoic collision between India and Asia. Proc. Natl. Acad. Sci. Unit. States Am. 109, 7659–7664.
Wang, B., Ho, L., 2002. Rainy season of the Asian–Pacific summer monsoon. J. Clim. 15, 386–398.
Wang, K.F., Yang, J.W., Li, Z., Li, Z.R., 1975. On the tertiary sporo-pollen assemblages from Lunpola Basin of xizang, China and their palaeogeographic significance. Sci. Geol. Sin. 4, 366–374.
Wang, W., Xie, P., Yoo, S.-H., ZXue, Y., Kumar, A., Wu, X., 2011. An assessment of the surface climate in the NCEP climate forecast system reanalysis. Clim. Dynam. 37, 1601–1620.
Wang, E., Kirby, E., Furlong, K.P., van Soest, M., Xu, G., Shi, X.G., Kamp, P.J., Hodges, K., 2012. Two-phase growth of high topography in eastern Tibet during the Cenozoic. Nat. Geosci. 5, 640–645.
Wang, C.S., Dai, J., Zhao, X., Li, Y., Graham, S.A., He, D., Ran, B., Meng, J., 2014. Outward-growth of the Tibetan plateau during the cenozoic: a review. Tectonics 621, 1–43.
Wang, Y., Zhang, P., Schoenbohm, L.M., Zheng, W., Zhang, B., Zhang, J., Zheng, D., Zhou, R., Tian, Y., 2018. Two-phase exhumation along major shear zones in the SE Tibetan Plateau in the Late Cenozoic. Tectonics 37, 2675–2694.
Wang, L., Kunzmann, L., Su, T., Xing, Y.-W., Zhang, S.-T., Wang, Y.-Q., Zhou, Z.-K., 2019. The disappearance of *Metasequoia* (cupressaceae) after the middle Miocene in yunnan, southwest China: evidences for evolutionary stasis and intensification of the asian monsoon. Rev. Palaeobot. Palynol. 264, 64–74.
Webster, P.J., Fasullo, J., 2003. Monsoon: Dynamical Theory. In: Holton, J.R. (Ed.), Encyclopedia of Atmospheric Sciences. Academic Press, London, pp. 1370–1385.
Weedon, G.P., 2005. Time-Series Analysis and Cyclostratigraphy: Examining Stratigraphic Records of Environmental Cycles. Cambridge University Press, Cambridge.
Weedon, G.P., Coe, A.L., Gallois, R.W., 2004. Cyclostratigraphy, orbital tuning and inferred productivity for the type kimmeridge clay (late jurassic), southern england. J. Geologi. Soc. london 161, 656–666.
Whatley, R., Bajpai, S., 2006. Extensive endemism among the Maastrichtian non-marine Ostracoda of India with implication of palaeogeography and "out of India" dispersal. Rev. Espanola Micropaleontol. 38, 229–244.
Wheeler, E.A., Srivastava, R., Manchester, S.R., Baas, P., 2017. Surprisingly modern latest cretaceous – earliest Paleocene woods of India. IAWA J. 38, 456–542.
Wissink, G.K., Hoke, G.D., Garzione, C.N., Liu-Zeng, J., 2016. Temporal and spatial patterns of sediment routing across the southeast margin of the Tibetan Plateau: insights from detrital zircon. Tectonics 35, TC004252.
Writing Group of Yunnan Vegetation, 1987. Vegetation of Yunnan. Science Press, Beijing.
Wu, Z.Y., 1979. Flora of Yunnan. Science Press, Beijing.
Wu, Z.Y., 1988. Hengduan Mountain flora and her significance. J. Jpn. Bot. 63, 297–311.
Wu, Z.Y., Zhu, Y.C., 1987. Vegetation of Yunnan. Science Press, Beijing.
Wu, Z.-Y., Zhou, Z.-K., Sun, H., Li, D.-Z., Peng, H., 2006. The Areal-Types of Seed Plants and Their Origin and Differentiation. Kunming: Yunnan Publishing Group Corporation Yunnan Science & Technology Press, Kunming, pp. 1–566.
Wu, G., Liu, Y., He, B., Bao, Q., Duan, A., Jin, F.-F., 2012. Thermal controls on the Asian summer monsoon. Sci. Rep. 2, 404.
Wu, F., Herrmann, M., Fang, X., 2014. Early Pliocene paleo-altimetry of the Zanda Basin indicated by a sporopollen record. Palaeogeogr. Palaeoclimatol. Palaeoecol. 412, 261–268. https://doi.org/10.1016/j.palaeo.2014.08.006.
Wu, F.-X., Miao, D., Chang, N.-M., Shi, G., Wang, N., 2017. Fossil climbing perch and associated plant megafossils indicate a warm and wet central Tibet during the late Oligocene. Sci. Rep. 7, 878–885.
Wu, F.-X., He, D., Fang, G., Deng, T., 2018. Into Africa via docked India: a fossil climbing perch from the Oligocene of Tibet helps solve the anabantid biogeographical puzzle. Sci. Bull. 64, 455–463. https://doi.org/10.1016/j.scib.2019.03.029.
Xiong, Z., Ding, L., Wang, X., Spicer, R.A., Farnsworth, Wang, X., Valdes, P.J., Su, T., Zhang, Q., Zhang, L., Cai, F., Wang, H., Li, Z., Song, P., Guo, X., Yue, Y., 2020. The early Eocene rise of the Gonjo Basin, SE Tibet: from low desert to high forest. Earth Planet Sci. Lett. 543, 116312. https://doi.org/10.1016/j.epsl.2020.116312.
Xu, Q., Ding, L., Zhang, L.Y., Cai, F.L., Lai, Q.Z., Yang, D., Zeng, J.L., 2013. Paleogene high elevations in the Qiangtang terrane, central Tibetan plateau. Earth Planet Sci. Lett. 362, 31–42.
Xu, Q., Ding, L., Hetzel, R., Yue, Y., Rades, E.F., 2015. Low elevation of the northern Lhasa terrane in the Eocene: implications for relief development in south Tibet. Terra. Nova 27, 458–466.
Xu, H., Su, T., Zhang, S.-T., Deng, M., Zhou, Z.-K., 2016. The first fossil record of ring-cupped oak (*Quercus* L. subgenus *Cyclobalanopsis* (Oersted) Schneider) in Tibet and its paleoenvironmental implications. Palaeogeography, Palaeoclimatology,. Palaeoecology 442, 61–71.
Xu, Q., Ding, L., Spicer, R.A., Liu, X., Li, S., Wang, H., 2018. Stable isotopes reveal southward growth of the Himalayan-Tibetan Plateau since the Paleocene. Gondwana Res. 54, 50–61.
Yan, Y., Xia, B., G., L, Cui, X., Hu, X., Yan, P., Zhang, F., 2007. Geochemistry of the sedimentary rocks from the Nanxiong Basin, South China and implications for provenance, paleoenvironment and paleoclimate at the K/T boundary. Sediment. Geol. 197, 127–140.
Yanai, M., Wu, G.X., 2006. Effects of the Tibetan plateau. In: Wang, B. (Ed.), The Asian Monsoon. Springer, Berlin, pp. 513–549.
YBGMR, 1990. Regional geology of yunnan province.
Yi, T.-M., Li, C.-S., Xu, J.-X., 2003. Late Miocene woods of taxodiaceae from yunnan, China. Acta Bot. Sin. 45, 384–389.
Yin, A., Harrison, T.M., 2000. Geologic evolution of the Himalaya-Tibet orogen. Annu. Rev. Earth Planet Sci. 28, 211–280.
Yu, H., Miao, S., Xie, G., Guo, X., Chen, Z., Favre, A., 2020. Contrasting floristic diversity of the hengduan mountains, the himalayas and the qinghai-tibet plateau sensu stricto in China. Front. Ecol. Evol. https://doi.org/10.3389/fevo.2020.00136.
Zachos, J., Pagani, M., Sloan, L., Thomas, E., Billups, K., 2001. Trends, rhythms, and aberrations in global climate 65 Ma to present. Science 292, 686–693.
Zachos, J., McCarren, H., Murphy, B., Röhl, U., Westerhold, T., 2010. Tempo and scale of late Paleocene and early Eocene carbon isotope cycles: implications for the origin of hyperthermals. Earth Planet Sci. Lett. 299, 242–249.
Zhang, S., Wang, B., 2008. Global summer monsoon rainy seasons. Int. J. Climatol. 28, 1563–1578.
Zhang, W., Yan, M., Fang, X., Zhang, D., Zhang, T., Zan, J., Song, C., 2019. High-resolution paleomagnetic constraint on the oldest hominoid- fossil-bearing sequence in the Xiaolongtan Basin, southeast margin of the Tibetan Plateau and its geologic implications. Global Planet. Change 182, 103001.
Zhao, Y., Tzedakis, P.C., Li, Q., Qin, F., Cui, Q., Liang, C., Birks, H.B., Liu, Y., Zhang, Z., Ge, J., Zhao, H., Felde, V.A., Deng, C., Cai, M., Li, H., Ren, W., Wei, H., Yang, H., Zhang, J., Yu, Z., Guo, Z., 2020. Evolution of vegetation and climate variability on the Tibetan Plateau over the past 1.74 million years. Sci. Adv. 6, eaay6193.
Zhou, Z.-K., Deng, T., 2020. The Tibetan Plateau is a natural laboratory for studying organic evolution and environmental change. Sci. China Earth Sci. 63, 169–171. https://doi.org/10.1007/s11430-019-9563-x.
Zhou, Z.-K., Wang, T.-X., Huang, J., Liu, J., Deng, W.-D., Li Shihu, Deng, C.-L., Su, T., 2020. Fossil leaves of berhamniphyllum (rhamnaceae) from Markam, Tibet and their biogeographic implications. Sci. China Earth Sci. 63, 224–234. https://doi.org/10.1007/s11430-019-9477-8.